TÉCNICO LISBOA

WindFloat design for different turbine sizes

Johannes George

Thesis to obtain the Master of Science Degree in

Energy Engineering and Management

Supervisors: Prof. Antonio José Nunes de Almeida Sarmento
Eng. Cyril Gilles Emile Gordreau

Examination Committee

Chairperson: Prof. José Alberto Caiado Falcão de Campos
Supervisor: Prof. Antonio José Nunes de Almeida Sarmento
Members of the Committee: Prof. Luís Manuel de Carvalho Gato

September 2014

This thesis is based on work conducted within the KIC InnoEnergy Master School, in the MSc programme SELECT - Environomical Pathways for Sustainable Energy Systems. This programme is supported financially by the KIC InnoEnergy. The author also received financial support from KIC InnoEnergy, which is gratefully acknowledged.

The thesis is integrated in the IST effort on the OTS - Offshore test Station project funded by KIC InnoEnergy. The project is realized in collaboration with WavEC – Offshore Renewables and coordinated by Professor Antonio Sarmento.

KIC InnoEnergy is a company supported by the European Institute of Innovation and Technology (EIT), and has the mission of delivering commercial products and services, new businesses, innovators and entrepreneurs in the field of sustainable energy through the integration of higher education, research, entrepreneurs and business companies. Shareholders in KIC InnoEnergy are leading industries, research centres, universities and business schools from across Europe.

Acknowledgements

I would like to express my gratitude to my supervisor Professor Antonio Sarmento who suggested the topic for my master's thesis and who made it possible for me to work in the interesting field of floating offshore wind turbines.

I am sincerely grateful to my thesis advisor and co-supervisor Cyril Godreau from IST for sharing his time and in-depth knowledge throughout the thesis-writing process. His constant support and remarks were highly valuable and provided me with guidance and motivation whenever needed.

Special thanks go to PhD candidate and edp-engineer Tiago Duarte. His comments and apposite answers helped me very much.

I also would like to acknowledge the PhD candidates and researchers Matthieu Guérinel, for the WAMIT-simulations, and Yannick Debruyne for his help concerning the scaling methodology.

A special thanks to Melinda Minen for translating the thesis summary into Portuguese and Nadirah Porter-Kasbati for proofreading this work.

Abstract

This thesis presents the evaluation of two different floating semi-submersible platform designs to support large offshore wind turbines. Based on the 5MW-platform used in the OC4-project (Offshore Code Comparison Collaboration Continuation), two different models - straight upscale, increasing all dimensions by the same factor, and a design with a draft limited to 20m - were developed to carry 7.5MW and 10MW wind turbines. The main focus is set on the analysis and comparison of the platforms' stability for various load cases representing European offshore conditions in time- and frequency-domains, based on numerical simulations. In pitch-motion, the most critical of the six degrees of freedom of the platform, larger platforms show a slightly higher response to acting forces. The slightly changed platform type with the reduced draft shows better stability in pitch in comparison with the straight upscale. Resonant behavior and damping are also discussed. The large platforms for 10MW turbines show a high resonant response in sway and yaw for extreme conditions. This might cause problems for the structural stability of the whole system, which is not examined in this work. The nacelle acceleration does not exceed the threshold value of 1.96m/s^2 in any of the analyzed load cases.

The infrastructural conditions, mainly harbors, shipyards, dry docks, and natural conditions, such as wind-speeds and distance to shore, seem to allow an implementation of semi-submersible platforms for offshore wind farms.

A brief economical evaluation indicates that the economy of scale would justify the deployment of large-scale floating wind turbines.

Keywords: semi-submersible, floating offshore wind turbine, platform stability, numerical simulation

Resumo

Esta tese apresenta a análise de duas plataformas semi-submersíveis para suportar grandes turbinas offshore. Com base na plataforma de 5MW usada no projecto OC4, foram desenvolvidas duas plataformas para suportar turbinas de 7.5MW ou 10MW. Essas plataformas foram desenvolvidas com base em dois modelos por semelhança geométrica, um por aumento linear idêntico nos três eixos e outro por aumento apenas nos eixos horizontais, mantendo o calado da plataforma em 20m. Em ambos os casos o aumento linear é determinado pela impulsão necessária para suportar o peso da turbina. Uma maior atenção é dada à análise e comparação da estabilidade das plataformas para diferentes condições offshore típicas na Europa no domínio do tempo e frequência, com base em simulações numéricas. O *pitch* é o mais crítico de entre os DOF, sendo que as plataformas maiores demostram uma reacção maior às forças. A plataforma ligeiramente alterada com menos *draft*, mostra uma estabilidade maior no *pitch* comparada com a *streight-up scale*. A ressonância e o amortecimento são analisados também. As plataformas de 10 MW demonstram uma alta ressonância no *sway* e *yaw* em condições extremas. Isto pode causar problemas na estabilidade estrutural do sistema completo, que não é examinado neste trabalho. A aceleração da nacelle não supera o limite de 1.96m/s^2 em nenhum caso analisado.

A condições em termos de estruturas, tais como portos, estaleiros ou docas secas, e em termos de natureza, como a velocidade do vento e a distância à costa, permitem a implementação de plataformas semi-submersíveis para parques eólicos offshore.

Uma avaliação económica indica que a economia de escala justifica a instalação de grandes plataformas.

Palavras-chave: semi-submersível, turbina eólica off-shore, estabilidade da plataforma, simulações numéricas

Contents

List of Figures

List of Tables

Nomenclature

Symbol	Unit	Description
A	[m^2]	area
$B_{ZZ,Visc}$	[Ns^2/m^2]	linearized quadratic drag coefficient (linear modes)
$B_{\theta\theta,Visc}$	[Nms^2/rad^2]	linearized quadratic drag coefficient (rotational modes)
C_D	[-]	drag coefficient
H_S	[m]	significant wave height
H_{Steady}	[m]	steady state wave height
R	[m]	radius
ω	[Hz]	frequency
ρ	[kg/m^3]	density
s	[-]	scaling factor
S(ω)	[m^2/Hz]	wave spectrum
T_p	[sec]	peak-spectral period of incident waves
T_{Steady}	[sec]	wave peak period
Θ	[rad]	angle of the rotational motion
U_{Steady}	[m/s]	steady wind speed
U_{mean}	[m/s]	mean wind speed (turbulent wind)
z_a	[m]	amplitude of the linear motion

List of Abbreviations

API	American Petroleum Institute
CAD	Computer Aided Design
CAPEX	Capital Expenditures
DoF	Degree of Freedom
DTU	Technical University of Denmark
EDP	Energias de Portugal
IEA	International Energy Agency
IEC	International Electrotechnical Commission
FAST	Fatigue, Aerodynamics, Structures, and Turbulence
FOWT	Floating Offshore Wind Turbines
GIS	Geographic Information System
HVDC	High voltage direct current
JONSWAP	Joint North Sea Wave Project
LCOE	Levelized cost of energy
MI&T	Marine Innovation & Technology
MSL	Mean sea level
NREL	National Renewable Energy Laboratory
NTNU	Norwegian University of Science and Technology
NWTC	National Wind Technology Center
OC3/OC4	Offshore Code Comparison Collaboration/ (Continuation)
OPEX	Operational Expenditures
PSD	Power spectral density
WAMIT	Wave Analysis at MIT (Massachusetts Institute of Technology)
WavEC	Offshore Renewables Center (previously: Wave Energy Centre)

1. Introduction

The first windmills were used for pumping water and grinding grain more than 2000 years ago (WEF, 2012). In 1887 electricity was generated from a wind turbine for the first time. However, the discovery of oil as a cheap fuel that is easy to store and has a high energy density impeded the further development of wind-generated energy. Due to the 1970s oil shock, research and development of wind turbine technology received enhanced funding from several governments (Nixon, 2008). This started a fast and ongoing evolution of the design of wind turbines. The rated power, size and efficiency of turbines continue to increase while the levelized cost of energy (LCOE) decreases. With the first offshore wind farm going into operation in 1991, new possibilities and challenges were added to the already complex field of wind turbine technology. Highly productive and larger turbines have to be installed in new areas with good wind resources to ensure the compatibility of the whole industry. Favorable wind conditions can often be found far off the coast, where water depths exceed several hundred meters.

Floating structures, able to carry wind turbines with power ratings well above 5MW might be an applicable solution to exploit these energy resources. Thereby the electricity generation has to be reliable to ensure the economic feasibility. The economy of scale takes effect only if the platform provides enough stability in a long variety of conditions. Furthermore infrastructural limitations regarding the construction and maintenance efforts have to be considered.

Therefore the scope of this thesis is to evaluate the platform behavior of two different semisubmersible designs being designed for a 7.5 and a 10MW wind turbine. These designs are derived from and are compared to a floating 5MW system. The scaling approaches are presented in this thesis. The central part of this work consists of the simulation and evaluation of the different designs and sizes under a variety of conditions. A brief overview on the infrastructural circumstances of the European North Atlantic and North Sea area is given. Finally the influence of the different designs and dimensions on the costs is examined.

1.1. Current Background and Motivation

Climate change, particularly its social, economical and environmental consequences, is one of the biggest challenges faced by humankind. It is mainly caused by the use of non-renewable and finite primary energy sources (fossil fuels) for energy supply, paired with the simultaneous increase in energy demand at an unprecedented rate. Thus a shift towards renewable and sustainable sources of energy is inevitable. A large part of the energy demand can be provided by wind power, which, converted to electricity by wind turbines, already satisfies 2% of the global energy demand (Sun, Huang, & Wu, 2012). Wind turbines are a proven technology on- and offshore. In Europe alone there is 110.7 GW of installed wind capacity onshore, representing 13% of the total generating capacity (EWEA, 2014a). Especially in densely populated parts of the world like Europe, with a relatively high

number of onshore wind turbines installed, the productive and lucrative locations are developed already. As stated by EWEA (2014), “Europe is the most maritime of all continents. “ This motivates decision-makers to deploy wind turbines offshore, where larger areas are available, with high mean wind speeds, less turbulent wind, and reduced visual impact (Sun, Huang, & Wu, 2012). The average capacity factor of a European offshore wind turbine is 41%, compared with 24% for a turbine located onshore. The biggest offshore wind farm “London Array” is currently under construction and will reach the same rated electricity output as a conventional coal powered block-unit power station. Once finished, the total rated power will be 1 GW (London Array Limited, 2014). Currently, offshore wind farms are being installed on fixed foundations on the seabed at an average water depth of 20m and with an average distance to shore of 30km.

Three quarters of all European offshore wind turbines are installed on Monopile structures, allowing an application of maximum water depths of up to 30m. Other commercially deployed substructures allow a construction in water depths of up to 50m, such as the Jacket and Tripod structures visualized in Figure 1-1 (EWEA, 2013). The installation costs rise with increasing depth.

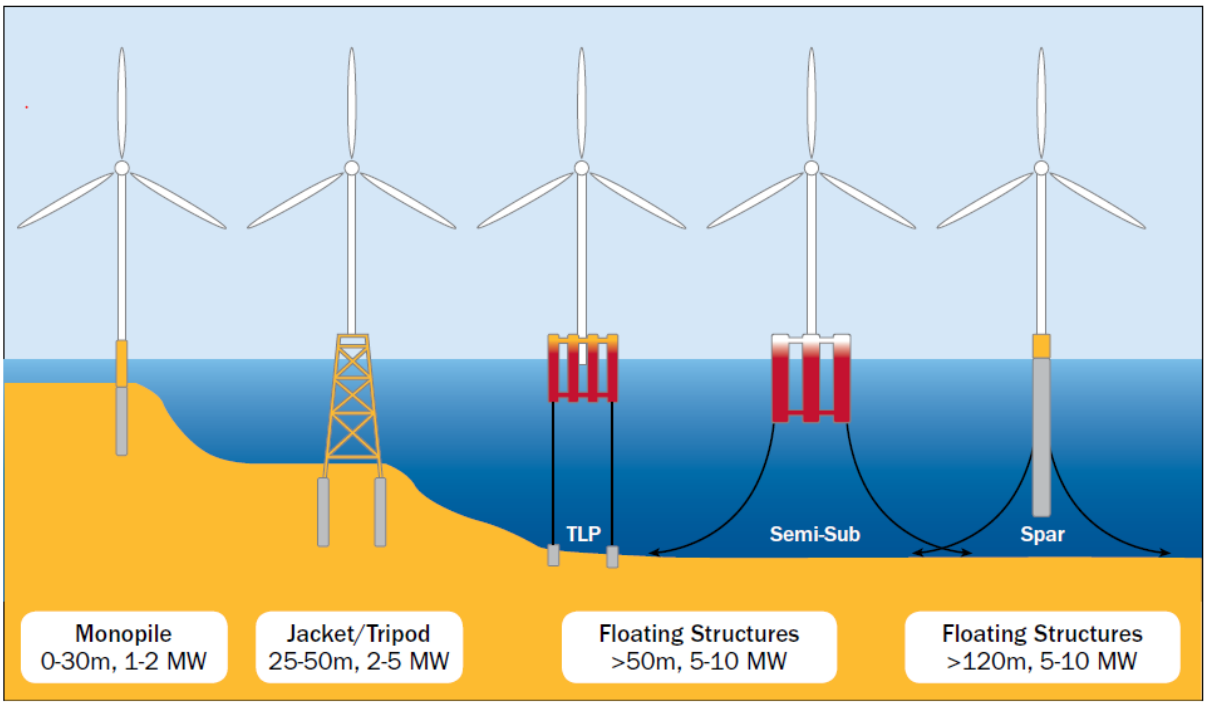

Figure 1-1 Summary of platform concepts for offshore wind turbines (EWEA, 2013)

Floating structures, inspired by and based on the knowledge from the oil and gas industry, open up the possibility to move towards water depths over 50m. Two thirds of the North Sea´s area has a water depth between 50m and 220m. The wind resources in this area are enough to generate four times the electricity being used in Europe today. The map depicted in figure Figure 1-6, at the end of chapter 1, illustrates these favorable areas in Europe. Floating Offshore Wind Turbines (FOWT) are not in the commercial phase yet, but the first full- and small-scale prototypes are being tested under

real conditions. An overview of the different designs and the current efforts in research and Development is given in section 1.2.2. To ensure compatibility, the power capacity and costs of a FOWT has to meet the benchmarks set by bottom-fixed installations. Power ratings of those turbines will be in the range of 5 to 10MW in the next decade (Smith P. , 2014b).

1.2. Previous and Ongoing Research

The capacity ratings and dimensions of wind turbines have steadily risen since the introduction of the first commercial wind turbines in the 1980s. The main driving force behind this development is the minimization of the levelized generation costs. In contrast to onshore turbines, where size limitations might occur due to logistical constraints, the design of offshore wind turbines will increase as long as technically possible and economically justifiable (Wiser, et al., 2011). Thus support structures, whether bottom-fixed or floating, must be designed and adjusted accordingly. The following passage gives an overview of the development in turbine and floating platform design, as well as introducing the software used for the simulations in this thesis.

1.2.1. Wind turbine development

In the last 10 years, the rated capacity of commercial three-bladed upwind turbines has increased threefold. The expected average capacity for newly installed offshore wind turbines in the year 2014 is 4MW, mainly due to the dominance of market leader Siemens and its 3.6 MW turbine (EWEA, 2014b). The trend is clearly going towards significantly higher power ratings, as Siemens had already installed a 6MW wind turbine onshore in May 2011 (Siemens, 2011). It is expected that 6 MW will be the next standard for offshore installations. So far, the largest fully operational turbine that has been installed offshore is the Alstom 6-MW Haliade™ 150 in December 2013 (Alstom, 2013a). At the same time, the largest turbine with respect to height (196m) and rotor diameter (171m) was installed onshore by Samsung Heavy Industries (PE, 2013). Vestas constructed a first prototype of its 8MW wind turbine in January 2014. Developed especially for offshore North Sea conditions (Garus, 2014), Vestas confirmed first orders for construction in 2016 (Smith P. , 2014a). This fast development is visualized in the figure below.

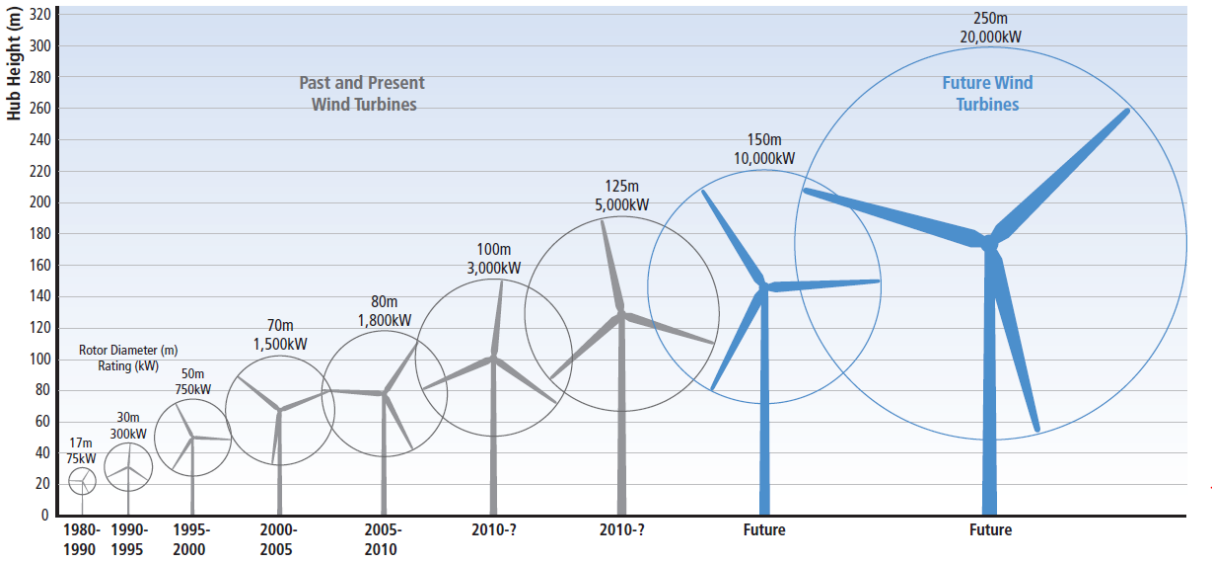

Figure 1-2 Increase of turbine sizes (Wiser, et al., 2011)

The main benchmark for the near future is the construction of a 10MW wind turbine. For such sizes, no data is available from manufacturers, but research institutes and universities present preliminary complete designs. The Technical University of Denmark (DTU), in cooperation with Vestas, developed the “DTU 10-MW Reference Wind Turbine (DTU 10MW RWT)” (Bak, et al., 2013). This model is used for considerations in this thesis and is described in more detail in chapter 2. An overview and comparison between commercially available and scientifically used turbines can be found at the end of that section.

General Electrics and Gamesa have started the concept phase in two independent projects with the aim of developing a 15MW offshore turbine by the year 2020 (4COffshore, 2014c). The theoretical design of an offshore wind turbine with a rated power of 20MW is presented by Peeringa et al. (2011).

1.2.2. Floating structures for Floating Offshore Wind Turbines

As FOWT have been subject to intense Research and Development efforts only recently, no design clearly prevails over the others. Different advantages and disadvantages might determine the choice of the floating platform depending on the particular site of deployment. In Crozier (2011) a list of key parameters to assess and compare different floating structures is presented:

- Platform stability
- System operational and shut-down dynamics
- Platform mass and mooring system
- Survivability
- Installation

• Logistics

• Maintenance

Depending on the platform´s performance with regard to these parameters, the costs and overall competitiveness with bottom fixed offshore constructions is defined. For the scope of this thesis, only the semi-submersible type is investigated. Therefore the evaluation of the overall stability and operation is of main interest. The other aspects do not change significantly between the examined designs. The motions along the six Degrees of Freedom (DoF) have an influence on different parameters of the whole floating system.

Sway/Surge & Roll	-> stress on mooring
Pitch & Roll	-> fatigue, operation and shut down dynamics
Heave	-> internal stress & stress on mooring

Main types of Floating Platforms

Three main types of floating structures in different modifications are the subject of most projects, as shown in Figure 1-1. All designs are based on the experiences of the offshore oil and gas industry. Namely these are: the Tension Leg Platform (TLP), Spar buoy, Barge type and the Semi-submersible, stabilized through mooring, ballast and buoyancy, respectively. The semi-submersible platform type, as analyzed in this thesis and depicted in Figure 1-3, is a hybrid concept. It combines restoring modes of all three previously presented platform types.

Tension Leg Platform:

The very buoyant platform is connected to the sea bed through tensioned mooring lines, ensuring very good stability. The main drawback lies in the difficulty of construction and securing the anchors to withstand the high forces induced by the platform motions.

Spar Buoy:

The cylindrical, ballast-stabilized structure has a center of gravity far below the sea surface and its center of buoyancy. Advantages are the minimum sensitivity to wave motions and the comparable ease of anchor installation. The main disadvantage lies in the size of the construction, increasing the material and installation costs. Furthermore the size only allows installations under calm water conditions at depths higher than 120 meters (Matha & Jonkman, 2009) & (Bossler, 2014).

Barge type:

The stability of the barge type platform is ensured primarily by its water plane area moment due to the comparably large diameter and shallow draft. It is ballasted with seawater. A catenary mooring system is used. Of all platform designs the barge type has the most sensitive reaction to wave motions (Matha & Jonkman, 2009).

Semi-submersible:

As is the case for the Spar buoy, the center of gravity lies below the center of buoyancy. This is achieved by adding ballast to the bottom of the columns. At the same time, the semi-submersible platform is deployable at depths similar to the tension leg platform. The great economical advantage over other FOWT-concepts is that its assembly can be realized completely in the harbor and it can be transported to its final destination by simple tug vessels. This makes an installation under rougher conditions more manageable than with the other concepts. Therefore it decreases the need for expensive offshore vessels and reduces the risks of offshore operations. Consequently, a wider period of time for the offshore installation is available.

History

The idea of installing floating wind turbines has existed since the 1970s. However, serious research with industry involvement began only in the mid-1990s. The first offshore test configuration was installed in 2008 near the Italian coast by Blue H technologies. The system, equipped with a 80kW wind turbine, was dismantled after a year of data collection (EWEA, 2013). The same year, Poseidon Floating Power launched an offshore demonstration plant in Denmark, consisting of a floating wave energy converter with a wind turbine placed on top. According to the plans, a full-scale plant might be able to have a power of 7.5MW, of which 5MW would be produced by the wind turbine (Poseidon Floating Power, 2013). The first large-scale, grid-connected FOWT was installed in 2009 by Statoil in Norway. The wind turbine with a rated power of 2.3MW is placed on a spar buoy structure. In 2011 Principle Power in cooperation with EDP (Energias de Portugal) and Repsol commissioned the WindFloat structure, with a 2MW wind turbine mounted on top. This semi-submersible platform is located 5km off the Portuguese coast (EWEA, 2013). As the system was assembled in the harbor, this was “the first multi-megawatt offshore wind turbine to be installed without the use of any heavy lift offshore vessels” (MarineLink, 2013). In 2013, a joint venture between several Japanese research institutes and the Ministry of Environment installed a 2MW Hitachi-turbine, based on the spar concept (Foster, 2013).

In total, there are more than 30 projects worldwide at different stages of development. Many of them are undertaking tests on small scale models. The main actors are from Europe, the US and Japan. The first systems, the three most mature projects leading ahead, are planned to enter the pre- and/or serial production phase in 2 to 3 years. Please see (EWEA, 2013) pages 21-24 for a complete overview on all R&D efforts in the field of floating platforms.

Not only the platform, but also the wind turbine design is subject to research efforts. While the largest deployed prototypes, as presented in the following paragraph, use 3-bladed upwind turbines, some developers investigate 2 bladed downwind turbines or vertical axis Darrieus-type turbines (Nautica Winpower, 2011) & (MODEC Inc., 2013).

1.2.3. DeepCwind, OC3/4, and WindFloat project

The platform to be examined in this work and its origin are presented in this chapter. Furthermore, the platform is put in context with other current research efforts.

DeepCwind Consortium

This research group aims to develop deep-water offshore wind technology towards a mature state, with the ultimate goal of installing a total of 5GW of floating wind farms off the coast of Maine (USA). The consortium is led by the University of Maine, funded by the U.S. Department of Energy and involves other universities, research institutes, nonprofits and industrial partners. Several platform designs have been developed and tested in wave tanks, as well as in 1:3 scale models offshore (Lindyberg, et al., 2012). One of these models is the subject of considerations in this work and will be presented below. One member of the DeepCwind consortium is the National Renewable Energy Laboratory (NREL). The NREL developed coupled aeroelastic/hydrodynamic models of the platform designs that were and are validated in tests at a later stage of the DeepCwind-project (University of Maine, 2014).

OC3/4 – Offshore Code Comparison Collaboration / Continuation

Simulation tools are used for the design and analysis of wind turbines to predict the system´s reaction and dynamics on externally applying loads. For land-based turbines aero-servo-elastic codes are used, simulating the coupled aero- and structural-dynamic motions together with the control system (servo) in a time domain. As FOWT experience additional dynamics, such as waves and current, hydrodynamics and the dynamics of the platform, the codes have to be enhanced. As data for validating these complex “aero-hydro-servo-elastic codes” is rare, the OC3 – “Offshore Code Comparison Collaboration” – was established between 2005 and 2009 to verify the correctness of the simulation tools. The NREL initiated a code-to-code comparison “which analyzed shallow, transitional, and deep water offshore wind turbine concepts” (Musial & Jonkman, 2010). Universities, research institutes and industrial partners from across the world compared their software. Three different bottom fixed and one floating platform of the spar-type were analyzed in the OC3 (Musial & Jonkman, 2010).

The semi-submersible platform

The OC4-project (Offshore Code Comparison Collaboration Continuation), finalized in 2013, is a continuation of the OC3 project. In the second phase, a semisubmersible floating platform was examined, as shown in a 5MW-configuration below in Figure 1-3. This design originated from the activities of the DeepCwind consortium and marks the starting point for the scaling approaches in this thesis. Three offset columns are arranged in a triangular array, ensuring the buoyancy and stability of the platform. These bodies consist of two parts, the upper and base column. The base columns have

the same effect as heave plates. They improve the motion performance of the FOWT. The damping of the system increases significantly, primarily in Pitch, Roll and Heave motion. Because of its good stability performance they may carry commercially available wind turbines. A separating wall lies in between the upper and lower cylinder of the column. This allows the adjustment of the center of mass by changing the amount and distribution of the ballast water. The central main column serves as the foundation of the wind turbine. These four main cylindrical floaters are connected to each other by horizontally positioned pontoons and vertical cross bars. A more detailed description of the platform can be found in Robertson A. et al. (2013b).

The three catenary mooring lines are arranged at a 120° angle to each other. The anchors are pre-laid drag embedded. In comparison to taut mooring, used for Tension Leg platforms, this type of mooring causes reduced stress on the components and is cheaper to install.

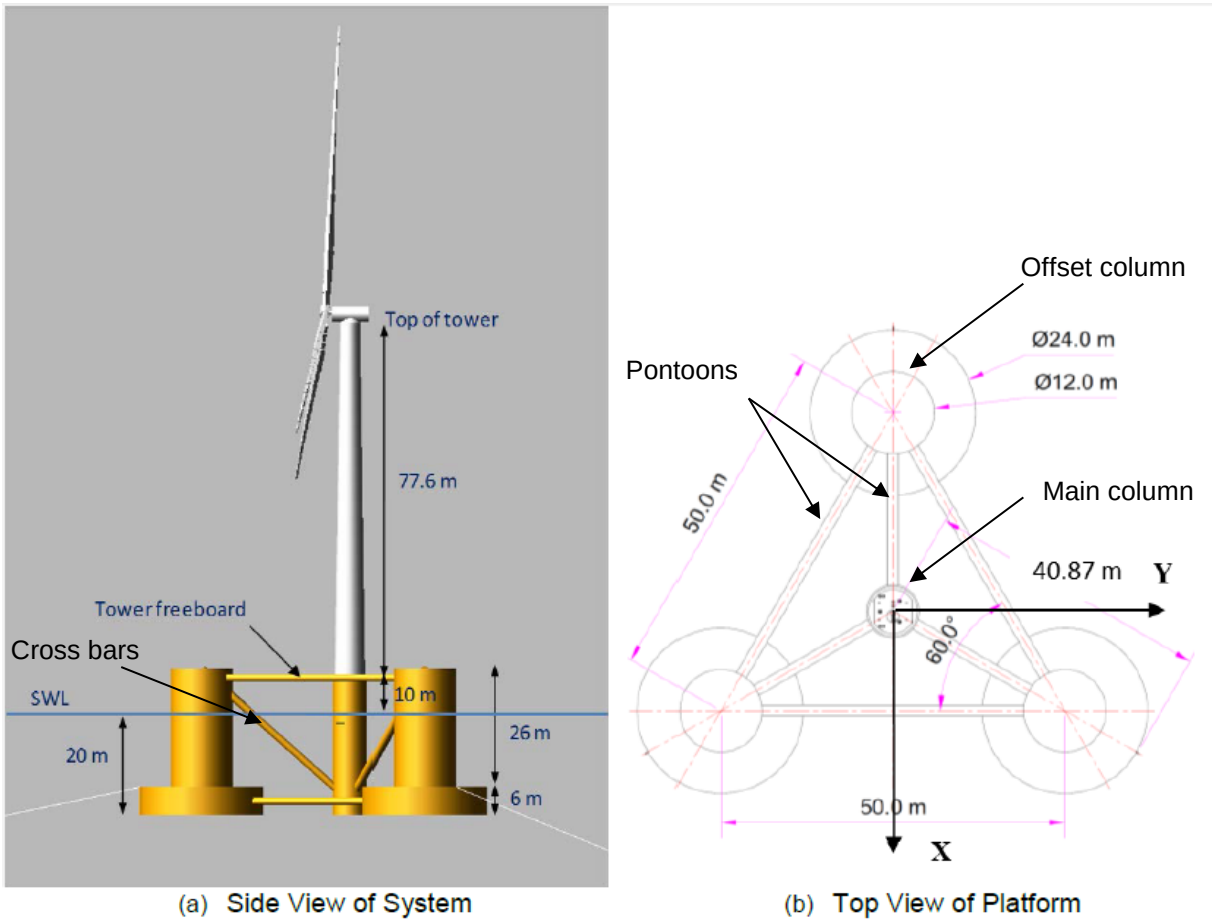

Figure 1-3 OC4 semi-submersible 5MW-configuration (modified after (Robertson A. , et al., 2013b))

WindFloat project

The foundation for the WindFloat platform was laid by MiniFloat^{TM}, a floating semi-submersible, triangular platform patented in 2003 by the offshore engineering consulting company MI&T (Marine Innovation & Technology) (MI&T, 2014). As the turbine is sustained by one of the columns the stresses on the connecting structure to the other two columns is very small. Furthermore the restoring moments originated in the two other columns is much higher due to the increased arm.

The company Principle Power acquired the patent for WindFloat and in a cooperation with EDP (Energias de Portugal) realized the deployment of the platform off the Portuguese coast, equipped with a 2MW wind turbine. The WindFloat project marks the first large-scale testing of a semi-submersible floating structure and offshore wind turbine installation without any heavy-lifting vessels (MarineLink, 2013). The WindFloat platform is depicted in the figure below. A comparison between the two presented floating structures is given in chapter 3.3.

Figure 1-4 The WindFloat platform (Bornemann, 2011)

1.2.4. Numerical simulation

Different software is used to realize the simulation of the floating systems´ response to forces. Most work is done with a publicly available aero-servo-hydro-elastic code developed by the National Wind Technology Center (NWTC). Other programs are mainly used for the preprocessing of additional inputs needed for the simulations.

FAST 8

The FAST (Fatigue, Aerodynamics, Structures and Turbulence) Code, developed by NREL´s National Wind Technology Center (NWTC), is a capable of simulating the response of a FOWT to most environmental loads it is exposed to offshore. Furthermore the servo-elastic properties of the structure, foundation, control and power system are considered. Originally designed for modeling onshore wind turbines, the tool was extended to simulate platform and mooring dynamics under waves and currents. In addition, FAST facilitates the calculation of the internal stresses of the tower and blades. The software was used for the previously mentioned aeroelastic/hydrodynamic simulations in the DeepCwind consortium and has been verified in the OC3/4 project. Wave tank tests have been done to validate the FAST-code and examine how accurately the platform behavior is modeled (Masciola, et al., 2013). For the simulations in this report the latest version FAST 8 is used. In contrast to earlier versions, it enables the user to define complex platform geometries. In earlier versions bodies were approximated by a cylinder. This restriction only allowed the user to accurately simulate spar-buoy concepts. To model other platform types, such as a semi-submersible, adaptations in the code were necessary. The platform geometry has a huge impact on its overall stability, damping and drag against induced motions. Therefore additional values had to be added in the input-files to compensate for the simplification of the platform model. Those additional damping and drag coefficients resulted from iterative wave-tank tests and code comparisons, until the simulation and test results matched. To check the accurate running of FAST 8, the OC4 load cases were re-simulated in the start of this thesis work and compared to the results simulated with FAST 7. In this work, a simplified platform model is used together with adjusted coefficients. This procedure is presented in detail in section 3.4. The general structure of FAST 8 is presented below in Figure 1-5. Several modules calculate the aerodynamic, hydrodynamic, servo dynamics, etc. behavior of the system, based on previously defined inputs. In one output file, all desired information is collected in the time domain. Some input files can be found in the appendix and meaningful results are presented in form of graphs throughout the thesis. Detailed information on the theory behind FAST is available in Jonkman & Buhl (2005).

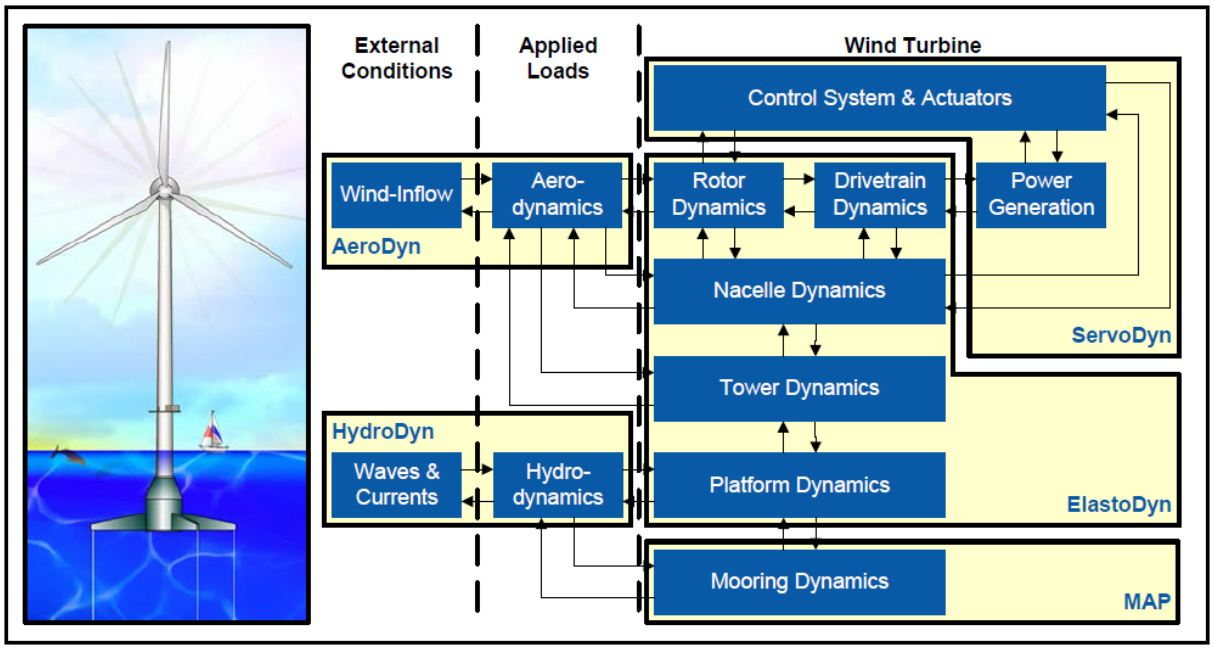

Figure 1-5 The program setup of FAST 8 (Jonkman & Jonkman, 2013)

TurbSim

Turbulent wind flow files are generated with the TurbSim - stochastic inflow turbulence code. For further information please see Kelley & Jonkman (2007). This wind data is vital for the AeroDyn-module of FAST.

WAMIT®

The computations of WAMIT (Wave Analysis at MIT) give additional hydrodynamic inputs for the HydroDyn module of FAST. “WAMIT® is a computer program based on the linear potential theory for analyzing floating or submerged bodies, in the presence of ocean waves” (WAMIT, Inc., 2013b). Using inputs describing the platform geometry, its inertias and the analyzed water depth, WAMIT computes the added mass, damping and stiffness matrices.

Solid Edge ST6

The CAD-software Solid Edge ST6 is used to construct 3-dimensional models of the scaled platform designs. The total mass of a scaled model and its mass moments of inertia, both necessary for the FAST and WAMIT-simulations, are then easily obtained.

1.3. Objectives

The objectives of this master´s thesis are to:

- Develop two scaled platform models based on the 5MW semisubmersible design as used in the OC4, for both 7.5MW and 10MW wind turbines
- Show the influence of the turbine with regard to the platform size.
- Compare the dynamic behavior of the two different semisubmersible floating platform designs and different sizes.
- Investigate the technical and economic feasibility of increasing the system´s rated power from 5MW to 7.5MW and 10MW.

1.4. Assumptions and boundary settings

For the simulation, as well as the cost comparison a number of assumptions, simplifications and restrictions are applied. Some are chosen due to the time-limitations of this work, other to ensure the validity of the model.

1.4.1. Assumptions

The FOWT-system consists of 3 major parts: „the floating platform, the wind turbine, and the mooring system" (Wayman, 2006). It is assumed that the wind turbine and the platform are one rigid body, neglecting bending motions in the tower, the blades and the platform. The rotational DOF of the drivetrain and the rotor-blades around the shaft is permitted, as well as the ability of pitching the blades for controlling the rotational speed at high wind speeds. The internal stresses are not considered in this work either, as the focus lies on testing the overall dynamic stability behavior of the system and not on testing the structural solidity. The three translational modes (surge, sway and heave) along the axis and rotational modes (roll, pitch and yaw) around the axis of the whole system are of main interest. The coordination system is located at the center of gravity for the x- and y-axis, as visualized in Figure 1-3 and z equals 0 at the calm water surface.

The mooring was chosen to be identical to the 5MW-system of the OC4-project, in order to allow a better comparability between the different platform sizes and designs. The only change is made to the radius at which the mooring lines are attached to the platform. In reality the anchor point radius and mooring line thickness would be increased. As the applying forces on the anchors and connection points (fairleads) on the platform are calculated, conclusions on necessary adaption of the mooring system can be drawn. This has an influence on the costs.

The water depth of 200 m is chosen for all simulations as it was examined in the OC4 project and a mooring design was thus readily available.

The steel wall thickness of all platforms´ offset columns is assumed to be 60mm, as in the OC4-5MW-platform. The same applies to the main column and the crossbars and pontoons with 30mm and 17.5mm thickness, respectively. This thickness of 60mm is considered to be relatively high. A closer look at this issue is taken in chapter 3.2, in the context of the platform scaling.

In the simulation, the presence of currents is neglected. The waves` incident propagation direction is in positive x-direction with reference to the coordinate system presented in section 1.2.3.

1.4.2. Geographical and natural boundaries

FOWT are expected to be cost efficient for water depths greater than 50m (Roddier, Cermelli, Aubault, & Weinstein, 2010). If wind energy is to be harvested in areas where depths exceed 60m – (that is the maximum technically feasible depth for fixed bottom structures) – wind turbines on floating structures seem to be one of the most promising solutions. In the scope of this thesis, water depths between 60m and 200m are considered. The deployment at greater depths is feasible, but will most probably entail higher costs for the mooring and installation.

The main focus is placed on European waters, mainly the European Atlantic and North Sea. This limitation is important for infrastructure and cost consideration, concerning the distance to shore and availability of shipyards and harbors.

Wind speed

Most offshore wind farms in the North Sea, from planning to operational stage, are located in areas with mean wind speeds of at least 8m/s at 10m above Mean Sea level (MSL). To be able to compete economically with these bottom-fixed installations, only sites with mean wind speeds above 8m/s are considered. This prerequisite excludes the Baltic Sea from further consideration for the moment. In the Mediterranean Sea, only a few areas have the desired mean wind speeds. Those locations mainly lie off the French and Greek coast.

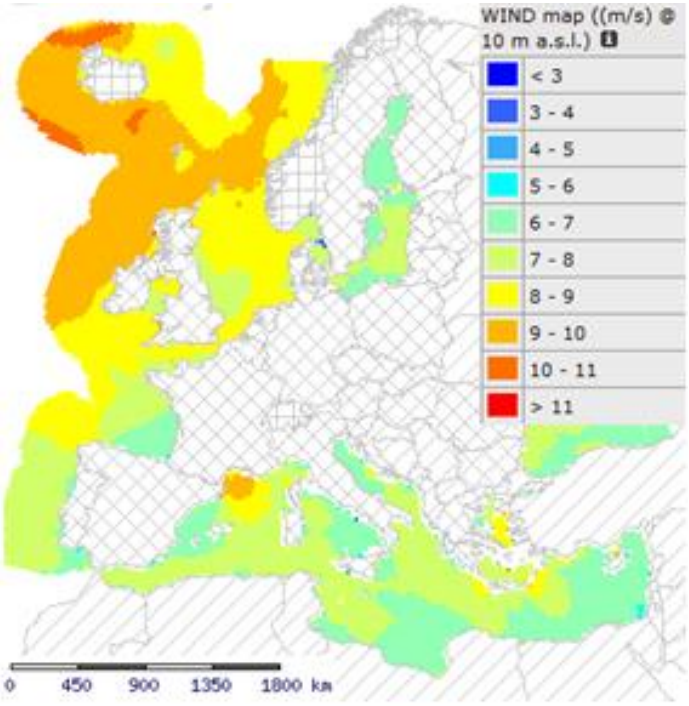

Figure 1-6 Mean wind speeds over European waters (based on (RSE, 2012))

Depth

Most areas of the North Sea have depths between 25 and 200m, with slightly deeper trenches of up to 500m depths along the Norwegian coast. The North Atlantic Ocean off the Irish, British and French coasts has the desirable depths between 60-200m, as visualized in cyan color in the map below.

The exclusive economic zones are marked by the orange/black solid lines. This shows that in particular France, Norway, the United Kingdom, the Republic of Ireland, Iceland and the Faroe Islands have privileged access to the most favorable water depths. This might be one reason for Norway´s state owned company Statoil to be one of the main drivers in the research field of FOWT.

As the waters in almost all of the Mediterranean Sea are deeper than 500m, this region is excluded from the scope of this thesis as well. Only water depths of 200m are analyzed due to time constraints. This does not imply that the deployment of floating wind turbines is unfeasible in the Mediterranean Sea.

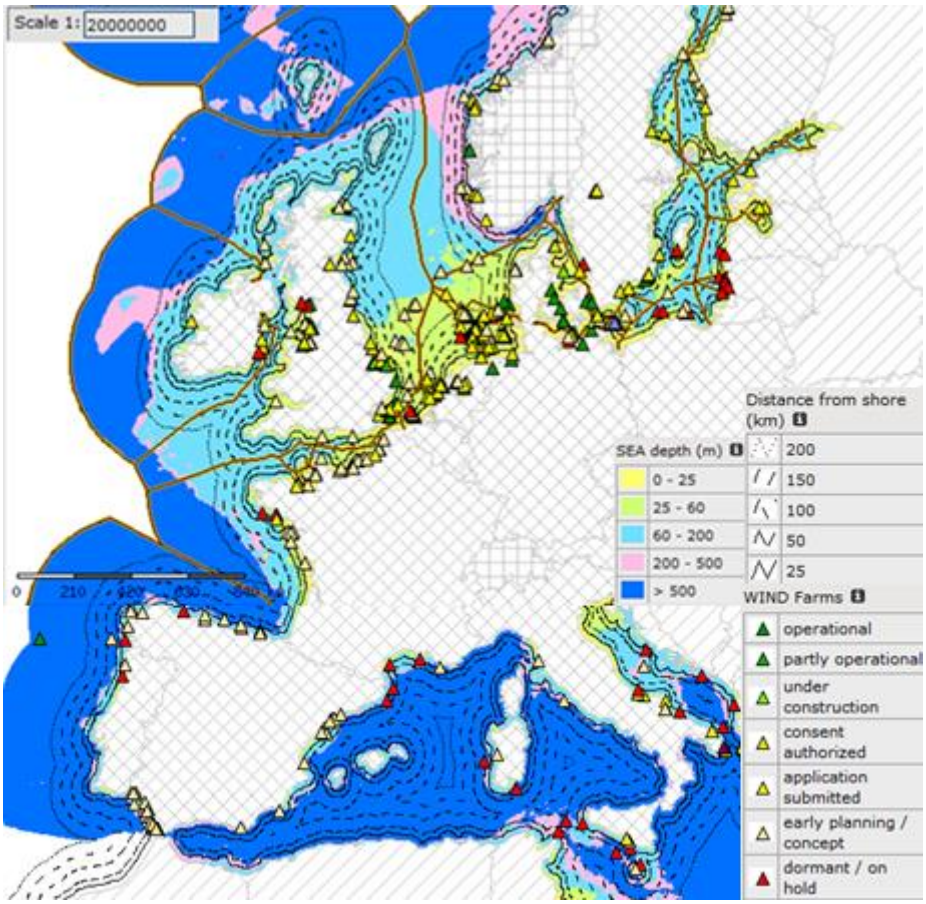

Figure 1-7 Sea depth of European waters (based on (RSE, 2012))

The triangular marks represent all offshore wind farms from conceptual to operational stage. They show that several projects are planned or under construction at around 300km offshore. Based upon on this fact, it is assumed that the costs for operation and maintenance (O&M), as well as connection costs, are within a reasonable scope for a maximum distance to shore of 300km. Information is retrieved and maps are created with the WebGIS (Geographic Information System) software ORECCA by Ricerca sul Sistema Energetico (RSE, 2012).

2. Wind turbines used for the simulation

Upwind, 3 bladed, horizontal axis turbines are the predominant design in the multi megawatt range of wind turbines. Some manufacturers have introduced the direct drive system, most notably Siemens (4COffshore, 2014a). In this case, the rotor and the generator are on one shaft without a gearbox. Other producers use gearboxes even for large designs. All wind turbines presented in the following chapter are specially designed for offshore application. The three wind turbine sizes of 5MW, 7.5MW and 10MW are examined for feasibility of installation on semi-submersible floating platforms. These sizes´ power ratings represent the current and near-future standards in the offshore wind sector, as previously presented. The input files for the description of the turbines in FAST are available in the appendix B.

2.1. The 5MW and 10MW Reference Wind turbines

Reference turbines were developed for research activities, allowing easier comparison with a standardized design. Since wind turbine manufacturers keep most data as a company secret, only reference turbines come with all the specific information needed for a meaningful simulation.

The following two designs are chosen because they are both published by internationally recognized research institutions and specifically designed for offshore cases.

2.1.1. NREL 5-MW Offshore Baseline Wind Turbine

The NWTC, under the umbrella of the NREL, published detailed specifications of the “NREL offshore 5-MW baseline wind turbine” (for short: “NREL 5MW OWT”) in 2006. The design is largely influenced by the “REpower 5M wind turbine”, which was the largest and most powerful turbine prototype at that point (Jonkman, Butterfield, Musial, & Scott, 2009). While the Repower 5M wind turbine is designed for onshore application, the NREL 5MW OWT is adjusted for offshore conditions in accordance with IEC 61400-3 design standards (IEC, 2005). The main “objective was to establish the detailed specifications of a large wind turbine that is representative of typical utility-scale land- and sea-based multi-megawatt turbines, and suitable for deployment in deep waters (Jonkman, Butterfield, Musial, & Scott, 2009).”

The tower height in the original design is dimensioned for an application onshore and at the MSL. For an offshore case on a (floating) platform the tower height is shortened by the same magnitude as the foot of the tower is elevated by the platform. The length of the tower is adjusted to ensure an operation at the designed hub-height. For example, since the center column of the platform in the OC4-project juts out by 10m, the NREL 5MW-OWT had to be shortened by this length. A direct comparison of all designs can be found in section 2.3.

2.1.2. DTU 10 MW Reference Wind Turbine

As the development in the wind power industry strives towards larger wind turbines the scientific community also needs a comparable standard for a 10MW wind turbine. The DTU 10MW Reference Wind Turbine (DTU 10MW RWT) was developed to serve this purpose. Other than the blades, the structural definition is mainly based on scaling the NREL 5MW turbine using classical similarity rules. The same is done for the platform scaling described later on in this thesis. Furthermore, the construction partly follows the design of the Vestas V-164 8MW, which is also included in the comparison at the end of this chapter. The mass of the nacelle and hub for example are based on scaling the values of the Vestas turbine. The development of the 10MW reference turbine started with the efforts to develop new rotor designs in the “Light Rotor project” (Bak, et al., 2013).

The tower design as presented in Bak, et al. (2013) only covers the details for a turbine based onshore. The tower development was an iterative process starting from the NREL design. Relative to the other dimensions the tower of the DTU 10MW RWT was made shorter than that of the NREL 5MW turbine. Its length has to be adjusted with regards to the type of platform being looked at. The procedure of adjusting the tower properties in accordance with the different platform designs for the purposes of this thesis is presented in the section below.
The DTU 10MW RWT is chosen for the simulations as it is a based on the NREL 5MW turbine, allowing a good comparability and its design is specifically adapted to operate in offshore conditions present in the North Sea.

Determining the tower properties

The tower characteristics of the onshore design have to be adjusted to fit on an application on the floating platform. First the length and mass of the shortened 10MW tower is calculated. Afterwards the properties of the 7.5MW tower result from interpolation between the 5MW and the 10MW design.

Two alternatives for defining the shortened tower of the 10MW turbine were considered. The first approach was to take the ratio of the tower masses from the shortened 5MW tower and the designed tower height and apply this factor to the mass of the 10 MW designed tower. The tower design of the 10MW differs from the 5MW reference turbine. In particular the mass distribution and mass per length data has changed. Therefore the results obtained from this method are slightly imprecise.

The second approach uses the height ratio instead of the masses, as the masses are defined relative to the length of the tower. This is the approach that was ultimately used to determine the masses.

$$h_{DTU\ 10MW\ tower\ (short)} = \frac{h_{NREL\ 5MW\ tower\ (short)}}{h_{NREL\ 5MW\ tower\ (design)}} * h_{DTU\ 10MW\ tower0\ (design)} \quad (1)$$

$$= \frac{77.6m}{87.6m} * 115.63m$$

$$= 102.5m$$

Thus, the bottom 12.5m of the tower is going to be removed. This corresponds to a mass of 107,588kg. This result is obtained by using the average cross-sectional area of the specified tower section, multiplied by its height and mass density. The values are obtained from the wall thickness distribution table in Bak, et al. (2013) and can also be found in the appendix. After doing this, the total mass of the shortened 10MW tower is 520,854kg.

The FAST simulations require a control strategy to initiate the appropriate response of the turbine to changing wind conditions, e.g. blade pitch or nacelle yaw. The control strategies for the 7.5MW and 10MW turbine were adapted from the NREL 5MW OWT, as available from the OC4-project.

2.2. The 7.5 MW Wind turbine

This thesis includes the evaluation of a FOWT with a rated power of 7.5MW. The benchmark for the next generation offshore wind turbines in terms of power rating is around 7.5MW. This makes a study of a 7.5MW FOWT being especially interesting. Such a study also contributes to a better understanding of the development of the economies of scale. As no data is publically available for this specific turbine size, the necessary data was obtained from the available information of the previously discussed NREL 5MW OWT and DTU 10MW RWT.

2.2.1. Methodology for scaling towards a 7.5 MW turbine

Most of the dimensions of the 7.5MW turbine resulted from linear interpolation between the 5MW and 10MW turbines discussed above. The total tower mass does not increase linearly but follows a slight logarithmic trend. The 7.5MW turbine tower properties result from linear interpolation of the tower heights and the tower mass density along the tower. The tower mass density expresses the mass per tower length [kg/m] and decreases from the bottom to the top. The values were interpolated based on the relative height fractions of the respective towers, as visualized in the figure below.

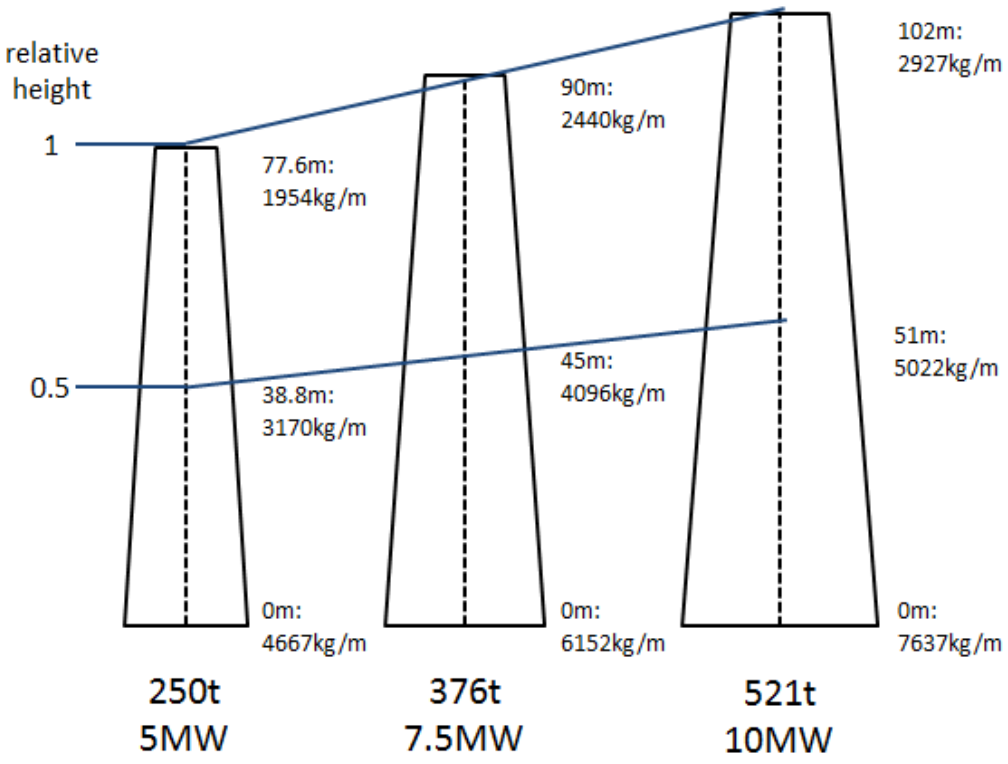

Figure 2-1 Scaling of the tower parameters

The blade geometry is taken from the DTU 10MW design. Relative to the rotor length the airfoil and blade twist are the same. Simulations in which the 10MW blade profile was used for the 5MW turbine showed that the consequent power curve is almost identical to the designed one. That means that either of the two airfoils can be used for the 7.5MW, without obtaining distorted results regarding the main objective – analyzing the dynamic response of the platform. The blade mass is determined according to the same methodology as the tower mass properties. The blade length is scaled according to the linear relation between swept area and power of a wind turbine. Consequently, the rated power is proportional to the squared scaling factor of the rotor length: $P \sim s^2$. The key parameters of the 7.5MW wind turbine are presented in the subsequent chapter. More details are included in the appendix.

2.3. Comparison and verification of all 3 turbines

This section aims to confirm the validity of the 5MW and 10MW reference turbines and, in particular, the 7.5MW design that was developed for this thesis. The most relevant characteristics for this comparison are the sizes and masses, as well as rated conditions of the different turbine designs. The commercially available wind turbines used in this verification represent a variety of well-established manufactures, namely Vestas, Siemens, Alstom and REpower system (now called Senvion). As those companies supply a large share of the market demand for on- and offshore installations, the validity of

the comparison is ensured. The wind turbines of the offshore market leader Siemens and Alstom´s Haliade 150-6MW are equipped with the direct drive mechanism. All other systems have a gear box coupling the rotor and the generator shaft.

The biggest deviations can be seen in the mass of the nacelles and rotors. For example the relatively light design of the Siemens SWT-6.0-154 results from the application of a direct drive generator. This turbine is also available in a slightly different configuration with a rotor diameter of just 126m, included in the table below.

Table 2-1 Comparison of commercial and scientific wind turbine designs

Turbine property	REpower 5M[1]	NREL 5MW OWT[2]	Alstom Haliade™ 150-6MW[3]	Siemens SWT-6.0-154[4]	7.5 MW Wind turbine[5]	V164-8.0 MW®[6]	DTU 10 MW RWT[7]
Rating	5MW	5MW	6MW	6MW	7.5MW	8MW	10MW
Rotor, Hub Diameter	126m, 3m	126m, 3m	150.95m, 3.95m	154m, 4m	154m, 4.3m	164m, 4m	178.3m, 5.6m
Hub Height	85m – 95m	90m	100m	120m onshore	104.5m	-	119
Cut-In, Rated, Cut-Out Wind Speed	3.5 m/s, 13 m/s, 30 m/s	3 m/s, 11.4 m/s, 25 m/s	3 m/s, -, 25 m/s	3 m/s, 12 m/s, 25 m/s	4m/s, 11.4m/s, 25m/s	4 m/s, 11 m/s, 25 m/s	4m/s, 11.4m/s, 25m/s
Cut-In, Rated Rotor Speed	7.7rpm 12.1rpm	6.9rpm, 12.1rpm	4rpm 11.5rpm	5rpm 11rpm	6rpm, 9,6rpm	4.8rpm 12.1rpm	6rpm, 9,6rpm
Rotor Mass	120t	110t	-	360t (rotor + nacelle)	169t	105t	228t
Nacelle Mass	290t	240t	400t		343t	390t	446t
Total mass (including tower)		599.7t			887.5t		1,194t

The tower length and related hub height heavily depends on the site chosen for installation. As a consequence, the tower and total mass might vary considerably. For that reason only, the total masses of the reference turbines used in this work are included in the table.

The tower of the NREL 5MW wind turbine was reduced by 10m compared with the tower length given in the turbine specification in Jonkman, Butterfield, Musial, & Scott (2009). This length accounts for the

[1] (REpower Systems SE, 2005)
[2] (Jonkman, Butterfield, Musial, & Scott, 2009)
[3] (Alstom, 2013b) & (Alstom, 2014)
[4] (4COffshore, 2014a)
[5] The 7.5MW specifications are developed for this thesis
[6] (Vries, 2013) & (4COffshore, 2014b)
[7] (Bak, et al., 2013)

10m elevation above MSL of the tower base due to the height of the platform. Since the turbine mass has essential influence on the platform size, it is important to adjust the tower length of the DTU 10MW RWT in an appropriate way.

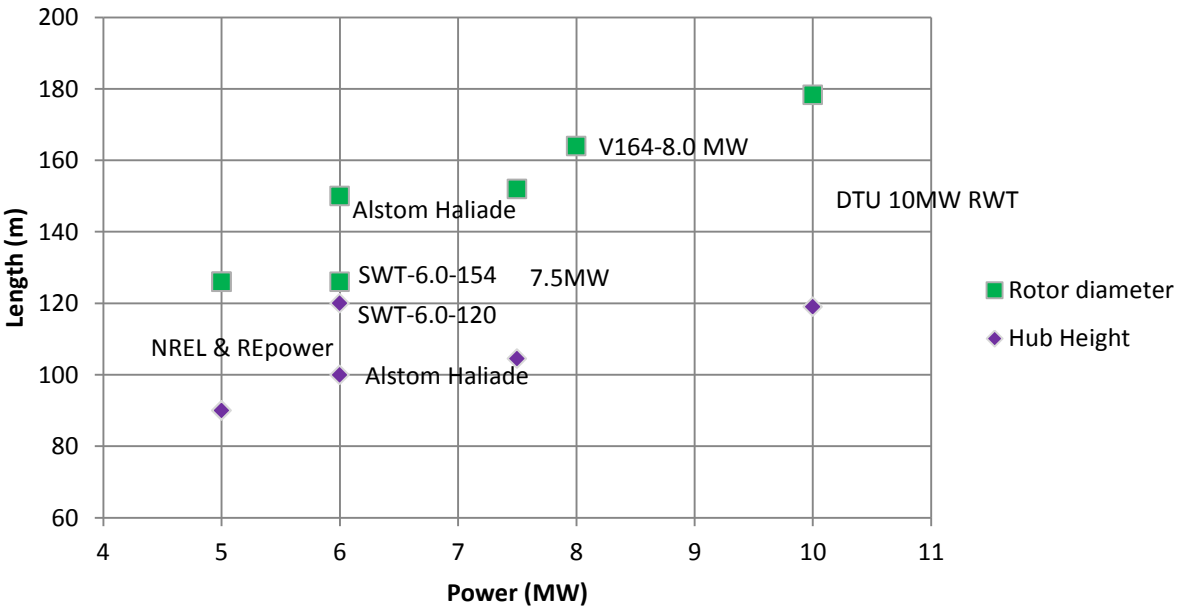

Figure 2-2 Relation between rotor diameter, hub height and rated power

Figure 2-2, depicted above, shows the rotor diameter and hub height for the different wind turbines and their respective power ratings from the previous comparison table. The commercially available turbines and the reference turbines both follow the same linear trend for each of the two comparison parameters. For these parameters the NREL 5MW OWT follows the specifications of the REpower 5M.

3. Scaling of the Platform

The main cost driver of a FOWT is the platform. In the WindFloat project, it accounted for 42% of the total costs (Maciel, 2010). The structural design has a decisive influence on the technical and economical feasibility of the system. The methodology of scaling the OC4-platform from supporting a 5MW wind turbine towards 7.5MW and 10MW turbines is thus one of the key aspects in this work. Two methods for adapting the platform's size to the additional load are examined in this work. In the first approach, the design and proportions of the 5MW DeepCWind-structure are maintained. Only its dimensions are changed to accomodate the higher masses and forces. In the second approach, the draft is limited to 20m. In the following, thsee designs are referred to as "Scaled" (S) and the "Reduced Draft" (RD), respectively. The second concept is investigated for 7.5MW and 10MW wind turbines, but not for the 5MW version. This is mainly because the trend in offshore installations clearly moves towards larger sizes, as demonstrated above.

3.1. Methodology for the platform up-scaling

The most important consideration in scaling the floating platform is ensuring its buoyancy. A superstructure (and thus a wind turbine) with higher mass, requires a larger water displacement and thereby a larger volume for the support structure. Thus the exact mass of the nacelle, rotor and tower has to be determined for both platform designs. The 10MW wind turbine developed by DTU is designed for offshore conditions, but with a tower to be placed onshore or at MSL. Therefore the tower length and mass has to be adjusted similar to how it was with the NREL 5MW OWT-tower for the OC4-project. This procedure was explained in chapter 2.

3.1.1. Model 1: Scaling all platform´s dimensions by a mass-depending factor

The same geometry that is used for the OC4-5MW platform (presented in section 1.2.3) is used for this scaling approach. All dimensions are enlarged by the same factor, in order to realize the higher displacement that is needed to carry the increased mass of the larger turbine. The factor by which all dimensions are increased is referred to as the scaling factor *s*. According to basic geometry the scaling factor *s* is proportional to the cubic root of the increase in mass as a result of the weight and buoyancy balance of the platform.

$$s \sim \sqrt[3]{m} \tag{2}$$

The platforms created following this direct scaling method are referred to as 7.5MW-**S** and 10MW-**S** in the remainder of this thesis.

As the 10MW wind turbine is twice as heavy as the 5MW turbine, s equals 1.26.

$$\sqrt[3]{2} = 1.26 \tag{3}$$

The mass of the 7.5MW turbine increases by slightly less than 1.5. This is mainly due to the fact that the tower mass does not result from linear interpolation of the absolute masses, but rather from the interpolation of the mass per length tables. As a result, the scaling factor *s* for the platform supporting the 7.5MW turbine is 1.13.

$$\sqrt[3]{1.46} = 1.13 \tag{4}$$

As the wall thickness is kept constant, the relative mass of the platform compared to the wind turbine mass is smaller. Therefore the 10MW platform is more buoyant than the 5MW design. The reason for not choosing a slightly smaller platform is to ensure its stability in the direction of the other degrees of freedom. The location of the CM as well as the pre-defined draft is tuned by adjusting the ballast water in the lower and upper cylinders of the offset columns. The overall dimensions of the platforms are presented in chapter 3.3.

3.1.2. Model 2: Scaling the platform while keeping a constant draft

This second method is evaluated to ensure that one of the elementary advantages over other FOWT-structures – complete construction on land or in the dry dock – can be maintained. The infrastructural conditions of European port facilities are presented in chapter 4.2. The draft is important for fitting the semi-submersible support structure into harbors and allowing the assembly of the whole system in shipyards. This platform type will be referred to as the “reduced draft”-design, or 7.5MW-**RD** and 10MW-**RD**. The center of mass is kept at the same position as in the 5MW design. The spacing between the offset columns is identical to the respective scaled platform model. Table 3-1 displays these relations.

Methodology

The numerical values used in this methodology description are for the 10MW-case.

The total displacement should be equal to that of the scaled version, which is 27295m^3. By subtracting the displaced volume of the main column and neglecting the pontoons and cross bars, the total needed volume for each of the offset columns is 8746m^3. A number of additional boundary conditions

are chosen to ensure sensible geometrical relations. These relations are the same in the 5MW design and are listed and visualized below.

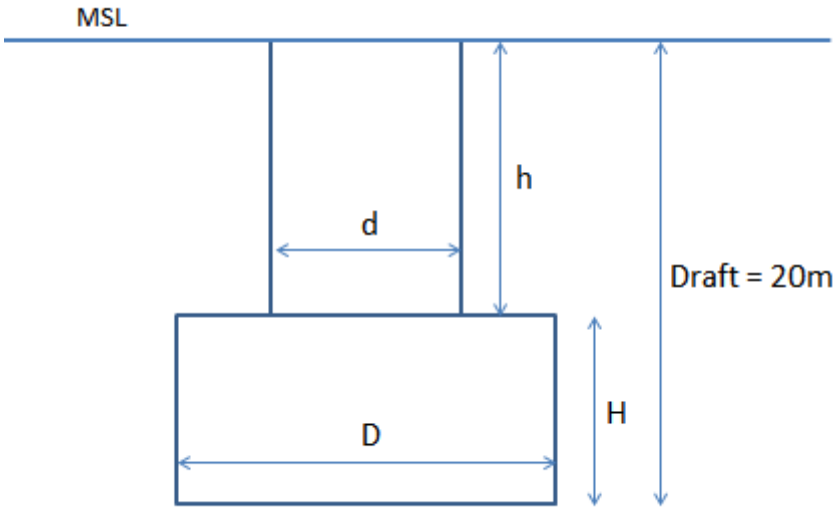

Figure 3-1 Cross sectional view of the submerged offset column

The figure shows the submerged part of the offset column.

- The diameter of the base (or heave plate) D is twice the diameter of the top column d

$$D = 2d \tag{5}$$

- The base height H is a quarter of its diameter D

$$\frac{H}{D} = \frac{1}{4} \rightarrow H = \frac{d}{2} \tag{6}$$

- Consequently, the height of the upper column is equal to the difference between the maximum draft of 20m and the base height H.

$$h = Draft - H \rightarrow h = 20 - \frac{d}{2} \tag{7}$$

The following figure shows a direct comparison of the scaled and the reduced draft design to support the DTU 10MW RWT turbine. The reduced draft design, depicted in transparent green, has a higher heave plate H, and an increased diameter of the upper and lower column, d and D respectively.

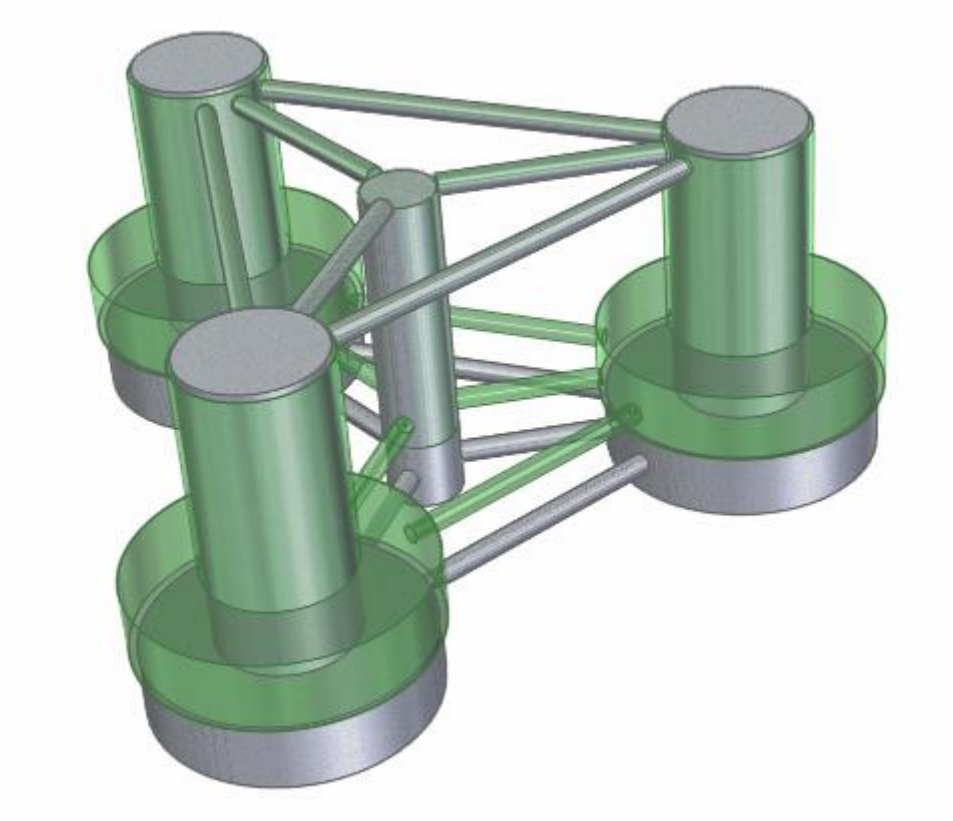

Figure 3-2 CAD-model of the 10MW S (grey) and the 10MW RD (green) design

In summary the main difference between the scaled and the reduced draft design lies in the geometry of the offset columns. The offset columns' relative position to each other and to the main column in the center of the platform stays unchanged for the respective power rating of the system. The diameter of the main column of the reduced draft and scaled platforms stays the same for the particular turbine size, as it has to fit the tower dimensions of the wind turbine. The diameters of the cross-bars and pontoons, connecting the main column with the offset columns, are taken from the scaled platform specifications.

Designing new offset column geometry changes not only the draft, but also the total mass of steel. The reduced draft design is a little lighter and will thereby lead to slightly reduced material costs. The overall weight is still kept constant by adjusting the amount of ballast water. Hence, the displaced volume of the whole FOWT stays the same when comparing both scaled versions of the 7.5MW and 10MW system.

3.2. Uncertainty regarding the wall thickness

There are several alternatives to be considered in determining the wall thickness. In this work the same steel wall thicknesses of the 5MW-DeepCWind system are used for the larger platforms as well. Instead of thicker walls, additional stiffeners could be used to prevent the buckling of the walls. The

bottom plates of the heave plates especially should be equipped with braces. The large dimensions of the cylinder walls might also demand additional structural support by reinforcing ribs for example. The steel wall thickness in the works of Wayman (2006) and Crozier (2011), investigating TLPs, is set to 15mm. However, Crozier (2011) argues that this thickness will not be sufficient for the main cylinder of the particular designs without further stiffening. The wall thickness and thus the total amount of steel needed, have a major impact on the costs. The biggest part of the platform's construction costs comes from the material expenses. The applied wall thickness is expected to be over-dimensioned. If a thinner wall is chosen, a similar total weight, draft and CM could be realized by increasing the amount of ballast water or other ballast material, such as concrete.

3.3. Final dimensions of the platforms

The following table gives an overview of the key dimensions of the platforms. Furthermore, it summarizes the similarities and differences between the platform designs. The paragraph and figure thereafter contribute to a better understanding of the table. Technical drawings showing the dimensions of all designs are included in the appendix C. Only the 5MW model is excluded as it is specified in Robertson (2013b).

Table 3-1 Significant parameters of the five evaluated platform configurations

		5 MW	7.5 MW		10 MW	
		DeepCWind-Design	Scaled (s=1.13)	Reduced Draft	Scaled (s=1.26)	Reduced Draft
Total draft [m]		20	22.61	20	25.21	20
Spacing between offset columns [m] (center to center)		50.00	56.52	56.52	63.04	63.04
Center of mass below SWL [m]		13.46	15.21	13.46	16.97	13.46
Minimum platform width [m]		67.30	76.08	77.54	84.85	86.45
mass of steel [t]		3`852	4`659	4`547	5`796	5`575
Total mass [t] (incl. ballast water)		13`437	19`403	19`403	26`988	26`988
Mass moments of inertia around CM	Pitch/Roll [kg*m^2]	6.8E+09	1.2E+10	1.3E+10	2.0E+010	2.0E+10
	Yaw [kg*m^2]	1.2E+10	2.2E+10	2.2E+10	3.6E+010	3.8E+10

The total draft of the scaled platforms corresponds to the value of the 5MW-DeepCWind structure times the corresponding scaling factor s. The spacing between the offset columns is measured from the center of one column to the center of the other. It is derived for the scaled platform in the same way, just by multiplying by *s*. This value was also taken for the reduced draft design of the corresponding size. The position of the center of mass is kept at the same relative distance to the draft

as in the 5MW design. The width of the platform (in addition to the draft) puts a limitation on suitable dry docks. It is a result of the spacing between the offset columns. The mass of steel of the reduced platform is slightly lower than that of its scaled counterpart. The total weight is designed to be the same or the scaled and the reduced draft design. The total mass is derived from the 5MW-platform by applying the particular scaling factor. The mass moments of inertia are a necessary input for the FAST simulations. They were derived from CAD-models in Solid Edge, based on the fully ballasted and trimmed platforms.

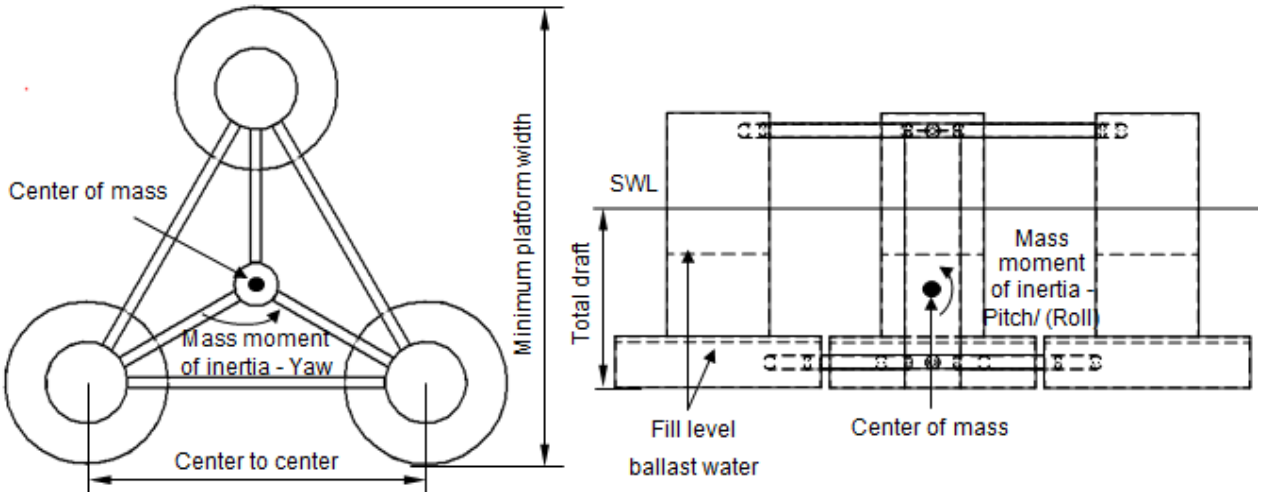

Figure 3-3 schematic top and side view of the semi-submersible platform

A comparison of some platform key dimensions between the 5MW initial design, the 10MW scaled and the 5-10MW WindFloat is presented in Table 3-2. Most dimensions of the WindFloat platform, which was designed to support a 5MW to 10MW wind turbine, are between the 5MW structure of the DeepCWind project and its 10MW up-scaled version. However, due to the reduced column diameter of the WindFloat design compared with the two others, its overall volume, and consequently the buoyancy, is smaller. This has the consequence that the platform itself has to be lighter, meaning that less steel is used. Thus the wall thickness of the offset columns is most likely far less than the 60mm of the WindFloat structure.

Table 3-2 Comparison between the DeepCWind and WindFloat design

	DeepCWind 5 MW	DeepCWind 10 MW (x1.261)	WindFloat 5 - 10 MW
Platform dimensions	**Length [m]**	**Length [m]**	**Length [m]**
Depth of platform base below SWL (total draft)	20	25.2	22.9
Elevation of wind turbine tower base above SWL	10	12.6	10.7
Spacing between offset columns	50	63.0	56.4
total length offset column	32	40.3	33.6
Diameter of offset (upper) columns	12	15.1	10.7
Diameter of base columns / heave plate	24	30.3	38.1
Diameter of pontoons	1.6	2.0	1.8
Diameter of cross braces	1.6	2.0	1.2

3.4. The platform model in FAST and additional inputs

As the focus of this thesis is platform design and behavior, the modeling of the systems' hydrostatic- and dynamic behavior in FAST is presented in detail in this section. As with the wind turbine, all FAST input files can be found in the appendix.

Through Solid Edge generated CAD-models, several platform characteristics are evaluated. These values are the steel mass, mass moments of inertia and the amount and distribution of the ballast water. The trim compensation is adjusted to the center of mass and designed total weight. The mass, mass moments of inertia and CM are needed for the ElastoDyn module of FAST. The ElastoDyn module determines the structural dynamics of the FOWT-system.

3.4.1. Modeling of the platform elements' geometries in HydroDyn

Earlier FAST codes allowed the simulations of single cylinder platform shapes (e.g. the spar buoy) only. If the viscous drag effect of only one column is modeled, the system damping is underestimated. This was also shown when results from FAST and wave tank tests were compared. The main drag and damping of the DeepCWind-floating structure is due to the geometry of the offset columns and especially the heave plates. Additionally to the WAMIT results, more inputs are needed to achieve a realistic response of the floating structure in simulations. These additional damping and drag coefficients are set in the "Floating platform additional stiffness and damping"-matrices of the HydroDyn file for all six DOF. The entries were calibrated "such that the FAST simulations matched the damped behavior of the systems during the free-decay tests" (Masciola, et al., 2013). The diagonal entries of the Additional quadratic drag matrix in the HydroDyn file are shown for the 5MW platform design from the OC4 in Table 3-3. This approach was chosen for the OC4-simulations with FAST 7.

As the platform used in the OC4-project marks the starting point for the simulations presented hereinafter, this methodology is chosen for this work as well.

Please see Robertson A., et al. (2013b) for a detailed description of the DeepCWind-platform-components and the appendix for the HydroDyn input file, containing the model descriptions.

Table 3-3 Quadratic drag coefficients ($B_{ZZ,Visc,5MW}$) for the FAST model of the 5MW DeepCwind platform, after (Robertson A. , et al., 2013b)

Surge	**Sway**	**Heave**	**Roll**	**Pitch**	**Yaw**
Ns^2/m^2	Ns^2/m^2	Ns^2/m^2	Nms^2/rad^2	Nms^2/rad^2	Nms^2/rad^2
3.95E+5	3.95E+5	3.88E+6	3.70E+10	3.70E+10	4.08E+9

The subscripted characters Z define the matrix position of the value. The quadratic drag coefficients are the same for surge and sway, as well as roll and pitch motion, as the platform geometry is the same looking along the x and y-axis.

$$\begin{pmatrix} B_{11,Visc} & \cdots & 0 \\ \vdots & \ddots & \vdots \\ 0 & \cdots & B_{66,Visc} \end{pmatrix}$$

The diagonal entries of the quadratic drag matrix are the previously defined values. All off-diagonal entries are equal to zero.

FAST 8 features an alternative and more elaborate way to estimate viscous drag over the column. However, due to a lack of documentation and information on the topic, this work uses the same method than in FAST7's model of DeepCWIind.

3.4.2. Scaling of the additional quadratic drag matrix

A simplified platform model together with an adjusted quadratic drag matrix is used in the simulations for this thesis. As much of the platforms hydrodynamic behavior in the simulations can be ascribed to this matrix, it is important to choose an appropriate way of scaling it, starting from the values presented for the 5MW DeepCWind design used in the OC4. The procedure for calibrating the quadratic drag factors for linear and rotational motions is presented in the following paragraphs.

Translational displacements

For the up-scaled models, an adjustment of the given values is necessary. The viscous damping for linear motions, namely heave, surge and sway, is calculated according to the equation shown below (Cozijn, Uittenbogaard, & Brake, 2005). It represents the same translational factors as presented in table 3-3 above, multiplied by the velocity in the particular direction.

$$B_{ZZ,Visc} = \frac{4}{3\pi} * \rho * C_D * \mathrm{A} * \omega * z_a \quad (8)$$

In equation 8 above, ρ and C_D represent the water density and non-dimensional drag coefficient, A is the cross-sectional area, ω and z_a represent typical values of the frequency and amplitude of the particular motion. The value C_D is identical for the same geometry for a sufficiently high Reynolds number. The only variable that changes for a platform with different dimensions is the cross sectional area A. For the heave motion, A is equal to the area of the heave plates only, as seen along the z-axis. Since A changes proportionally to the square of the applied scaling factor, the values of the quadratic drag for linear motions for the scaled version also changes with this factor.

$$A \sim s^2 \rightarrow B_{ZZ,Visc,upscale} \sim s^2 \quad (9)$$

The same approach is chosen to determine the entries of the quadratic drag matrix for the platforms with reduced draft. However, not all dimensions are increased by the same scaling factor. To obtain the additional quadratic drag values here, the change of the cross sectional areas is looked at. As an example, the procedure for obtaining the quadratic viscous drag coefficient for the heave motion of the 10MW-reduced draft platform is shown.

$$B_{33,Visc,10MW-RD} = B_{33,Visc,5MW} * \frac{A_{Heaveplate,10MW-RD}}{A_{Heaveplate,5MW}} = 3.88 * 10^6 * 1.762 = 6.84 * 10^6 \quad (10)$$

An overview of the results for the scaling of the quadratic drag coefficients for linear motions is given in the following table.

Table 3-4 Quadratic drag coefficients of the linear modes (S – scaled, RD – reduced draft)

	Heave				**Surge/Sway**			
Platform design	7.5MW -S	7.5MW -RD	10MW -S	10MW - RD	7.5MW - S	7.5MW -RD	10MW -S	10MW -RD
Factor multiplied by $B_{ZZ,Visc,5MW}$	1.277	1.42	1.589	1.762	1.277	1.244	1.589	1.45
$B_{ZZ,Visc}$ [Ns²/m²]	4.95E+6	5.51E+6	6.17E+6	6.84E+6	5.04E+5	4.91E+5	6.28E+5	5.73E+5

Rotational displacements

The viscous damping for rotational motion, namely pitch, roll and yaw, is calculated according to the equation shown below (Cozijn, Uittenbogaard, & Brake, 2005). It represents the same rotational displacement factors as presented in table 3-3 above, multiplied by the velocity in the particular direction.

$$B_{\theta\theta,Visc} = \left(\frac{4}{3\pi}\right)^2 * \rho * C_D * \mathrm{A} * \mathrm{R}^3 * \omega * \theta_a \tag{11}$$

The radius R defines the location at which the local drag loads is assumed to apply and $\theta_a$the angle of the rotational motion. Increasing the dimensions by the factor s, changes the values of the area and the radius in formula 11. As explained for the linear motion, the area A increases proportionally to the square of the applied scaling factor. The radius increases linearly by the factor s, but is cubed in the previous formula.

$$(A * R^3) \sim s^5 \rightarrow B_{ZZ,Visc,upscale} \sim s^5 \tag{12}$$

As a result the quadratic drag coefficient for rotational motions is proportional to the applied scaling factor to the power of five, for the scaled platform design.

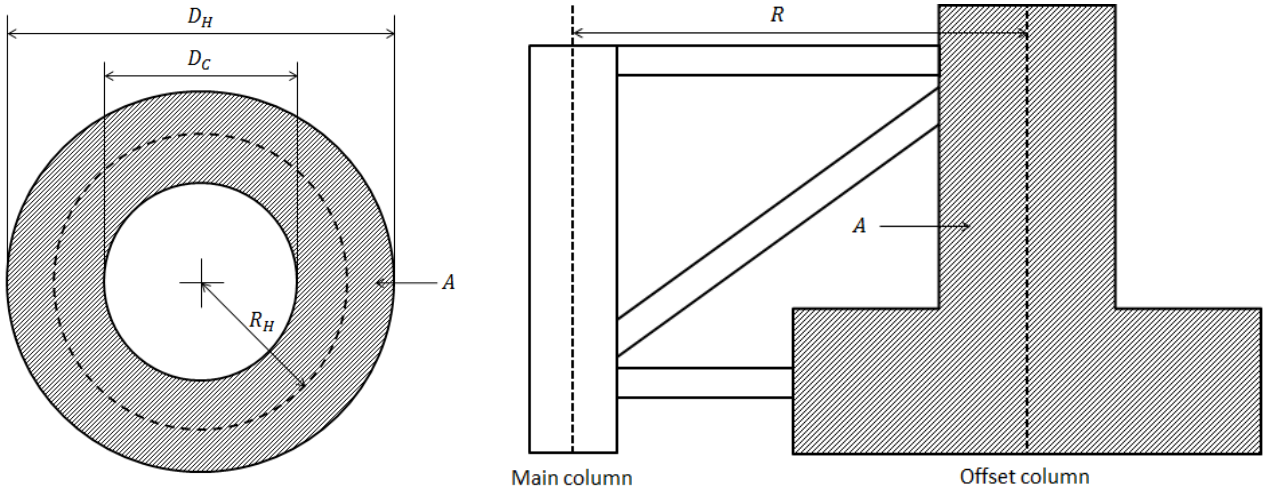

Figure 3-4 left: top view on offset column, based on Cozijn, Uittenbogaard, & Brake (2005)
right: side view on a part of the platform's cross section (not to scale)

The heave plate area is larger for the reduced draft design than for its scaled counterpart. In contrast, the cross sectional area of the offset column of the scaled version is larger than that of the reduced draft version. The quadratic drag coefficients for the reduced draft design are obtained by looking at the relative change of the cross-sectional areas.

Table 3-5 Quadratic drag coefficients for rotational modes

	Roll/Pitch				Yaw			
Platform design	7.5MW -S	7.5MW -RD	10MW -S	10MW - RD	7.5MW - S	7.5MW -RD	10MW -S	10MW -RD
Factor multiplied by $B_{ZZ,Visc,5MW}$	1.733	2.194	2.829	3.577	1.733	1.796	2.829	3.236
$B_{ZZ,Visc}$ [Nms^2/rad^2]	6.41 E+10	8.12 E+10	1.05 E+11	1.32 E+11	7.07E+9	7.33E+9	1.15E+10	1.32E+10

The influence of the choice of the particular adjustment of the quadratic drag coefficients can be seen in Figure 3-5. This underlines the high importance of selecting a reasonable approach for modifying the quadratic drag matrix to assure comparability between the results of the 5MW and 10 MW platforms. This is especially true, as the stability in pitch is one of the most critical performance indicators.

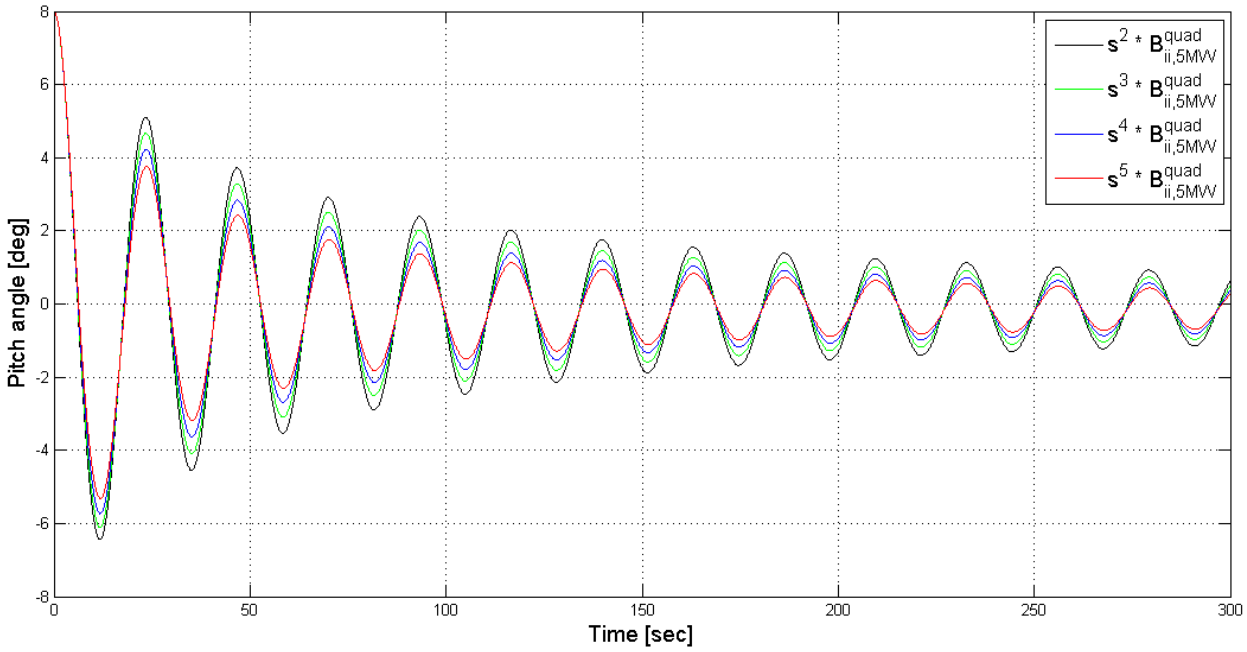

Figure 3-5: Restoring from initial pitch for different quadratic drag coefficients

3.4.3. The mooring system

The catenary mooring system designed for the 5MW OC4 project is used for all platforms in the simulations. This is a simplification to ensure better comparability between the different floating structures. Otherwise, differences in the platform's response to excitation forces could be due to the moorings. The only parameter that changes is the radius of the fairleads on the platform at which the mooring lines are connected. The fairlead radii are 40m for the 5MW design, 45.75m for both 7.5MW designs and 50.5m both 10MW designs. These radii are based on the specific scaling factor used for each platform. The stability against pitch is higher if the mooring lines are installed as far away from the platform center as possible.
Three mooring lines are used to fix the FOWT to its desired position. One is installed in positive x-direction. The other two are positioned symmetrically in a 120° angle to each other. The ground distance between platform and anchor is 837.5m. The properties are uniform along the whole mooring line. In reality they are a combination of chains, steel cables and synthetic fiber ropes (Duarte, 2014).

The actual needed mooring strength

Even though being neglected in this work, the required mooring chain diameter and corresponding mass per meter is presented in the following. The calculation is based on the maximum force applying on the fairlead as calculated in chapter 4.1.3 for 50-year storm conditions. By applying a safety factor of two, the break load of the mooring is determined. Corresponding to this value, the diameter and weight can be found according to the American Petroleum Institute (API)-regulations from the "Studless Chain Loads"-table of Vicinay Cadenas (Vicinay Cadenas, S.A., 2011).

Table 3-6 Suggested mooring diameter and weight

	5MW-OC4	5MW	7.5MW-S	7.5MW-RD	10MW-S	10MW-RD
Diameter [mm]	76.6	70	76	81	95	107
Weight [kg/m]	113.35	98	116	131	181	229

The mooring line parameters of the OC4-project, which are presented as "5MW-OC4" in the table above, are used for all platforms in this thesis. The deviation to the "5MW" results might be caused by the slightly different settings for the 50-year storm event.

4. Simulation and evaluation criteria

Several factors have an influence on the technical feasibility and competitiveness of FOWT. On one hand, a certain stability of the whole system under the influence of applying loads is required. On the other hand the efforts for construction, transportation, installation and operation and maintenance play an important factor. These two aspects are considered in this chapter. The focus is set on the evaluation of the platform's dynamic behavior while being exposed to environmental loads.

4.1. First order criteria: dynamic behavior of the platform

The results presented in this chapter are based on fully coupled dynamic models of the previously defined platforms. A variety of load cases are simulated with FAST 8 in the time domain. The complexity of the external natural impacts is increased steadily. As time and computer resources are limited, approximations are made in some aspects of the simulations. Waves are defined in one direction along the x-axis only. The wind inflow is mainly directed along the same axis. The presence of currents is neglected. Fatigue, lifetime evaluations and structural studies go beyond the scope of this work. The performance analysis is based on a time- and frequency domain analysis, as proposed in the guideline by the American Bureau of Shipping (ABS, 2013).

The most critical offset for FOWT is in pitch. The critical offset value of the system in pitch is at a five and ten degree angle for the mean and maximum angle respectively (Duarte, 2014). The crucial point is not the danger of capsizing, but that the turbine has to shut down for safety reasons if the ten degree angle is exceeded. There is the risk that the blades hit the tower in their rotational movement. The pitch intensifies the blades' bending, caused by the gravitational force and the wind induced thrust. This worst-case scenario could lead to the destruction of the floating wind turbine system, despite the fact that the rotor shaft has a predefined, upwards-directed tilt angle and the clearance between tower and blades is several meters. Even though this danger can be eliminated through a number of measures to shut down the wind turbine, the pitch angle should be reduced to minimum possible value. As soon as the rotor blades are out of designed position, the efficiency and performance of the turbine deteriorates. Furthermore, the undesired loading on the blades due to an unwanted angle of attack might cause structural problems.

Another important performance indicator for the evaluation of the dynamic platform performance is the nacelle acceleration, which is elaborated on in the end of section 4.1.3.

4.1.1. Hydrostatic stability and natural frequency

Before testing the impact of the forces of nature on the system, a number of tests are run to review the platform's response in recovering from an initial offset to the designed equilibrium position. These simulations are run without wind or waves. More specifically, the air density is set to 0. All aerodynamic components are thereby filtered out. Furthermore, free decay tests are run to determine the natural periods and natural frequencies for all platforms DoF. A simulation time of 900sec is chosen, as this time is considered to be sufficient for identifying the trends and discerning the equilibrium value at which the platform should level out. The motions of all system components apart from the platform motions are suppressed for this first set of simulations.

Buoyancy

As the wall-thickness for both up-scaled models is kept constant, the ratio between the platform's deadweight and its volume decrease for larger platform dimensions. The ballast water is adjusted to match the designed draft and CM of every platform configuration. The first FAST simulations serve to validate the trimming and the integrity of the inputs. In its equilibrium position no motions should be noticeable for the six DoF of the support structure.

Free decay

To verify if and how the floating structures restore to the equilibrium position, free decay tests are run. These tests provide the first data to compare the restoring ability of the different systems and the intensity of the damping. The free decay tests are of special meaning for determining the natural periods and, in this way, the natural frequencies. These are important for the subsequent frequency domain analysis. Resonant behavior occurs if the natural frequency of a system and the induced frequency due to external loads coincide. The resonance leads to high amplitudes for the system´s response. The external loads here are wind and waves. A separate free decay test is run for each and every platform motion. As the results in surge and sway as well in pitch and roll motion are almost identical, not all graphs are pictured.

Surge

The restoration from an initial displacement along the x-axis of the system of 14m shows similar results for FOWTs with the same rated power. Furthermore, the 5MW and 7.5MW systems' damping is alike. The 10MW systems have less damping. This is depicted in the relatively higher amplitudes of the green and blue lines compared to the other ones. This means that it takes a longer time for the large floating structures to reach their idle or equilibrium position. The frequencies lower as the floating systems increase in size and weight, due to greater inertia. The minor difference between the peak amplitudes of the RD and S-design is due to the differing cross sectional area of the offset column in the two models.

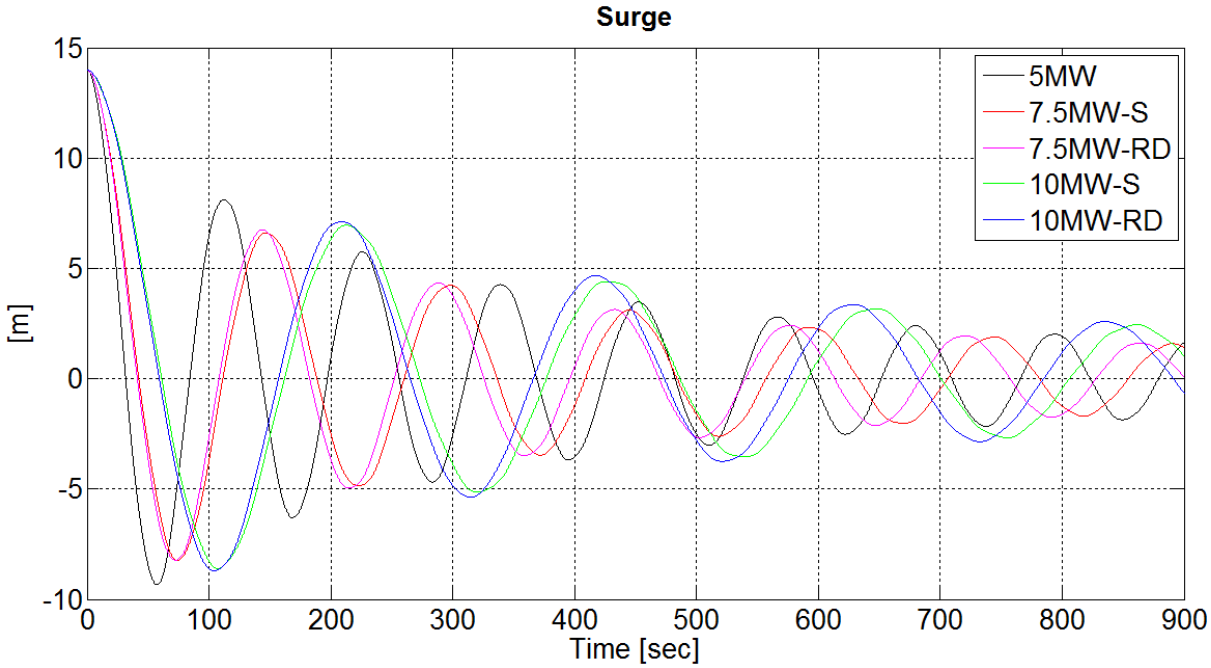

Figure 4-1 PSD-plot of Surge motion for free Decay load case

Nevertheless, the surge free decay tests are invalid for drawing conclusions regarding the stability characteristics of the different platforms, because the restoring from surge depends on the mooring to a significant degree. Furthermore, the viscous forces over the platform are approximated in this model.

Heave

Compared with surge, the differences between the amplitudes in heave motion lie in a smaller range. Moreover the damping of all systems is much higher compared to the surge decay test. This can primarily be explained by the plane shape of heave plates along the z-axis, which causes much more drag than the lateral cylinder shape of the structure. Additionally, the gravitational and buoyant forces apply along the same axis as the heave.

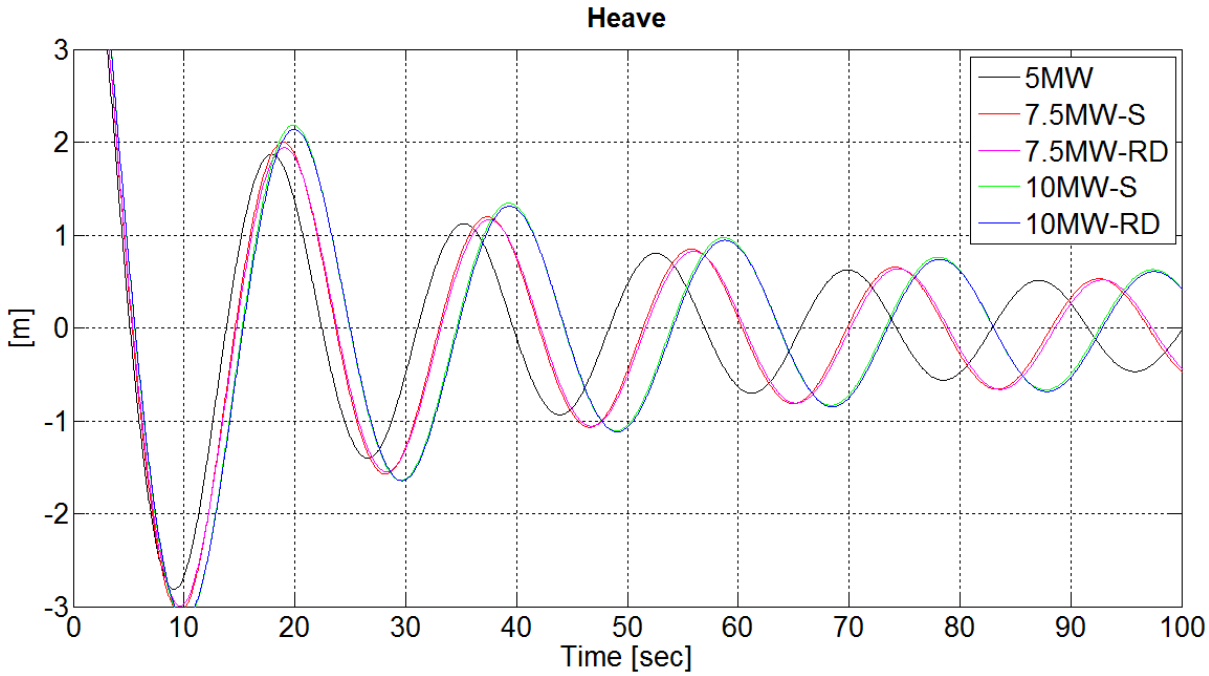

Figure 4-2 PSD-plot of Heave motion for free Decay load case

Although the differences are small, the graph shows decreasing frequencies and increasing amplitudes for larger system sizes. This means that the natural frequency of larger systems is lower and it has reduced damping characteristics compared to the smaller models.
The comparison of the scaled and the reduced platform designs reveals a slightly better restoring from heave of the RD-platforms. This is due to the larger heave plate area.

Pitch

The results of the restoring from an initial pitch of 8 degrees show better behavior from the RD-design than from the S-design. The 7.5MW-RD system experiences the most damping. The 10MW-S platform has the worst damping characteristics.

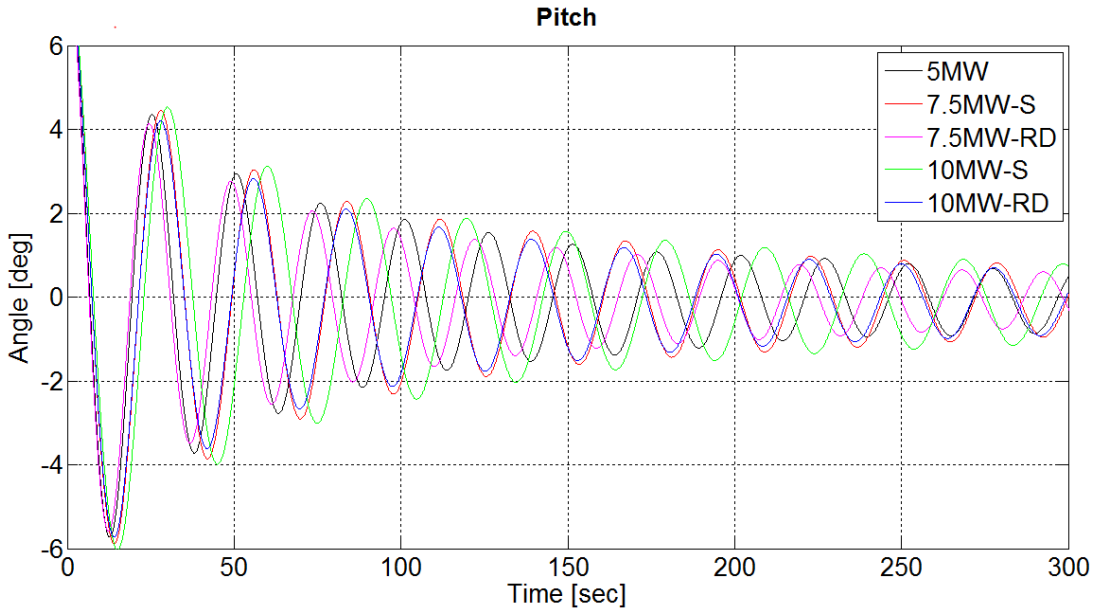

Figure 4-3 PSD-plot of Pitch motion for free Decay load case

Yaw

The yaw response after the 8 degree offset is very similar for systems with the same power rating. The smaller the platforms are, the greater the damping is.

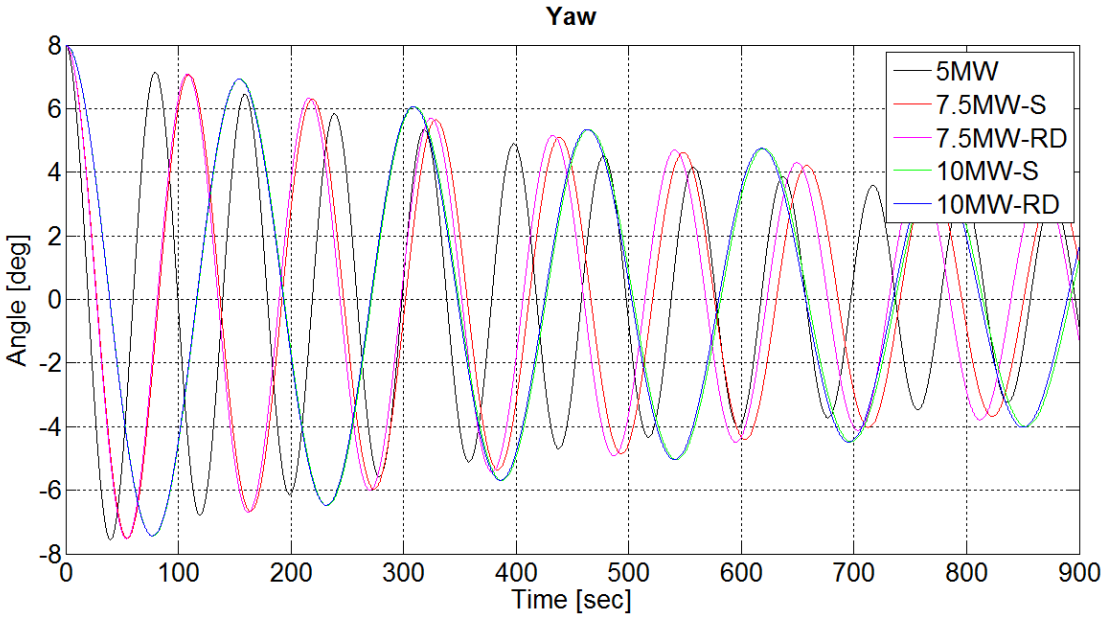

Figure 4-4 PSD-plot of Surge motion for free Decay load case

Fehler! Verweisquelle konnte nicht gefunden werden. and Table 4-2 show the natural periods and natural frequencies, respectively. These are extracted from the free decay tests. Pitch and roll, as well as surge and sway, have almost identical natural frequencies. They only differ to a minor degree through different relative angles of the mooring, which is negligible.

Table 4-1 Natural periods of the different platform designs

Mode	5MW	7.5MW-S	7.5MW-RD	10MW-S	10MW-RD
Surge	113	144	145	212	206
Heave	18	19	19	20	19
Pitch	26	28	25	30	28
Yaw	80	110	108	154	154

Natural periods [sec]

Table 4-2 Natural frequencies of the different platform designs

Mode	5MW	7.5MW-S	7.5MW-RD	10MW-S	10MW-RD
Surge	0.01	0.01	0.01	0.005	0.005
Heave	0.06	0.05	0.05	0.05	0.05
Pitch	0.04	0.04	0.04	0.03	0.04
Yaw	0.01	0.01	0.01	0.01	0.01

Natural frequencies [Hz]

Pierson-Moskowitz spectrum

The distribution of the energy density over the frequency of a wave spectrum is represented by the Pierson-Moskowitz spectrum. Published in 1964, it is based on data collected in the north Atlantic. For this thesis, it is of interest to see at which frequencies the peaks of the wave spectra lie and compare those to the natural frequencies. This can be seen in the following graph. The power spectral density (PSD) plots are generated from the time series simulation results with help of a MATLAB routine written by Amy Robertson of the NREL.

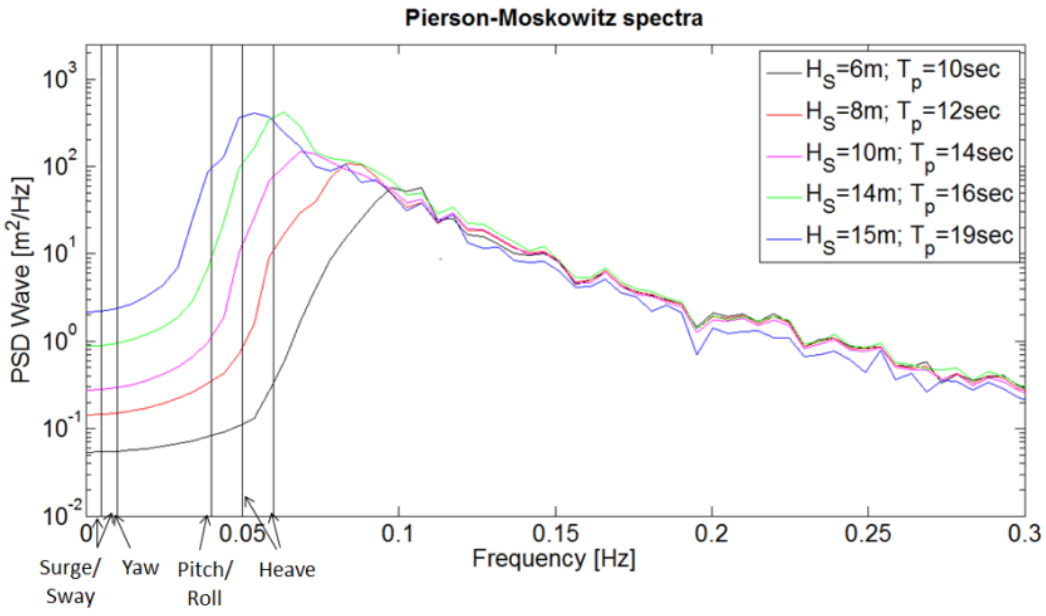

Figure 4-5 Pierson-Moskowitz spectra for examined wave conditions

If the peak-frequency of the wave coincides with the natural frequency of a platform motion, the waves will cause resonant behavior in the structure. Only the heave natural frequency is close to the peaks of the two extreme-wave spectra.

Free decay conclusion

The first simulations show that all systems eventually return to the equilibrium position without large differences in their behavior. Therefore the applied scaling methodologies for the dimensions and the damping matrix seem to be reasonable. However, the results need to be validated through wave tank tests.

It takes longer for all platforms to reach the equilibrium position in the yaw, surge and sway motions than in the heave, pitch and roll motions. This is mainly caused by the different shapes of the structure as seen along different axes. The heave plates cause a lot of damping with their plane areas and sharp edges, which is expressed by a high cd value (damping coefficient). The round surfaces of the cylinders as seen from a lateral view have a considerably lower cd value and cause less drag. Furthermore, the position in the horizontal or x-y-plane is fixed by the mooring only.

Sharper distinctions in the overall stability of the systems become clearer in the following load cases, in particular the operational ones.

4.1.2. Steady Conditions

Before examining the influence of dynamic loads on the floating structure, the steady state performance is tested. The system does not experience any acceleration. All wind- or wave-induced forces and moments are steady and the wind inflow is uniform. The simulations with steady conditions show if and how the platform is moving towards a new steady state position. Therefore three load cases with wind velocities below rated, at rated and above rated wind speed are examined. The regular waves have a height of 6m and arrive at the platform with a period of 10 sec. These wave characteristics are chosen, as they are close to the mean wave height at mean wind speeds in the North Sea and were used in the OC4-project as well (Schmidt & Ahrendt, 2006). The following table summarizes the investigated load cases. The simulation time is 1100 seconds, of which the first 200 seconds are ignored due to transient behavior.

Table 4-3 Steady state load cases

Case	Wind speed U_{Steady} [m/s]	Wave height H_{Steady} [m]	Wave peak period T_{Steady} [sec]
2.1	10	6	10
2.2	11.4	6	10
2.3	13	6	10

In the figure below, the platform pitch over time for the 10MW-S platform is imaged for different wind speeds according to load cases one to three. The graph shows that the highest platform pitch occurs at a wind speed of 11.4m/s. The simulations for the other designs underline this phenomenon. The reason for this is the turbine design. The highest thrust force on the rotors applies at rated wind speed. The blades are pitched at higher velocities which reduces the angle of attack.

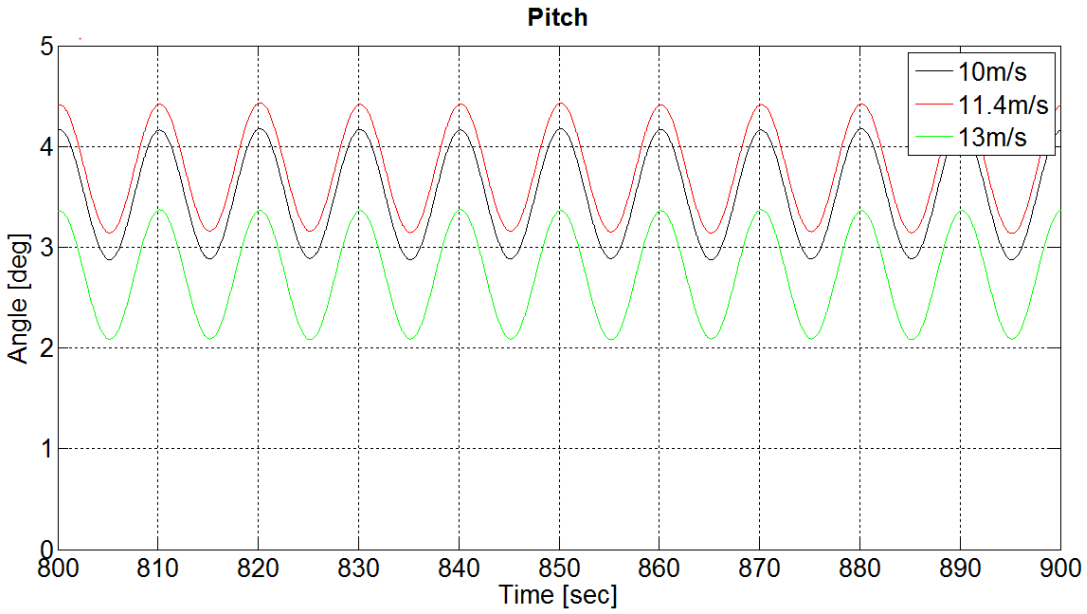

Figure 4-6 Steady state pitch response of the 10MW-S systems at different wind speeds

The significant results for the 10MW-S system are summarized in Table 4-4.

Table 4-4 Summarized results of the steady state simulations

U [m/s]	Thrust [kN]	Mean Pitch Angle [deg]	Max. Pitch Angle [deg]
10	1200	3.53	4.27
11.4	**1500**	**3.79**	**4.61**
13	1050	2.73	3.43

The graph below shows the thrust for different wind speeds of the DTU 10MW RWT. The results obtained from the simulations correspond to the values in graph.

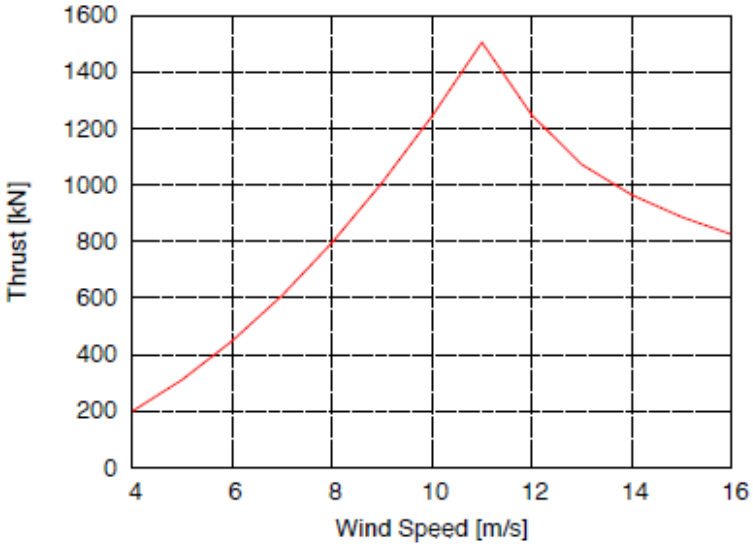

Figure 4-7 Thrust for various wind speeds on the DTU 10MW RWT (Bak, et al., 2013)

The pitch angle of the platform has an important influence on the performance and is a main factor in evaluating the platform's design. The rated wind speed is therefore chosen for most simulations hereafter as it marks the most critical wind velocity for the system. The three wind turbines used in this thesis operate with the same rated wind speed.

The steady state pitch response of the five floating structures to the steady conditions in load case two is displayed below.

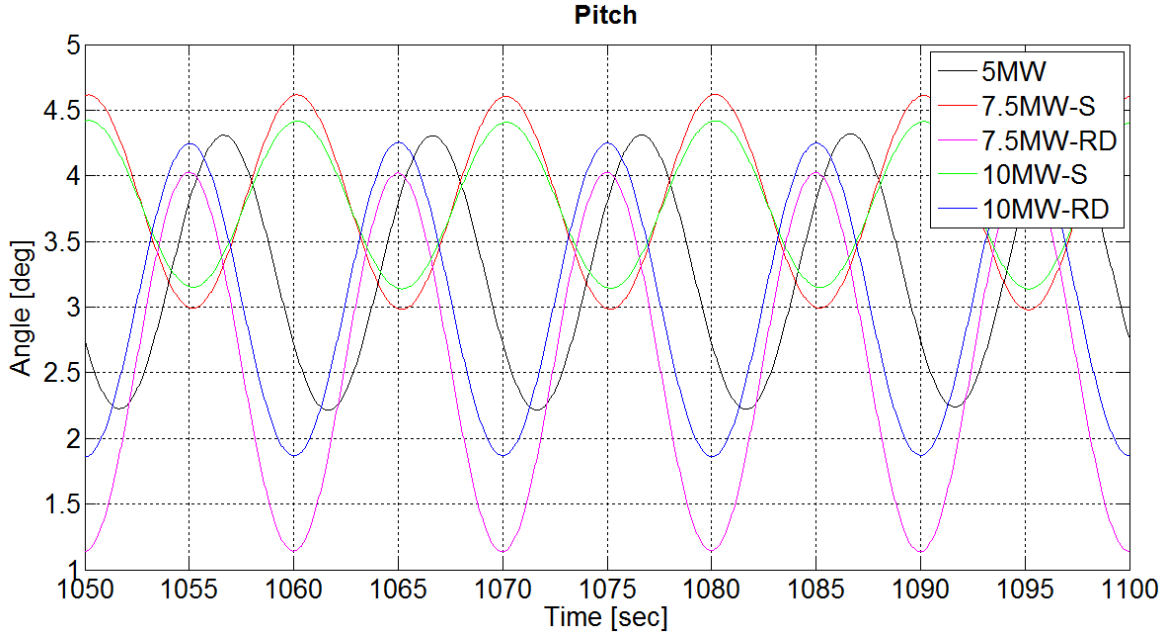

Figure 4-8 Steady state pitch response of all five systems

The pitch frequency in steady state conditions is the same for all designs. It corresponds to the wave frequency of 10sec. The mean and maximum pitch angle of the scaled designs is generally higher

than that of the reduced draft design for the same power rating. The amplitudes of the scaled design compared to the reduced draft design are decreasing for larger system sizes.

Table 4-5 summarizes the findings of the steady state simulations. For these steady conditions and with wind and waves only attacking along the x-axis, the results in sway, roll and yaw motion are not significant. Therefore they are not included in the overview.

Table 4-5 Summarized results of the steady state load case two

Platform design	Mean Pitch Angle [deg]	Max. Pitch Angle [deg]	Mean Surge [m]	Max. Heave [m]
5MW	3.3	4.4	11.4	0.6
7.5MW-S	3.6	4.5	19.1	0.4
7.5MW-RD	2.4	3.9	17.8	0.5
10MW-S	3.8	4.6	35.3	0.4
10MW-RD	3.1	4.3	34.9	0.5

The most important aspect that can be seen is that the RD-design has a better pitch response than the other design. This is valid for the heave motion, too, largely because of the slightly increased heave plate area. The increase in surge for larger system sizes is linked to the unchanging mooring. The larger underwater, vertical surface area of the scaled design causes slightly higher values in the surge displacement compared with the reduced draft system at the same rated power.

4.1.3. Operational Conditions

The following simulations show some representative offshore conditions under which the turbine is expected to operate normally. Turbulent wind profiles were created with TurbSim. The stochastic waves are generated by HydroDyn of FAST 8, using the Pierson-Moskowitz/JONSWAP-spectrum. The studied load cases are shown in the next table.

Table 4-6 Operational load cases

Case	Mean wind speed U_{mean} [m/s]	Significant wave height H_s [m]	Peak-spectral period of incident waves T_p [sec]
3.4	10	6	10
3.5	11.4	6	10
3.6	18	6	10
3.7	25	6	10
3.8	11.4	8	12
3.9	11.4	10	14
3.10	11.4	14	16

Load cases 9 and 10 do not actually represent operational conditions. The given wave height would cause a shutdown of the turbine. These extreme load cases are interesting for comparison due to the distinctive results. The wave conditions of load case 9 and 10 represent the expected values of an extreme event with a 50-year-return period (Freestone, 2014) & (OC4, 2013). In the case of such storm waves, the wind velocity would most probably be higher. Nevertheless, the rated wind speed is used to simulate the turbine in operation.

The influence of the platform motions on the power output of the 10MW wind turbine is presented in Figure 4-9. The red graph shows the 10MW turbine installed onshore and the blue graph representes the floating offshore system based on the scaled design platform. Both systems are exposed to the same wind profile corresponding to a mean wind speed of 11.4m/s. The wave conditions correspond to the inputs of load case 3.5.

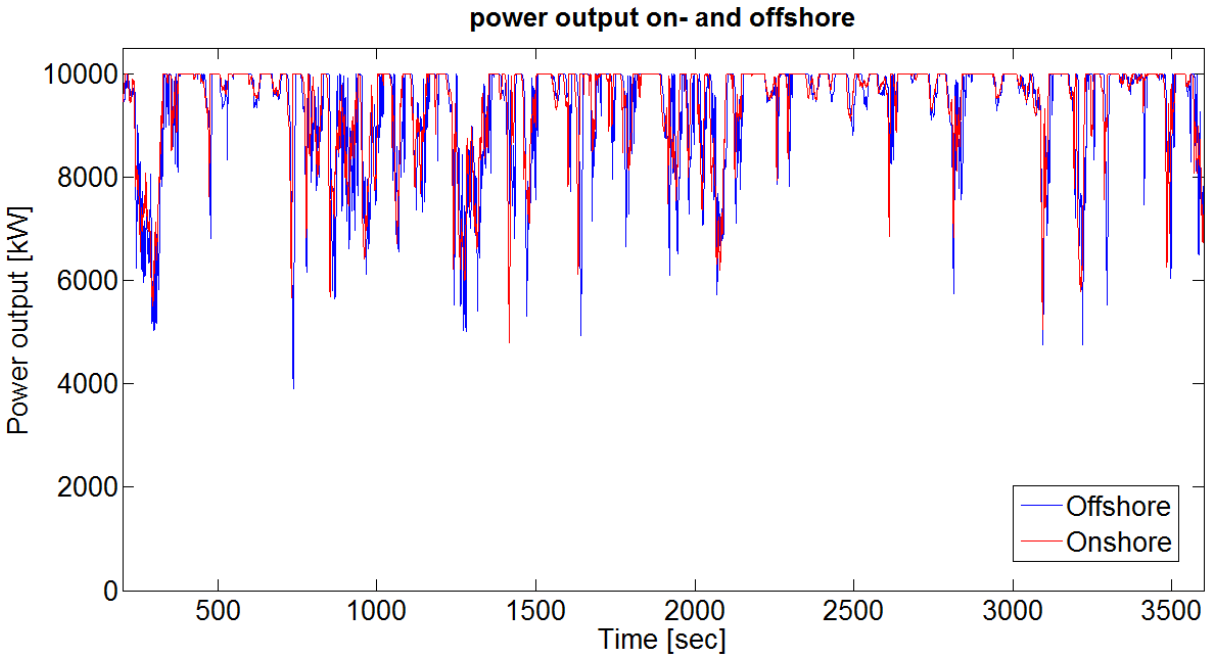

Figure 4-9 Power curves for an on- and offshore installation

The power curve for an offshore installation is subject to larger fluctuations than the onshore turbine. This results in reduced quality of the injected energy into the grid, even though the average power ratings do not differ to a great extent. (The onshore power output averages to 9.43MW and the offshore installation to 9.33MW.) Nevertheless, the wind conditions offshore are often better compared with onshore locations, as the mean velocities are higher and the wind profile has less vertical shear and is less turbulent.

The simulation results of load case 3.5 for all platforms are summarized in the table below. The same overall trends as for the steady state results of load case 2.2 can be seen.

Table 4-7 Summary of the simulation results of load case 3.5

Platform design	Mean Pitch Angle [deg]	Max. Pitch Angle [deg]	Mean Surge [m]	Max. Heave [m]
5MW	2.8	5.2	9.2	1.0
7.5MW-S	3.3	5.4	18.0	0.7
7.5MW-RD	2.4	4.6	17.9	1.1
10MW-S	3.6	6.5	33.3	0.6
10MW-RD	3.0	5.3	33.2	0.9

The mean and maximum values in pitch are slightly higher compared with the steady state conditions, presented earlier in table Table 4-5. The differences in surge displacement between the RD- and S-design for the same rated power vanish. This means that the mean displacement in surge is dependent mainly on the mooring and less on the platform geometry. A trend that becomes clearer in the evaluation of the operational behavior is that the heave motion reduces for larger system sizes. The free decay tests showed a slightly better damping in heave direction for the RD-design than the S-design of the same power rating due to the larger heave plate area. Nevertheless, the RD-platforms experience greater heave motions than the scaled counterpart for the same operational wind and wave loads. The explanation for this behavior lies in the natural frequencies, and hence the frequency response, of the different platforms. The heave natural frequencies of the 5MW, 7.5MW-RD and 10MW-RD platforms are closer to the frequencies of the peaks in the wave spectra. The frequency domain analysis of the heave motion in load case 3.5 is depicted with a logarithmic scale in Figure 4-10.

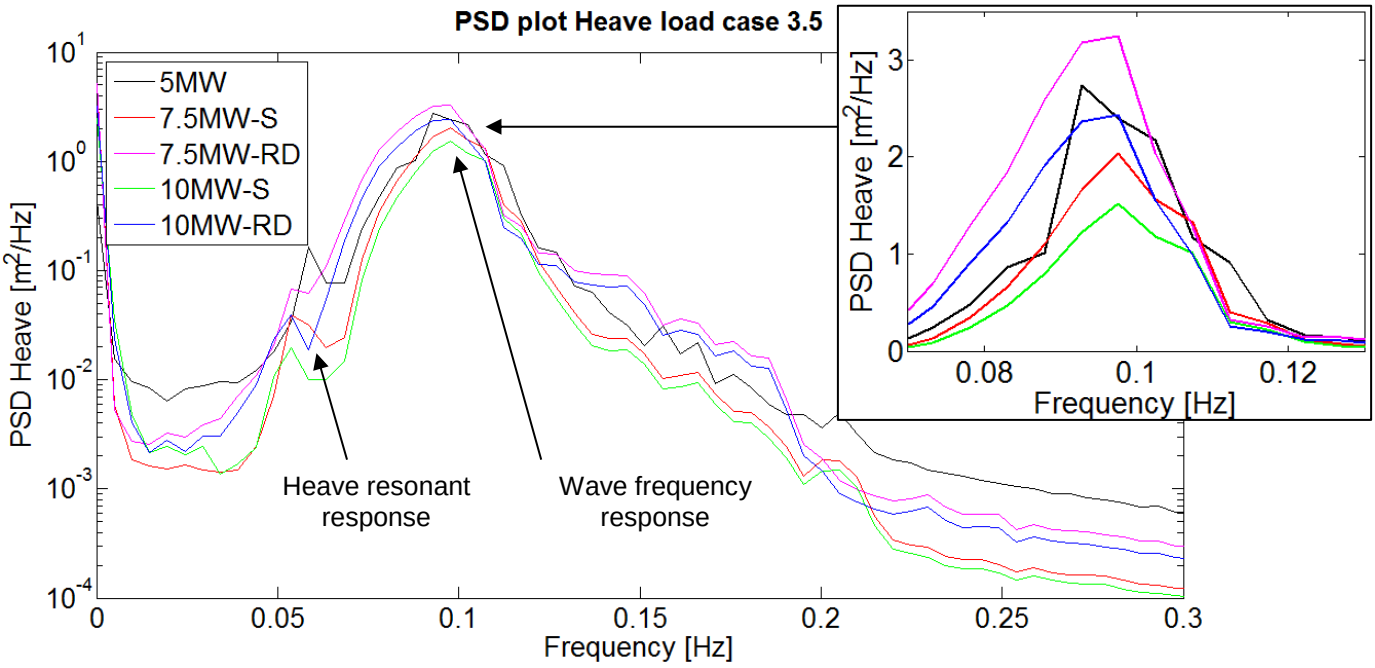

Figure 4-10 Response spectrum of heave motion in load case 3.5

The right peak in the graph depicted above shows the wave frequency response at a frequency of 0.1Hz. The relatively small peak to the left represents the resonant response in heave motion. The smaller platforms show a bigger resonant response than the larger systems. This is the reason for the lower maximum heave values of the bigger FOWT. The second peak is enlarged in the top right corner of the graph. It shows that the scaled designs, marked in red and green, have a significantly lower response to the wave frequencies than the RD-platforms, marked in magenta and blue. That is the reason for the larger amplitudes in heave for the RD platforms.

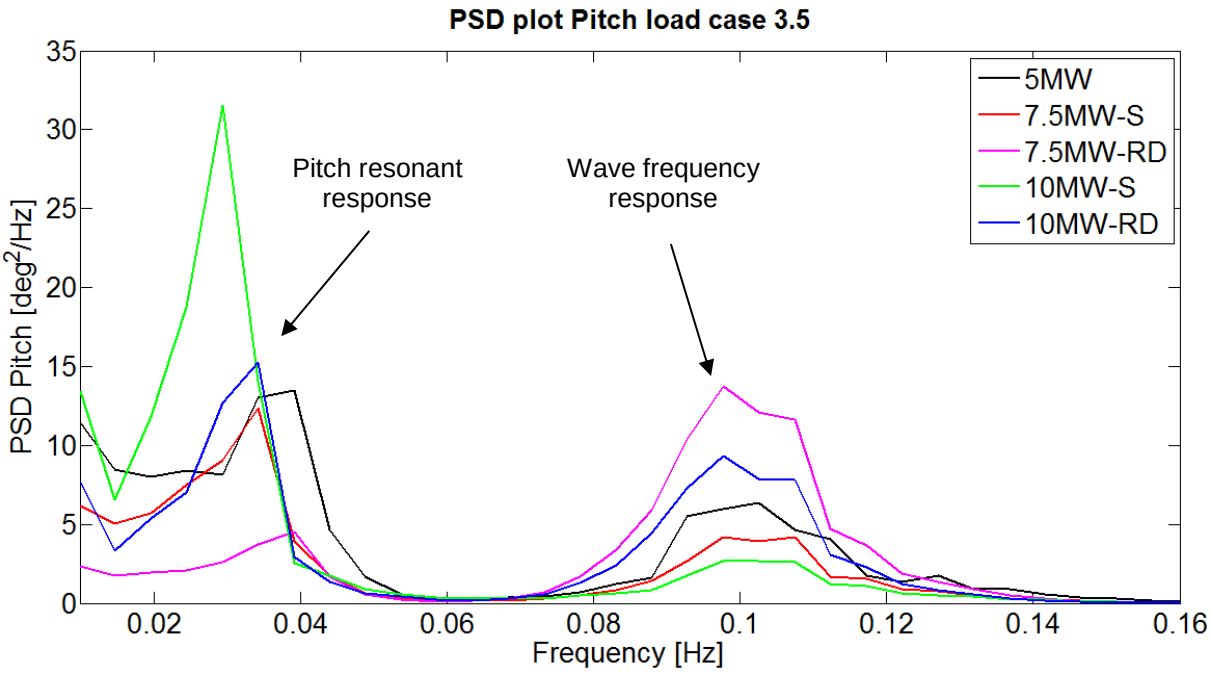

Figure 4-11 Response spectrum of pitch motion in load case 3.5

The PSD plot for the pitch motion of load case 3.5 indicates that the RD-platforms have a slightly stronger pitch response for wave-induced frequencies. This means that the wave conditions have a greater influence on the pitch stability of the RD- than on that of the S-platforms. Nevertheless, the RD-design shows a better overall pitch stability, as proven by the earlier results, because the pitch motion is more dependent on the wind than the wave conditions. Therefore, increased damping through larger heave plates has a bigger influence on the pitch stability than the higher wave frequency response of the system.

Furthermore, the left peaks provide an explanation for the greater mean and maximum pitch angles of the S-designs. The resonant behavior of the 10MW-S system (green) has a noticeably higher peak than the 10MW-RD configuration (blue). The same is true for the 7.5MW-S (red) and the 7.5MW-RD platform (magenta).

The minor differences in the surge displacement between the RD and S designs with the same rated power can be explained by looking at the PSD plot of the surge motion in Figure 4-12. A logarithmic

scale is used for the y-axis. The 7.5MW-S (red) and 10MW-S platform (green) have a slightly higher response in surge motion at the frequency of 0.1Hz, corresponding to the peak of the wave spectrum.

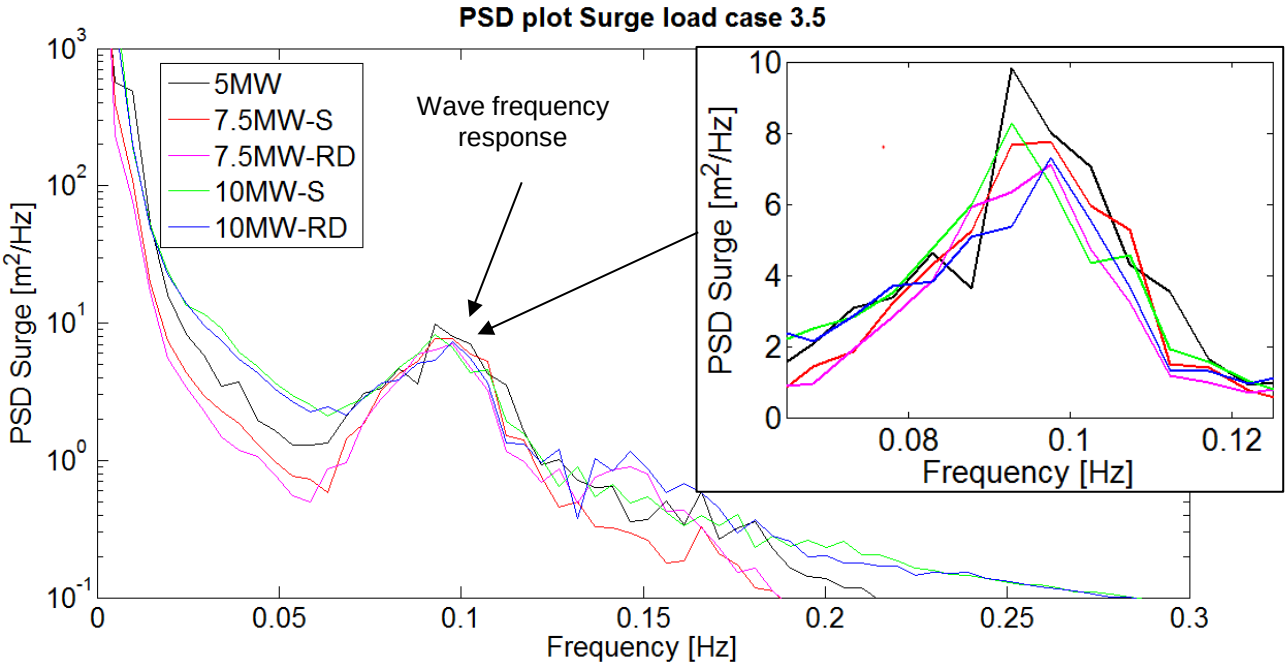

Figure 4-12 Response spectrum of surge motion in load case 3.5

The frequency response in roll motion is very similar to the pitch. The right peaks in Figure 4-13 represent the resonant response in roll motion. The peaks of the RD-platforms (magenta/blue) are smaller than the peaks of the S-platforms (red/green). There is no distinctive peak at wave-induced frequency at around 0.1Hz, probably because the waves only apply along the x-direction. The Yaw and Roll resonant response can be explained to the slightly changing angle of the wind inflow direction. The left peaks show the yaw resonant response at the yaw natural frequency of 0.01Hz.

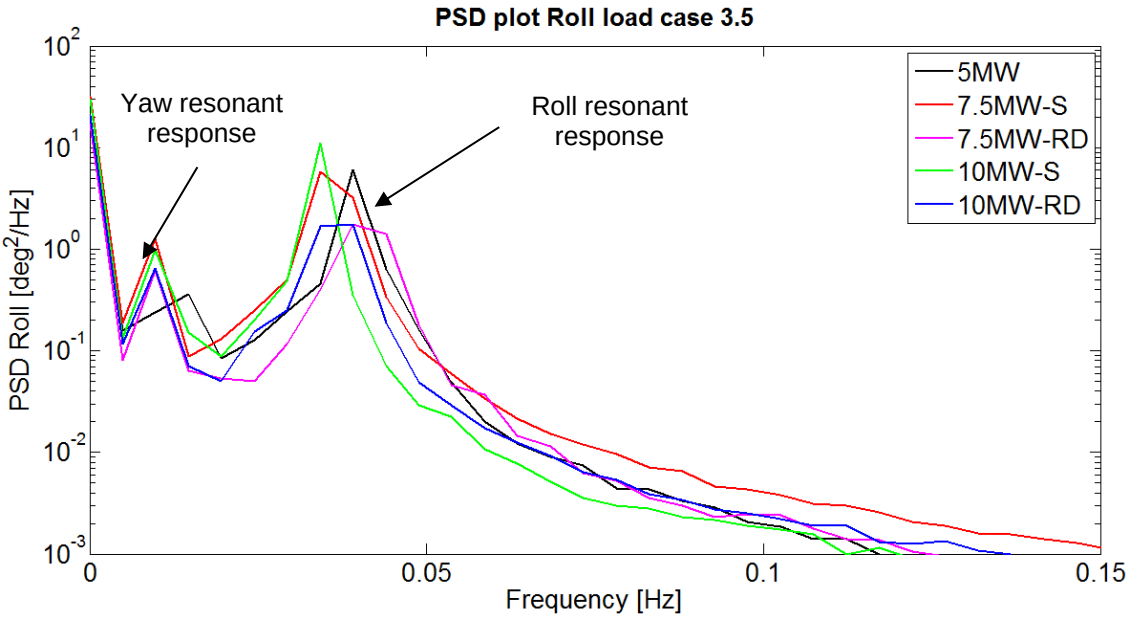

Figure 4-13 Response spectrum of roll motion in load case 3.5

Box plots of the pitch motion

A more in depth consideration of the pitch behavior is facilitated by the use of box-plots. Load cases 3.5 and 3.9 are compared. A box-and-whiskers plot is a graphical representation of statistical data. In the case under consideration, it depicts the minimum and maximum value that occurred during the simulations, marked by the end of the thin lines. Furthermore the 95% and 5% quantiles are marked by the ends of the red and blue boxes, respectively. This means that 90% of the time the pitch angle varies between these two values. The mean pitch angle is marked by the line where the red and the blue, or upper and lower 45% quantile, join together.

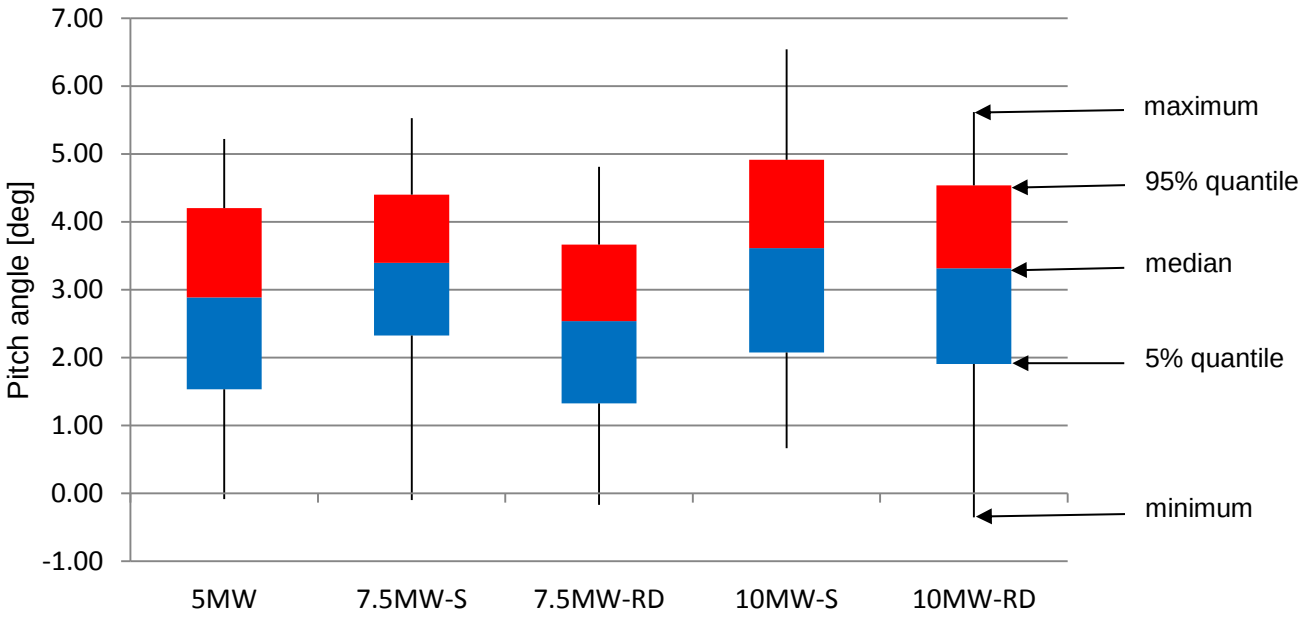

Figure 4-14 Box plot of pitch motion for load case 3.5

The results of the pitch stability under operational conditions summarized in the figure above confirm the conclusions drawn from the free decay and steady state tests. The pitch motion of the RD-systems is less than that of the S design. Mean and maximum pitch angles of all systems increase for larger systems.

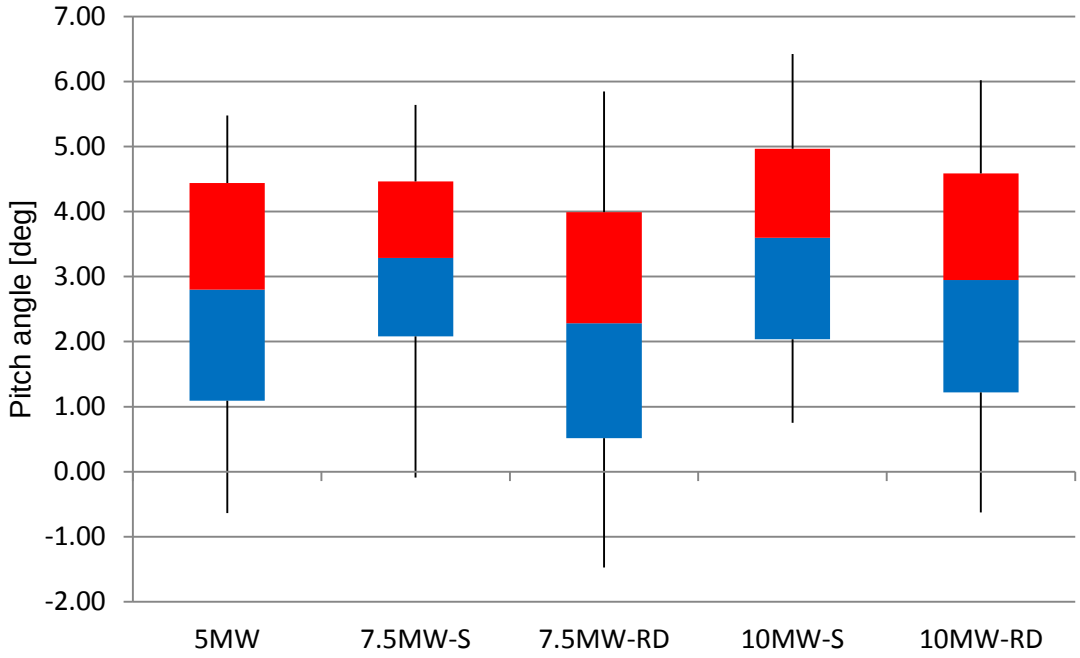

Figure 4-15 Box plot of pitch motion for load case 3.9

The pitch behavior in load case 3.9, presented in the figure above, shows a slightly increased movement for all the platforms compared to load case 3.5. The direct comparison shows that the significantly higher waves do not influence the stability of the semi-submersible platforms as much as a change in the wind velocity does, as shown in the steady state tests. This can be explained by looking at the Pierson-Moskowitz spectra in Figure 4-5 Pierson-Moskowitz spectra for examined wave conditions). The natural frequencies of all platforms are far away from the peaks of wave frequency spectra. Comparing load case 3.5 with 3.9, one can see that the response of the scaled design changes even less than that of the reduced draft. The minimum and maximum, as well as the 95% and 5% quantile of the RD-systems, suddenly attain a wider range of values for more extreme wave conditions. This does not imply that the S-design is more suitable for big wave conditions than the RD-platforms. The reduced draft design still shows lower pitch angles for most of the simulated time period. It verifies the previously presented results in the frequency domain plots, particular in Figure 4-11. The RD-systems' response to the frequencies of the waves is more extreme than that of the S-systems.

Nacelle acceleration

In addition to too-high wind speeds and large pitch angles, the nacelle acceleration can also lead to a shutdown of the system. A nacelle acceleration of 0.2*g or 1.96m/s^2 causes a cut-out of the wind turbine (Suzuki, et al., 2010). The nacelle acceleration describes the acceleration of the nacelle body and not the wind acceleration at nacelle-height. The effects of the wind accelerations on the turbine are site-dependent (Duenas-Osorio & Basu, 2007) and are not further discussed in this thesis.

As wind and waves apply along the x-axis, the maximum values of the positive and negative acceleration occur in x-direction. The absolute values are summarized for all platforms and a selection of convincing load cases in Table 4-8.

Table 4-8 Maximum nacelle acceleration all system

Load case	5MW [m/s^2]	7.5MW-S [m/s^2]	7.5MW-RD [m/s^2]	10MW-S [m/s^2]	10MW-RD [m/s^2]
3.5	1.10	0.96	1.38	0.85	1.25
3.8	1.13	0.97	1.38	0.86	1.26
3.9	1.19	1.02	1.46	0.93	1.24
3.10	1.32	1.19	1.66	1.08	1.44
survival	1.45	1.17	1.77	1.10	1.70

The values for the nacelle acceleration rise with increasing wave size for all systems. The RD-design experiences comparatively higher accelerations than the S-design. The larger the platforms of a particular design are, the smaller the maximum nacelle accelerations are. As previously explained, this is due to the fact that the RD-platforms show a higher response to the wave frequencies. Higher mean wind speeds of 18m/s and 25m/s examined in load cases 3.6 and 3.7, respectively, only have a minor influence on the maximum nacelle accelerations.

Load on mooring

The stress on the fairlead, the connection onto the platform, is usually greater than on the anchor for a catenary mooring system. On the fairlead also the gravitational force is applying, while a certain part of the chain is on the seabed before it pulls on the anchor. The stresses in the simulations for this work are the highest on the only mooring line directed upstream along the x-axis, as all external forces apply along this axis. These maximum values are presented in the following table for selected load cases. Furthermore, the stress on the mooring system is largest at rated wind speed, and increases with larger waves.

Table 4-9 maximum load on mooring

	5MW [MN]	7.5MW-S [MN]	7.5MW-RD [MN]	10MW-S [MN]	10MW-RD [MN]
3.5	1.85	1.94	1.87	2.64	2.47
3.8	1.91	2.00	1.94	2.70	2.56
3.10	1.94	2.29	2.62	3.37	4.24

The stronger response to large waves for the RD-platforms compared to the S-design becomes clear in the stress on the mooring lines as well. The maximum stress on the fairlead is slightly smaller for

the reduced draft platforms for waves with a significant height of six meters. This value drastically increases for extreme waves represented in load case 3.10. As these maximum values of the extreme load case determine required mooring strength, RD-platforms need stronger, thereby heavier and more costly moorings. This relation is discussed in chapter 5. The fatigue damage is not examined but should be considered for a complete mooring dimensioning.

4.1.4. Survival Condition

A 100-year storm event is simulated to evaluate the performance of the FOWT-systems under extreme conditions. The significant wave height amounts to 15m with a peak period of 19s. The mean velocity of the turbulent wind is 50m/s (Karimirad, Gao, & Moan, 2009). The blades are pitched 90 degrees and the rotational modes of the shafts and generator are suppressed. The results in pitch motion for all five platform configurations are summarized in the figure below.

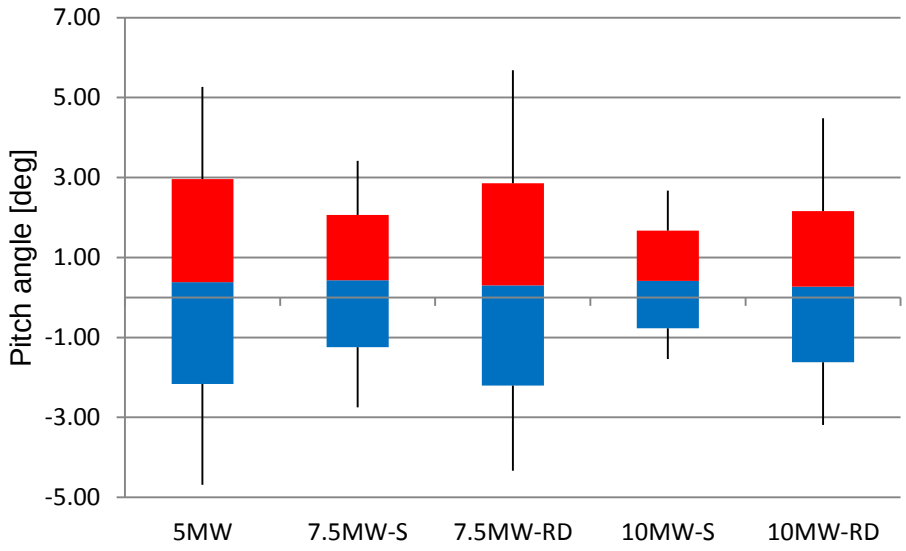

Figure 4-16 Box plot of pitch motion for the survival load case

The figure clearly shows that the pitch of the RD-systems is much more strongly influenced by the wave conditions than the pitch of the S-platforms is. The maximum and minimum pitch angles of the 7.5MW-RD, for example, vary by 10 degrees, while the different pitch angles of the 7.5MW-S lie in a range of 6.2 degrees.

Table 4-10 Summary of the simulation results of the survival load case

Platform design	Mean Pitch Angle [deg]	Max. Pitch Angle [deg]	Mean Surge [m]	Max. Heave [m]
5MW	0.4	5.7	1.2	6
7.5MW-S	0.4	3.4	2.3	6.2
7.5MW-RD	0.3	4.8	2.7	4.8
10MW-S	0.4	2.7	4.3	6.3
10MW-RD	0.3	4.5	4.1	5.1

The mean pitch angle of all platforms is comparatively low and similar for the different designs. This is mainly due to the fact that the blades are pitched. The waves thus have a higher relative influence on the pitch angle of the FOWTs. The maximum heave displacement of the RD-design is lower than the respective S-design. The case is reverse for the operational and steady state conditions. Furthermore, the maximum heave follows an increasing trend for larger systems. These circumstances are explained below in accordance with the heave PSD-plot shown in Figure 4-18.

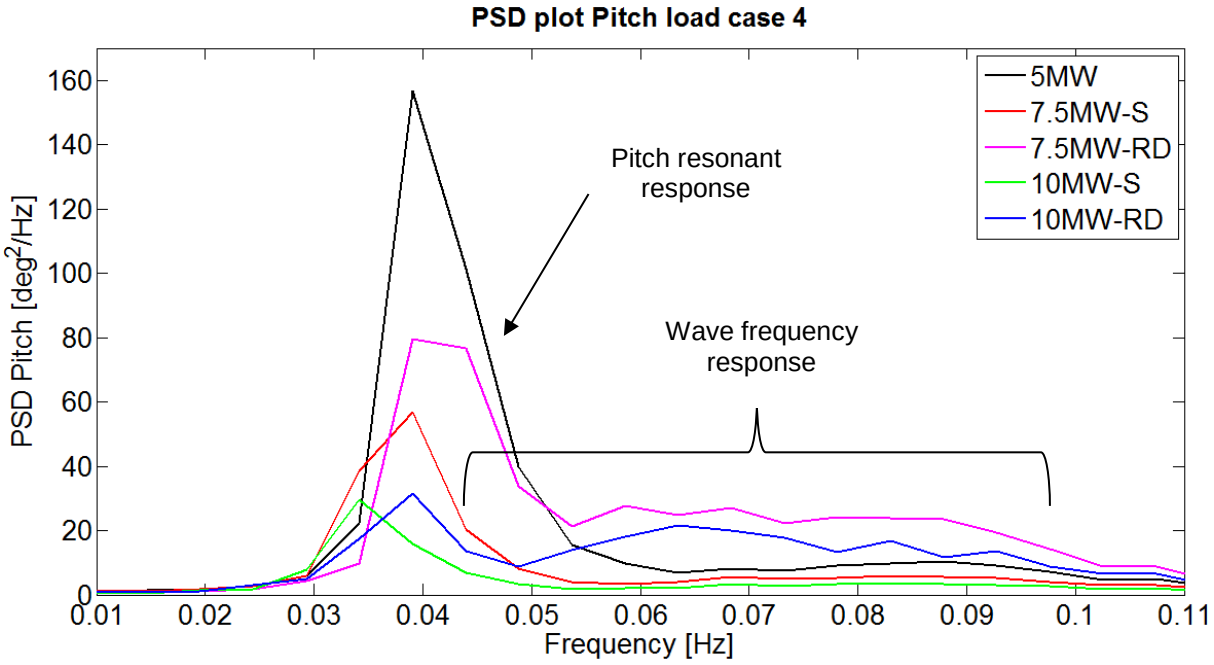

Figure 4-17 Response spectrum of pitch motion in a 100-year storm event

The Pitch resonant response for all evaluated systems is significantly higher for the survival conditions than for the load case 3.5, because the wave spectrum peak frequency lies closer to the natural frequencies in the survival state. The 5MW-system (black) shows the highest response. The previously discussed difference between the maximum and minimum pitch angle of the two 7.5MW

designs is explainable by looking at the greater response of the RD-design (magenta) compared to the S-design (red).

The wave-induced resonant behavior is especially significant for the heave motion as depicted in the figure below. The peak frequency of the survival wave spectrum, as presented in the Pierson-Moskowitz spectrum on page 39, coincides exactly with the heave natural frequencies of all platforms (0.05Hz). The scaled systems (green and red) have significantly higher peak than the reduced draft platforms (magenta and blue). This explains the higher values for the maximum heave in the previously presented in Table 4-10. Additionally, the 10MW rated systems show a greater response than the 7.5MW systems of the same S- or RD-design. This is the reason for the larger maximum heave displacement of the 10MW- compared with the 7.5MW platforms.

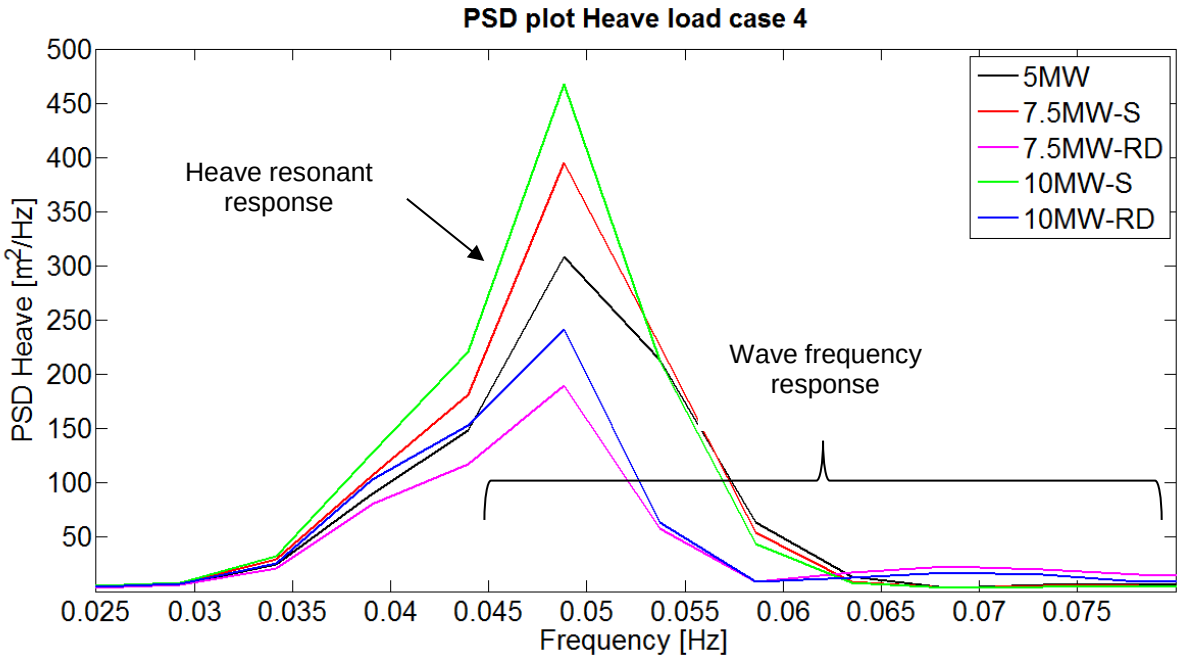

Figure 4-18 Response spectrum of heave motion in a 100-year storm event

As the Yaw motion in all evaluated cases of this work is negligible, the results of the PSD-plot in Yaw motion do not influence the overall outcomes significantly.

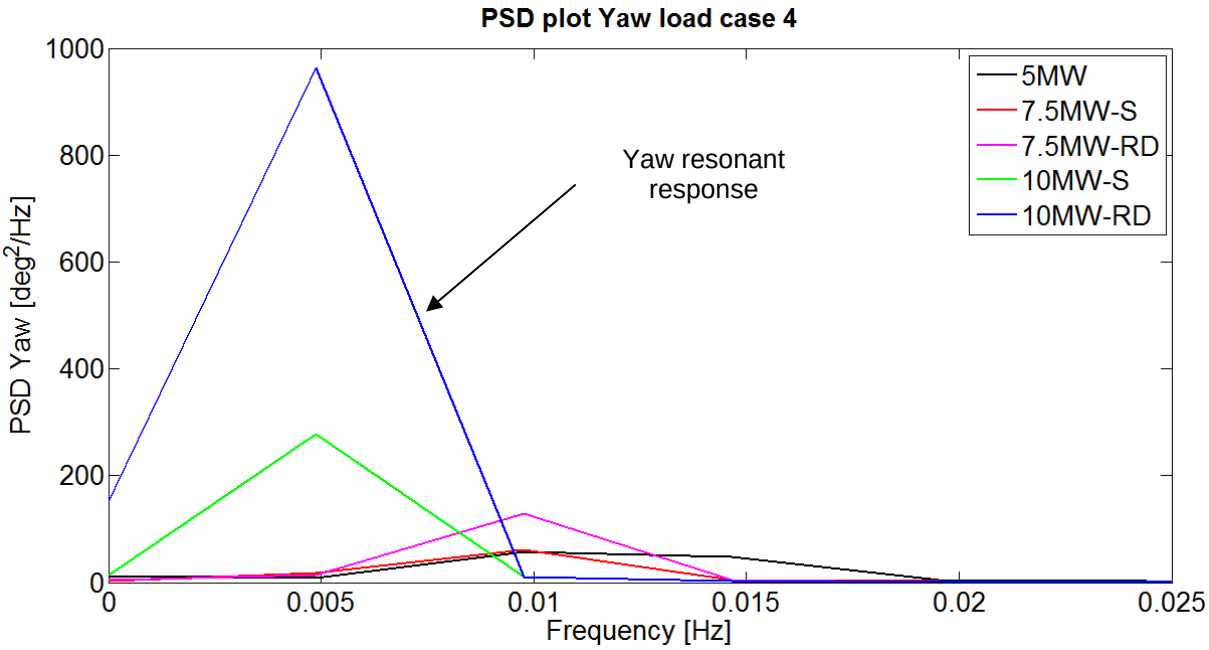

Figure 4-19 Response spectrum of yaw motion in a 100-year storm event

The 10MW-platforms, particularly the 10MW reduced draft design, have an extreme frequency response in yaw at their natural frequency of 0.005Hz, for 100-year storm event conditions. This might be problematic in terms of the structural stability and the yaw stability, if wind and waves apply multidirectional and the turbine components are not rigid. Further studies are needed to ensure the system's solidity.

An extreme resonant response of the two large platform designs can also be seen for the PSD-plot of the sway motion.

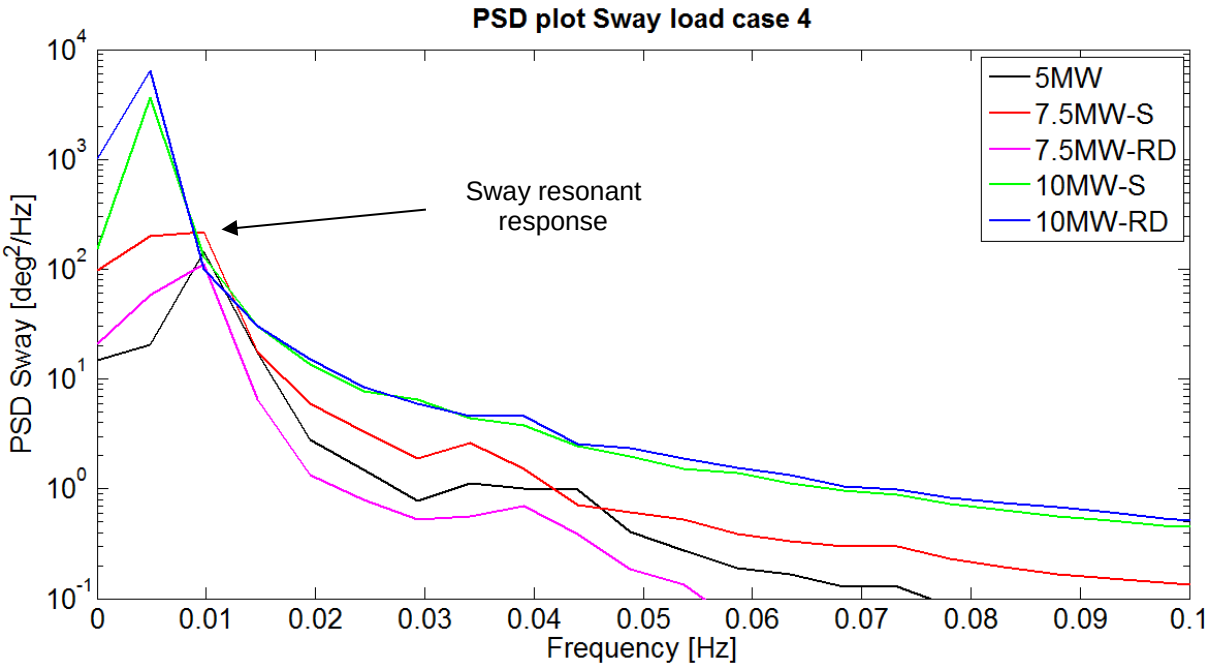

Figure 4-20 Response spectrum of sway motion in a 100-year storm event

As with the yaw motion, the sway displacement is not large since wind and waves are only applied in one direction. Nevertheless, the strong resonant behavior at the sway natural frequency in the 100-year storm conditions might cause considerable structural stress for the whole FOWT-system. The risk is especially high if other parts of the wind turbine have similar natural frequencies.

4.2. Second order criteria: Infrastructural limitations

One of the main advantages of semi-submersible structures over the other FOWT-platform designs from a technical and economic point of view is the possibility of complete construction in a harbor. After construction the FOWT is towed to the desired position, where the pre-laid mooring is connected to the platform. Construction in the shipyard allows a larger time window for offshore installation and reduces costs and risks significantly. If a dry dock is used for the construction, as it was in the WindFloat project, only a limited number of shipyards come into consideration for larger platform dimensions. This might lead to longer transport distances and thereby increased costs for the transportation and installation. Apart from these issues in transportation of technics and personnel, the grid connection has to be considered. The plans for a European “super grid” are being discussed on a national and EU-level. The motivation for these high voltage direct current (HVDC) cable connections is the (direct) conjunction of several EU-member and non-EU countries and integrating renewable offshore and remote energy generation units (House of Commons, 2012). These plans include linking several countries around the North Sea, which simplifies the use of the wind conditions there (BBC News, 2010). There are no technical barriers for an implementation of long distance cable connections through the sea (Subsea World News, 2012).

4.2.1. Overview of European shipyards to consider

The construction of the WindFloat platform showed the limited availability of dry-docks with suitable dimensions on the Portuguese coast. The “Lisnave” ship yard, located in Setúbal (close to Lisbon), is positioned roughly 400km away from the installation site. The transportation took two days, even though the system is positioned just 5km off the coast (Saygi, 2011) & (Valverde, 2014).

The increased dimensions of the up-scaled designs presented in this work drastically reduce the number of suitable European dry docks in this case as well. The minimum platform width, as presented in Table 3-1 on page 26, determines the most critical dimension. The 10MW-S platform has a minimum width of 84.85m and the 10MW-RD platform 86.45m. The dry dock length is usually not the limiting factor and theoretically allows the construction of more than one platform simultaneously. The platform draft is considerably lower in the dry dock, compared to its operating state, as the ballast water is let in later. Furthermore, it is possible to add extra floaters to the platform to further decrease the platform’s draft. This way shallow waters in the harbor area can be overcome until the open sea is reached. The maximum needed and available crane heights are not included in the following overview.

The dry docks in the table hereafter are sorted by their width. As a comparison, the largest dry dock in the Lisnave shipyard in Setúbal near Lisbon, which has been used for the construction of the WindFloat platform, has a length of 450m, a width of 75m, and a draft of 7.5m (Lisnave Estaleiros Navais, SA, 2014).

Table 4-11 Overview of the largest European dry docks

Company	Location	Length	Width	Draft
Able UK ltd[8]	Billingham, Great Britain	376m	120m	12.1m
Navantia[9]	Cadiz, Spain	525m	100m	9.0m
Harland & Wolff Heavy Industries ltd[10]	Belfast, Ireland	556m	93m	8.4m
Maersk[11] (closed since 2012)	*Odense, Denmark*	*415m*	*90m*	*11.0m*
STX Europe[12]	St. Nazaire, France	450m	90m	-
Keppel Verolme[13]	Rotterdam, Netherlands	405m	90m	11.0m
ThyssenKrupp Marine Systems[14]	Kiel, Germany	426m	88.2m	8.7m
Port Autonome de Marseille[15]	Marseille, France	465m	85m	9.2m
STX Europe[16]	Rauma, Finland	260m	85m	-
Lisnave[17]	Setùbal, Portugal	450m	75m	7.5m

The geographical distribution of these ship yards is visualized in the map below.

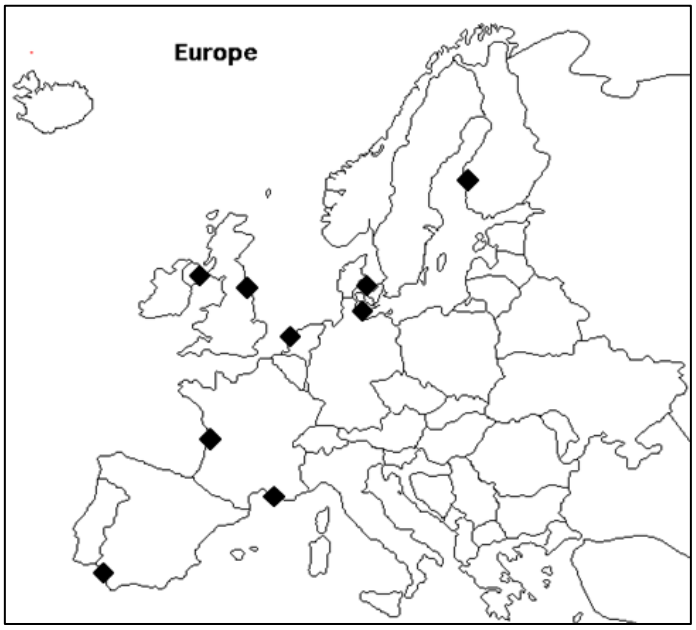

Figure 4-21 Map of Europe´s largest dry docks (Based on (EnchantedLearning, 2002))

[8] (Able UK ltd, 2014)
[9] (Navantia)
[10] (harland and wolff heavy industries ltd, 2010)
[11] (Jensen, 2009) – this ship yard was closed in 2012
[12] (stx France, 2014)
[13] (Keppel Verolme, 2013)
[14] (Reiff, 2009)
[15] (Capuzzo, 2012)
[16] (Sillanpää, 2009)
[17] (Lisnave Estaleiros Navais, SA, 2014)

The locations and size capacities of these dry docks indicate that large parts of the desirable offshore areas, as presented in chapter 1.4.2, are in a several hundred kilometer range around the ship yards. Especially in the southwestern North Sea, the Bay of Biscay and the Celtic Sea, good infrastructural conditions exist. Whether large dry docks in Norway and Scotland are necessary for reducing transport routes in the northern North Sea is mainly an economical question. The same is true for the North Atlantic off the Portuguese coast as large dry docks already exist in France and Spain. Furthermore, it might be an opportunity to forward Portugal's pioneering role in the FOWT-development.

4.2.2. Accessibility for Operation and Maintenance

The distance between the wind farm and the shore influences the installation costs and marks one of the main cost factors for later operation and maintenance efforts. The farthest offshore wind farm so far (BARD Offshore 1) is located 110km off the German coast, but several projects with greater distances to shore are planned (Fraunhofer IWES). A wind farm on the Dogger Bank in the North Sea will be located roughly 200km offshore (Green & Vasilakos, 2013). The distance restrictions are mainly determined by the costs. A representative maintenance vessel, the "Damen W2W Offshore Wind Support Vessel 9020", has a maximum speed of 14 knots, corresponding to roughly 25km/h (Damen, 2011). Assuming that the support harbor for a wind farm 100km off the coast lies at the shortest possible distance, this leads to a total travel time of 8hours, excluding onshore preparations.

4.2.3. Influence on the platform design

The platform dimensions analyzed in this thesis allow a construction in the largest European dry docks. The different ship-yard locations allow relatively good access to many potential floating offshore wind farm areas. Nevertheless, this result might not be satisfying, as the costs for these large scale dry docks are most probably significantly higher than for smaller sites. This economic constraint should be taken into consideration for a thorough evaluation and optimization of the platform sizes. A slightly reduced minimum width allows the assembly in a wider range of naval vessel building facilities. In this case, the influence on the platform stability would have to be reevaluated. The easiest adaption in the platform design might be the adaption of the pontoon- and cross-bar lengths, while keeping the geometry of the offset columns. Alternatively, the construction of new shipyards or the adaption of disused ones might enable the assembly of larger structures at reduced expenses.

New methods of semi-submersible platform assembly could also provide a solution. A semi-submersible oil rig was assembled offshore in Brazil in 2011. The pre-manufactured main components, such as the offset columns were towed and anchored to a sheltered position at the Angra dos Reis Bay, where they were put together (Technip, 2011).

5. Costs

The main motivation for larger offshore turbines is the desired economies of scale. The wind industry is experiencing an ongoing decrease in the levelized cost of energy for larger turbine sizes in the installation of fixed bottom structures. This motivates turbine manufacturers to further increase turbine dimensions and rated power, as described above. The future will show where the physical limitations are concerning floating structures, as the forces on the components not only increase with the size of wind turbines, but also with additional loads induced from the platform motions. The system's lifetime might be one of the main critical aspects concerning the economic feasibility of a large FOWT. The benchmark of the industry for fixed bottom offshore wind turbines is 20 years (RWE, 2013). The same lifetime is assumed for the economic evaluation of a floating offshore wind park by Saygi (2011). Other sources state that fixed bottom offshore wind turbines will have increased technical caused downtimes due to the rough environment, which leads to a realistic lifetime in the range of only 12-15 years (Hughes, 2012). Regardless of which lifetime really applies for bottom fixed installations, if similar wind turbines are used on floating foundations, the average life will most probably be lower.

The foundation costs for fixed bottom installations are around 20% of the total costs, depending, of course, on the chosen structure (Green & Vasilakos, 2013). This represents a benchmark for FOWT-platforms.

5.1. Cost drivers

Scaling the platform dimensions towards 7.5MW and 10MW systems has a different influence on the particular cost drivers. In the following section these cost drivers are classified as fixed and variable costs, depending on whether or not the size of the platform influences them.

5.1.1. Fixed costs

The following expenditures are not influenced by the design of the FOWT-system:

- environmental surveys (influence on the sea and atmospheric eco-system)
- wind, current and wave assessments
- management and taxes
- analysis of the geological condition of the sea bed
- cabling and offshore grid connection
- mooring and anchor lying vessels

The site assessment and preparation of all surveys can take up to two years (Saygi, 2011). The projected profitability of the wind farm is strongly determined by the quality of the site characteristics.

The currents and sea bed structure partly determines the choice of mooring and anchors. The fixed expense of building an offshore grid connection is one of the main arguments for installing large turbines offshore (Smith P. , 2014b).

The vessels needed for the mooring installation are not influenced by the platform size within the size limits being looked at in this work even though the mooring will be of increased dimensions for larger systems (Duarte, 2014).

5.1.2. Variable costs

The variable or marginal costs are those which change with different platform sizes. The variable costs can be further divided into those which follow a linear trend, those which are rising and those decreasing for different FOWT-system sizes.

Variable costs with a linear trend

The linear marginal costs are independent of the quantity. The price per unit stays the same.

Regarding the platform, these are:

- Steel
- Working hours for construction
- Decommissioning

Steel represents the main part of the variable costs with a linear trend and is significantly influenced by the platform size. The cost for structural, pre-manufactured sections and beams, as of February 2014 is approximately 571€ per ton of steel (MEPS International Ltd., 2014). The number of working hours in the ship yard might increase slightly for larger platforms, as the weld seams are longer, for example, and additional stiffeners might have to be installed. However, generally the platform is not becoming more complex; its structural elements merely get larger. Therefore the amount of working hours will not rise significantly. The decommissioning costs are expected to be relatively low compared to the total capital expenditures (CAPEX) (RAB, 2010). According to Saygi (2011) they are 1% of the capital costs.

Variable costs with a decreasing trend

The annual operational expenditures (OPEX) are estimated to be 4% of the total capital expenditures for a 100MW-wind farm consisting of 20 WindFloat systems with a rated power of 5MW each (Saygi, 2011). This cost factor is not expected to increase proportionally for larger systems, as 35% of the OPEX are labor costs. This value is derived from fixed bottom wind farm observations. Consequently, as the labor intensity of maintenance efforts are not expected to increase for larger FOWTs, this leads to lower OPEX relative to the initial investment costs. The magnitude of influence of long distances to shore on the operation and maintenance costs still needs to be evaluated (RAB, 2010).

Cost drivers with an increasing trend

Some marginal costs are likely to rise relative to the overall system expenditures for increasing platform sizes:

- Fees for dry dock
- Mooring and anchoring

The fees for dry docks vary significantly depending on the size and region. For large ships or small platforms the daily prices are between 16k€ and 25k€ (Berlinger, Clausen, & Siegel, 2013). The lowest fees are charged in China, where a large dry dock, which is needed for the 10MW platforms, is available for 30k€ per day. This does not consider expenses for renting cranes, additional ship yard space and manpower. The prices in Europe are considerably higher (Idwal Marine Services Limited, 2014). Nevertheless these costs per platform will be considerably lower for a production of larger quantities e.g. for a wind farm, as at least 3-4 platforms would fit in the previously presented dry docks simultaneously.

The mooring line cost is based on a factor of 0.31€/m-kN. This is multiplied by the length and maximum steady-state tension of the line (Hall, 2010). For the simulations as well as the following calculation, it is assumed that the entire mooring line is made from chain with a length of 835m. This simplification was made in the OC4-simulations as well. The total weight and costs are actually lower if a combined line of chains and cables is used. Nevertheless, an indication of the relative differences in mooring cost for the different platforms is given. The selection of moorings is based on the ultimate loads, as explained in chapter 3. For an exact evaluation of the strength and cost of the mooring system, fatigue damage might also be influential.

5.2. Cost development for increasing turbine sizes

The following graph shows the cost development of the mooring lines, the steel for the platform and the wind turbine.

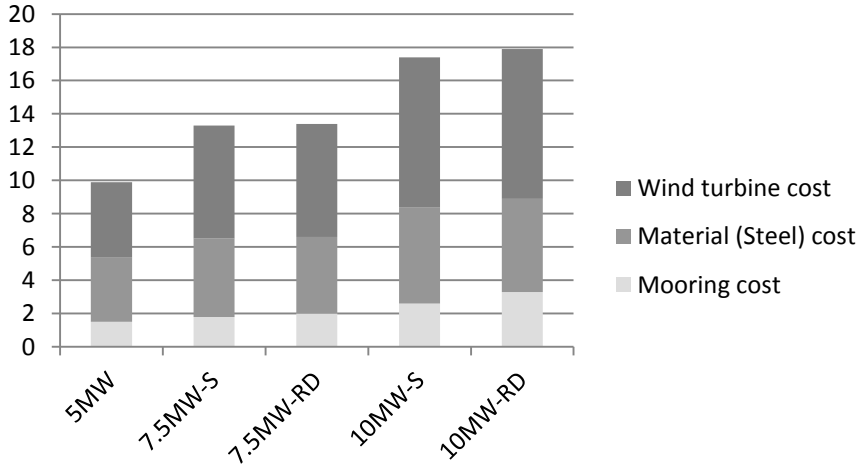

Figure 5-1 Costs of the main FOWT components (in million €)

The plot above shows that the mooring costs rise by a factor smaller than the relative increase of rated power for the scaled platforms, but by a slightly larger factor for the reduced draft design. The difference in cost between the S- and RD-design is 14% for the 7.5MW size and 25% for the 10MW size. A reverse trend can be seen for the material costs, as 2.4% more steel is needed for the 7.5MW-S-platform and 3.9% for the 10MW-S-platform, compared with the respective RD-platform.

It is expected that the future costs of offshore wind turbines in general and for increased power ratings in particular will be reduced (Maples, Hand, & Musial, 2010). The cost per MW of the wind turbine was around only 900€/kW in 2013 (IEA, 2013). As with the platform, one of the main cost drivers is the steel. In the future, savings can be realized by reducing the weight of the turbines through the development of new and more fatigue-resistant materials (EWEA, 2012). The exact costs for 10MW turbines are difficult to estimate, as “the world has no serial production of any industrial equipment of the relevant sizes”, e.g. bearings (Smith P. , 2014b).

Even without taking into account the fixed costs, economies of scale can be seen by looking at the cost figures above. This trend becomes even clearer if the fixed costs are included as well. As the wind turbine costs are also expected to decrease per MW and the mooring costs are probably over dimensioned, the conclusion can be drawn that it is economically justifiable to develop larger FOWT designs. The differences in the total cost between the S- and RD-platforms of the same size are negligible, due to the uncertainties in the mooring design.

6. Summary and Conclusion

The responses to dynamic loads of offshore wind turbines with rated powers of 5MW, 7.5MW and 10MW for two slightly different floating semi-submersible platform designs have been presented in this thesis. As wind and waves are the main environmental loads that act on the system, the consideration was limited to those factors. These turbine sizes were examined, as these will mark the future standards in offshore industry. The geographical and infrastructural conditions of European sites were also examined, and a brief cost consideration was performed. The platforms in the focus of current research efforts are largely influenced by the experiences of the oil and gas industry. The semi-submersible design is very promising, as it combines features of other different auspicious support structures. Specifically, these are the ballast stabilized spar buoy concept, the buoyancy stabilized barge concept and the mooring stabilized tension leg platform. Its main advantage over the other support structures is that, due to shallow draft and good stability behavior, complete construction in the harbor is possible. The starting point for all examined configurations is the semi-submersible platform developed in the DeepCwind-project and studied in the OC4-project (Offshore Code Comparison Collaboration Continuation). This phase of the OC4 was carried under the umbrella of the National Renewable Energy Laboratory (NREL). The NREL also developed the simulation tool FAST, capable of modelling the response of a floating offshore wind turbine to most environmental loads it is exposed to. This program was used for the simulations in this work.
In the following sections the main results and the principal conclusions are presented.

Platform scaling

Based on the 5MW platform design of the OC4-project, two different scaling methodologies were applied to support wind turbines of 7.5MW and 10MW power rating. The dimensions where determined based on the additional weight of the wind turbine to ensure the buoyancy of the structure. In the first methodology all dimensions were increased by the same factor. In the second scaling methodology, the 20m-draft of the initial 5MW-design is kept constant and only the horizontal dimensions were increased. This was done, because the relatively shallow draft of the semi-submersible platform marks one of the key advantages, as it allows a complete installation in the dry dock. The overall volume and total weight (including ballast water) of both scaled versions are identical for the respective turbine size.

Simulations

The main focus of this thesis is set on the analysis and comparison of the platforms' stability for various load cases. The complexity of the tests was increased from simple free-decay simulations, including steady state excitations, operational and extreme offshore conditions in European seas. The data was analyzed in the time and frequency domains, comparing the frequency and resonant responses as well as the absolute values of displacements in all six platform degrees of freedom.

The free decay tests indicate a slightly less damped response from the 10MW-systems compared with the smaller sizes. The natural frequencies in pitch, roll- and heave-motion lie close to the peak-frequencies of the wave frequency spectra for extreme waves. This leads to increased amplitudes in the motion along these degrees of freedom due to resonant response. In pitch-motion, the most critical of the six degrees of freedom of the platform, larger platforms show a slightly higher response to acting forces. In operational conditions, the slightly changed platform type with reduced draft shows better stability in pitch in comparison with the straight upscale. This can be explained by the slightly larger heave-plate area of the design with a draft reduced to 20m. Nevertheless, the platforms with a reduced draft showed a higher resonant response to the wave frequencies, which causes big pitch angles of these platforms in extreme wave conditions.
The large 10MW-platforms show a high resonant response in sway and yaw for extreme conditions. This might cause problems for the structural stability of the whole system, though this is not examined in this work.

Additionally, the larger the platform is, the greater the displacement in surge. This result is most probably influenced by the mooring system, which was kept the same for all systems to ensure a better comparability.

Another critical factor for the evaluation of a floating wind turbine is the nacelle acceleration. The tests showed that the threshold value of 1.96m/s^2 was not exceeded in any of the analyzed load cases and platform designs.

Infrastructural considerations

The examination of European ship yards and dry docks showed that facilities with sufficient dimensions for the construction of 10MW-systems are available in Europe to cover many potential floating wind farm areas. The main limitation is the width of the dry docks. The availability and costs of cranes with sufficient dimensions is not examined, but should also be taken into consideration for the selection of a construction side.

Costs

The influence of the scaling of the system on various cost drivers was examined. The costs for steel, mooring, working hours for construction and dry dock fees are expected to increase with platform size, while certain fixed costs such as environmental surveys, costs for renting installation vessel and the grid connection is not influenced by the size of the platform and turbine. Steel is the main cost driver for the platform. A basic cost comparison based on the main components of the floating system validates the assumption that an economy of scale is present at least up to power ratings of 10MW.

To conclude it can be said, that the development of larger semi-submersible platforms than the 5MW design is not just beneficial from an economical point of view, but also technically feasible due to the good stability characteristics.

7. Suggested further work

The proposals for further work are:

- Verify the findings with NREL's model of the semi-submersible platform using hydrodynamic calculations of the platform components, using Morrison equation. This has been made available in the new version of FAST 8.08.
- Perform a structural and fatigue analysis of the FOWT-systems. This includes investigating on designs with a minimized steel wall thickness for the platform. An increased structural stability could be achieved with reinforcing ribs.
- Optimize the platform design to decrease the extreme resonant response and evaluate the realistic life time of a large-scale floating wind turbine.
- Perform a profound economic analysis, including a cost-model to estimate an absolute value for the costs of each platform type and size and an estimation of the steel wall thickness` influence on the total costs. Furthermore, the economical justifiable distance to shore and shipyard needs to be determined.
- Simulations of the 7.5MW and 10MW designs with a specifically designed mooring system should be performed.

Bibliography

4COffshore. (2014a). *SWT-6.0-154*. Retrieved March 17, 2014, from 4COffshore: http://www.4coffshore.com/windfarms/turbine-siemens-swt-6.0-154-tid127.html

4COffshore. (2014b). *V164-8.0 MW*. Retrieved March 10, 2014, from 4COffshore: http://www.4coffshore.com/windfarms/turbine-vestas-v164-8.0-mw-tid89.html

4COffshore. (2014c). *Azimut Project*. Retrieved April 26, 2014, from 4C offshore: http://www.4coffshore.com/windfarms/turbine-gamesa-azimut-project-tid17.html

Able UK ltd. (2014). *ABLE Seaton Port - Dry Dock*. Retrieved June 24, 2014, from Able UK: http://www.ableuk.com/sites/port-sites/seaton-port/dry-dock/

ABS. (2013). *Guide for building and classing Floating offshore wind turbine installations.* Houston: American Bureau of Shipping, p.24.

Alstom. (2013a, December 3). *Alstom installing world's largest offshore wind turbine off the Belgian coast*. Retrieved March 17, 2014, from Alstom: http://www.alstom.com/press-centre/2013/11/alstom-installing-worlds-largest-offshore-wind-turbine-/

Alstom. (2013b, November 20). *Alstom's 6MW Haliade offshore wind turbine loaded at Ostend.* Retrieved March 11, 2014, from Alstom: http://www.alstom.com/press-centre/2013/9/alstoms-6mw-haliade-offshore-wind-turbine-loaded-at-ostend/

Alstom. (2014). *Haliade™ 150-6MW Offshore wind turbine.* Retrieved March 10, 2014, from Alstom: http://www.alstom.com/Global/Power/Resources/Documents/Brochures/offshore-wind-turbine-6mw-robust-simple-efficient.pdf

Bak, C., Zahle, F., Bitsche, R., Kim, T., Yde, A., Henriksen, L., et al. (2013). *Description of the 10 MW DTU Reference Wind Turbine.* Roskilde: DTU Wind Energy, pp.13-24.

BBC News. (2010, December 03). *European nations agree on offshore North Sea electric grid*. Retrieved June 23, 2014, from BBC News Business: http://www.bbc.co.uk/news/business-11909048

Berlinger, F., Clausen, C., & Siegel, H. (2013, September 23). *Students hope their ship inspection robot will significantly reduce dry-dock time for maritime transport industry, improve safety for inspectors*. Retrieved June 25, 2014, from Robohub: http://robohub.org/students-hope-their-ship-inspection-robot-will-significantly-reduce-dry-dock-time-for-maritime-transport-industry-improve-safety-for-inspectors/

Bossler, A. (2014). Japan`s Floating Offshore Wind Projects: An Overview. *energy ocean conference June 03-05 2014.* Atlantic City: Main(e) International Consulting LLC, p.4.

Capuzzo, N. (2012, July 9). *The largest drydock in Marseille officially handed over*. Retrieved June 23, 2014, from Ship to Shore: http://www.ship2shore.it/english/articolo.php?id=9816

Cozijn, H., Uittenbogaard, R., & Brake, E. t. (2005). Heave, Roll and Pitch Damping of a Deepwater CALM Buoy with a Skirt. *15th International Offshore and Polar Engineering Conference.* Seoul: The International Society of Offshore and Polar Engineers.

Crozier, A. (2011). *Design and Dynamic Modeling of the Support Structure for a 10 MW Offshore Wind Turbine.* Trondheim: NTNU - Norwegian University of Science and Technology, p.44;pp.87-94.

Damen. (2011). *Walk-to-work vessel*. Retrieved June 23, 2014, from Damen: http://www.damen.com/en/markets/walk-to-work-vessel

Duarte, T. (2014). *Offshore Wind Turbine Foundations - lecture.* Lisbon: IST.

Duenas-Osorio, L., & Basu, B. (2007). Unavailability of wind turbines due to wind induced accelerations. In *Engineering Structures Vol. 30.* Houston: Elsevier, pp.885-893.

EnchantedLearning. (2002). *Outline Map of Europe.* Retrieved June 23, 2014, from enchantedlearning: http://www.enchantedlearning.com/geography/europe/outlinemap/

EWEA. (2012). *Development of the Cost of Offshore Wind Power up to 2015*. Retrieved July 02, 2014, from Wind Energy - The Facts: http://www.wind-energy-the-facts.org/development-of-the-cost-of-offshore-wind-power-up-to-2015.html

EWEA. (2013). *Deep Water - The next step for offshore wind energy.* Brussels: European Wind Energy Association, pp.13-26.

EWEA. (2014a). *Wind in power - 2013 European statistics.* Brussels: European Wind Energy Association, pp.2-12.

EWEA. (2014b). *The European offshore wind industry - key trends and statistics 2013.* Brussels: European Wind Energy Agency, pp.5-15.

Foster, M. (2013, October 28). *Hitachi floating turbine generating power*. Retrieved April 23, 2014, from Wind Power Offshore: http://www.windpoweroffshore.com/article/1218417/hitachi-floating-turbine-generating-power

Fraunhofer IWES. (n.d.). *Locations*. Retrieved June 23, 2014, from windmonitor: http://windmonitor.iwes.fraunhofer.de/windwebdad/www_reisi_page_new.show_page?page_nr=417&lang=en&owa=&owa_own_header=0

Freestone, B. (2014, February 7). *The 50 Year Storm?* Retrieved June 17, 2014, from Magic Sea Weed: http://magicseaweed.com/news/the-50-year-storm/6070/

Garus, K. (2014, January 23). *Vestas builds the first V164-8.0*. Retrieved March 10, 2014, from Sun & Wind Energy: http://www.sunwindenergy.com/wind-energy/vestas-builds-first-v164-80

Green, R., & Vasilakos, N. (2013). *The Economics of Offshore Wind.* Birmingham: University of Birmingham, pp.8-9.

Hall, M. T. (2010). *Mooring Line Modelling and Design Optimization of Floating Offshore Wind Turbines.* New Brunswick: University of New Brunswick, p.103.

harland and wolff heavy industries ltd. (2010). *facilities*. Retrieved June 23, 2014, from harland and wolff heavy industries ltd: http://www.harland-wolff.com/Facilities-%282%29.aspx

House of Commons. (2012). *A European Supergrid.* London: The Stationery Office Limited, p.7.

Hughes, G. (2012). *The Performance of Wind Farms in the United Kingdom and Denmark.* London: Renewable Energy Foundation, p.16.

Idwal Marine Services Limited. (2014). *Dry-Dock Management*. Retrieved June 25, 2014, from http://www.imarserv.com/dry-dock-management.php

IEA. (2013). *Technology Roadmap - Wind Energy.* Paris: International Energy Agency, p.14.

IEC. (2005). *61400-1 Wind turbines - design requirements.* Geneva: International Electrotechnical Commission.

Jensen, T. (2009, August 10). *UPDATE 2-Maersk says to shut Odense shipyard*. Retrieved June 23, 2014, from Reuters: http://www.reuters.com/article/2009/08/10/maersk-shipyard-idUSLA32128520090810

Jonkman, B., & Jonkman, J. (2013). *ReadMe File for FAST v8.03.02b-bjj.* Golden: National Renewable Energy Laboratory, p.2.

Jonkman, J. M., & Buhl, M. L. (2005). *FAST User's Guide.* Golden: National Renewable Energy Laboratory.

Jonkman, S., Butterfield, S., Musial, W., & Scott, G. (2009). *Definition of a 5-MW Reference Wind Turbine for Offshore System Development.* Golden: NREL - National Renewable Energy Labratory, pp.15-16.

Karimirad, M., Gao, Z., & Moan, T. (2009). Dynamic Motion Analysis of Catenary Moored Spar Wind Turbine in Extreme Environmental Condition. *European Offshore Wind Conference 14.-16. September 2009.* Stockholm: EWEA, p.7.

Kelley, N., & Jonkman, B. (2007). *Overview of the TurbSim Stochastic Inflow Turbulence Simulator.* Golden: National Renewable Energy Laboratory.

Keppel Verolme. (2013). *Yard facilities*. Retrieved June 23, 2014, from http://www.keppelverolme.nl/en/over-ons/yard-facilities

Lindyberg, R., Viselli, A., Watt, A., Dagher, H. J., Elston, S., Graham, P., et al. (2012). *Maine Deepwater Offshore.* Orono: University of Maine.

Lisnave Estaleiros Navais, SA. (2014). *Drydocks*. Retrieved October 13, 2014, from Lisnave: http://www.lisnave.pt/yards.htm

London Array Limited. (2014). *How it all began*. Retrieved April 21, 2014, from http://www.londonarray.com/the-project/

Maciel, J. G. (2010). *The WindFloat project.* Lisbon: edp, p.24.

Maples, B., Hand, M., & Musial, W. (2010). *Comparative Assessment of Direct Drive High Temperature Superconducting Generators in Multi-Megawatt Class Wind Turbines.* Golden: NREL, p.10.

MarineLink. (2013, February 20). *Principle Power Names WindFloat Partners*. Retrieved March 23, 2014, from MarineLink: http://www.marinelink.com/news/principle-windfloat351815.aspx

Masciola, M. D., Robertson, A. N., Jonkman, J. M., Molta, P., Goupee, A. J., Coulling, A. J., et al. (2013). Summary of Conclusions and Recommendations Drawn from the DeepCWind Scaled Floating Offshore Wind System Test Campaign. *ASME 2013 32nd International Conference on Ocean, Offshore and Arctic Engineering 9-14 June 2013.* Nantes: NREL, p.8.

Matha, D., & Jonkman, J. (2009). *A Quantitative Comparison of the Responses of Three Floating Platforms.* Stockholm: NREL.

MEPS International Ltd. (2014). *MEPS - World Carbon Steel Prices - with individual product forecasts*. Retrieved June 25, 2014, from http://www.meps.co.uk/World%20Carbon%20Price.htm

MI&T. (2014). *MiniFloat™*. Retrieved April 24, 2014, from Marine Innovation & Technology: http://marineitech.com/index.php?option=com_content&view=article&id=46&Itemid=82

MODEC Inc. (2013, February). *Floating Wind & Current Hybrid Power Generation.* Retrieved April 23, 2014, from http://www.modec.com/fps/skwid/pdf/skwid.pdf

Musial, W., & Jonkman, J. (2010). *Offshore Code Comparison (OC3) for IEA Task 23 Offshore Wind Technology and Development.* Golden: National Renewable Energy Laboratory.

Nautica Winpower. (2011). *Design Advantage*. Retrieved April 23, 2014, from Nautica Windpower: http://www.nauticawindpower.com/

Navantia. (n.d.). *San Fernando-Puerto Real Shipyard Facilities.* Retrieved June 23, 2014, from http://www.navantia.es/eng/files/Datos_Tecnicos_Astilleros_San_Fernando_Puerto_Real_EN.pdf

Nixon, N. (2008, October 17). *Timeline: The history of wind power*. Retrieved June 11, 2014, from the guardian: http://www.theguardian.com/environment/2008/oct/17/wind-power-renewable-energy

OC4. (2013). *Description of Load Cases for OC4, Phase II.* Boulder: NREL.

PE. (2013, November 5). *Giant 7MW Fife offshore turbine completed*. Retrieved March 17, 2014, from Institution of mechanical engineers: http://www.imeche.org/news/engineering/giant-7mw-fife-offshore-turbine-completed

Peeringa, J., Brood, R., Ceyhan, O., Engels, W., & Winkel, G. d. (2011). *Upwind 20MW Wind Turbine Pre-Design.* Petten: Energy Research Centre of the Netherlands .

Poseidon Floating Power. (2013). *Wind and Wave in One*. Retrieved April 23, 2014, from Poseidon Floating Power: http://www.floatingpowerplant.com/?pageid=321

RAB. (2010). *Value breakdown for the offshore wind sector.* London: Renewable Advisory Board, pp.6-16.

Reiff, H. (2009, June 25). *Trockendock 8 und 8a von HDW in Kiel*. Retrieved June 23, 2014, from fotocommunity: http://www.fotocommunity.de/pc/pc/display/17590460

REpower Systems SE. (2005). *Das 5-Megawatt-Kraftwerk mit 126 Meter Rotordurchmesser.* Retrieved March 11, 2014, from http://www.senvion.com/fileadmin/download/produkte/RE_PP_5M_de.pdf?fromold=1

Robertson, A., Jonkman, J., Masciola, M., Song, H., Goupee, A., Coulling, A., et al. (2013b). *Definition of the Semisubmersible Floating System for Phase II of OC4.* Golden: NREL, p.6.

Robertson, Jonkman, J., Musial, W., Vorpahl, F., & Popko, W. (2013a). *Offshore Code Comparison Collaboration, Continuation: Phase II Results of a Floating Semisubmersible Wind System.* Golden: National Renewable Energy Laboratory.

Roddier, D., Cermelli, C., Aubault, A., & Weinstein, A. (2010). *WindFloat: A floating foundation for offshore wind turbines.* Seattle: AIP Puplishing LLC., p.9.

RSE. (2012). *Ricerca sul Systema Energetico*. Retrieved April 26, 2014, from Orecca WebGIS: http://map.rse-web.it/orecca/map.phtml

RWE. (2013). *Operation and maintenance*. Retrieved March 24, 2014, from Offshore wind farm Nordsee Ost: http://www.rwe.com/web/cms/en/962060/offshore-wind-farm-nordsee-ost/facts-and-figures/operation-and-maintenance/

Saygi, S. S. (2011). *Assessing the Economics of Offshore Renewable Energies and the Portuguese Supply Chain.* Lisbon: IST, p.10; p.23; p.28.

Schmidt, A., & Ahrendt, D. K. (2006). *Die Ökologie der Nordsee - Aktuelle Nutzungsprobleme und Trends.* Kiel, p.10.

Siemens. (2011, June 9). *Siemens starts operating its first 6 megawatt wind turbine*. Retrieved March 17, 2014, from Siemens: https://www.siemens.com/press/en/pressrelease/?press=/en/pressrelease/2011/renewable_energy/ere201106070.htm

Sillanpää, K. (2009, December 04). *Helsingin kaupungin kansainvälinen yhteistyö.* Retrieved June 23, 2014, from STX Europe: http://www.hel.fi/hel2/ajankohtaista/kavo/Sillanpaa.pdf

Smith, P. (2014a, February 18). *First order for Vestas V164 turbine*. Retrieved March 10, 2014, from Wind Power Offshore: http://www.windpoweroffshore.com/article/1281230/first-order-vestas-v164-turbine

Smith, P. (2014b, June 9). *Question of the week: Do we need a 10MW turbine?* Retrieved June 11, 2014, from Wind Power Monthly: http://www.windpowermonthly.com/article/1297819/question-week-need-10mw-turbine

stx France. (2014). *Industrial Facilities*. Retrieved June 23, 2014, from Industrial tools: http://www.stxfrance.com//UK/stxfrance-moyenstnazaire-0-moyens%20industriels.awp

Subsea World News. (2012, March 21). *Belgium: Five Grid Initiatives Call on Decision Makers to Accelerate European Supergrid*. Retrieved June 23, 2014, from Subsea World News: http://subseaworldnews.com/2012/03/21/belgium-five-grid-initiatives-call-on-decision-makers-to-accelerate-european-supergrid/

Sun, X., Huang, D., & Wu, G. (2012). The current state of offshore wind energy technology development. *Energy No. 41.* Shanghai: Elisier, pp.298-312.

Suzuki, K., Yamaguchi, H., Akase, M., Imakita, A., Ishihara, T., Fukumoto, Y., et al. (2010). *Initial Design of TLP for Offshore Wind Farm.* Tokyo: Mitsui Engineering and Shipbuilding Co., Ltd, p.1.

Technip. (2011). *World-class semi-submersible platforms.* Paris: Technip, p.5.

University of Maine. (2014). *Floating Turbine Design*. Retrieved April 24, 2014, from DeepCwind consortium: http://www.deepcwind.org/research-initiative/floating-turbine-design

Valverde, P. (2014). *The WindFloat Project - WindFloat 2 MW Floating Offshore Wind.* Lisbon: edp.

Vicinay Cadenas, S.A. (2011). *The future of mooring.* Bilbao: Vicinay Cadenas, p.29.

Vries, E. d. (2013, September 9). *Close up - Vestas V164-8.0 nacelle and hub*. Retrieved March 10, 2014, from Wind power monthly: http://www.windpowermonthly.com/article/1211056/close---vestas-v164-80-nacelle-hub

WAMIT, Inc. (2013b). Retrieved April 25, 2014, from WAMIT-website: http://www.wamit.com/index.htm

Wayman, E. (2006). *Coupled Dynamics and Economic Analysis of Floating Wind Turbine Systems.* Cambridge, USA: Massachusetts Institute of Technology, p.20; p.55.

WEF. (2012). *History*. Retrieved June 11, 2014, from Wind Energy Foundation: http://www.windenergyfoundation.org/about-wind-energy/history

Wiser, R., Yang, Z., Hand, M., Hohmeyer, O., Infield, D., Jensen, P. H., et al. (2011). *Wind Energy. In IPCC Special Report on Renewable Energy Sources and Climate Change Mitigation.* Cambridge: Cambridge University Press.

Wynn, G. (2012, October 03). *Offshore wind prospects hit by grid costs*. Retrieved June 24, 2014, from The Sydney Morning Herald: http://www.smh.com.au/environment/climate-change/offshore-wind-prospects-hit-by-grid-costs-20121003-26y5b.html

Appendix

A Wind Turbine Specification

Remark: More detailed information regarding the blade shapes can be read from the information provided in the AeroDyn files in part B of the Appendix.

NREL 5-MW Offshore Baseline Wind Turbine

Tower

NREL 5 MW OWT tower short		
real height	height fraction	tower section mass per unit length
(m)	(-)	(kg/m)
0.00	0.0	4667.0
7.76	0.1	4345.3
15.52	0.2	4034.8
23.28	0.3	3735.4
31.04	0.4	3447.3
38.80	0.5	3170.4
46.56	0.6	2904.7
54.32	0.7	2650.2
62.08	0.8	2406.9
69.84	0.9	2174.8
77.60	1.0	1953.9
total mass	**(kg)**	**249,718**

for FAST tower file input, based on (Robertson A. , et al., 2013b)

DTU 10 MW Reference Wind Turbine

Comparison of the actual DTU 10MW RWT-design and the parameters resulting from following a direct upscaling approach of the NREL 5MW

Parameter	DTU 10MW RWT	Upscaled NREL 5MW
Wind Regime	IEC Class 1A	IEC Class 1B
Rotor Orientation	Clockwise rotation - Upwind	Same
Control	Variable Speed	Same
	Collective Pitch	Same
Cut in wind speed	4 m/s	Same
Cut out wind speed	25 m/s	Same
Rated wind speed	11.4 m/s	Same
Rated power	10 MW	Same
Number of blades	3	Same
Rotor Diameter	178.3 m	Same
Hub Diameter	5.6 m	4.24 m
Hub Height	119.0 m	127.0
Drivetrain	Medium Speed, Multiple-Stage Gearbox	High Speed, Multiple-Stage Gearbox
Minimum Rotor Speed	6.0 rpm	4.9 rpm
Maximum Rotor Speed	9.6 rpm	8.6 rpm
Maximum Generator Speed	480.0 rpm	1173.7 rpm
Gearbox Ratio	50	97
Maximum Tip Speed	90.0 m/s	79.9 m/s
Hub Overhang	7.1 m	Same
Shaft Tilt Angle	5.0 deg.	Same
Rotor Precone Angle	-2.5 deg.	Same
Blade Prebend	3.332 m	0.000 m
Rotor Mass	227,962 kg	311,127 kg
Nacelle Mass	446,036 kg	678,823 kg
Tower Mass	628,442 kg	982,765 kg

(Bak, et al., 2013)

Tower

height m	outer diameter m	wall thickness mm
0.000	8.3000	38
11.500	8.0215	38
11.501	8.0215	36
23.000	7.7431	36
23.001	7.7430	34
34.500	7.4646	34
34.501	7.4646	32
46.000	7.1861	32
46.001	7.1861	30
57.500	6.9076	30
57.501	6.9076	28
69.000	6.6292	28
69.001	6.6291	26
80.500	6.3507	26
80.501	6.3507	24
92.000	6.0722	24
92.001	6.0722	22
103.500	5.7937	22
103.501	5.7937	20
115.630	5.5000	20

Table 4.15.: Wall thickness distribution of the tower.

(Bak, et al., 2013)

DTU 10 MW RWT tower short		
real height	height fraction	tower section mass per unit length
(m)	(-)	(kg/m)
0.00	0.0	7637.1
10.24	0.1	7395.0
20.49	0.2	6768.7
30.73	0.3	6160.3
40.97	0.4	5578.1
51.22	0.5	5022.3
61.46	0.6	4492.7
71.70	0.7	3989.5
81.94	0.8	3512.5
92.19	0.9	3060.6
102.43	1.0	2926.7
total mass	(kg)	525,072

7.5MW turbine

tower

7.5 MW turbine tower		
real height	height fraction	tower section mass per unit length
(m)	(-)	(kg/m)
0.00	0.0	6152.1
9.00	0.1	5870.1
18.00	0.2	5401.7
27.00	0.3	4947.9
36.01	0.4	4512.7
45.01	0.5	4096.4
54.01	0.6	3698.7
63.01	0.7	3319.8
72.01	0.8	2959.7
81.01	0.9	2617.7
90.02	1.0	2440.3
total mass	(kg)	375,550

B FAST input files

AeroDyn

7.5MW AeroDyn file

```
7.5 MW      offshore    baseline    aerodynamic input properties
SI          SysUnits    - System of units for used for input and output [must be SI for FAST] (unquoted string)
STEADY      StallMod    - Dynamic stall included [BEDDOES or STEADY] (unquoted string)
USE_CM      UseCm       - Use aerodynamic pitching moment model? [USE_CM or NO_CM] (unquoted string)
DYNIN       InfModel    -     Inflow model [DYNIN or EQUIL] (unquoted string)
SWIRL       IndModel    -     Induction-factor model [NONE or WAKE or SWIRL] (unquoted string)
0.005       AToler      -     Induction-factor tolerance (convergence criteria) (-)
PRANDtl     TLModel     -     Tip-loss model (EQUIL only) [PRANDtl, GTECH, or NONE] (unquoted string)
PRANDtl     HLModel     -     Hub-loss model (EQUIL only) [PRANdtl or NONE] (unquoted string)
..\WindData\NoShr_13.wnd    WindFile    -     Name of file containing wind data (quoted string)
104.5       HH          -     Wind reference (hub) height [TowerHt+Twr2Shft+OverHang*SIN(ShftTilt)] (m)
0.0         TwrShad     -     Tower-shadow velocity deficit (-)
9999.9      ShadHWid    -     Tower-shadow half width (m)
9999.9      T_Shad_Refpt      -     Tower-shadow reference point (m)
1.225       AirDens     -     Air density (kg/m^3)
1.46E-05    KinVisc     -     Kinematic air viscosity [CURRENTLY IGNORED] (m^2/sec)
0.0125      DTAero      -     Time interval for aerodynamic calculations (sec)
6           NumFoil     -     Number of airfoil files (-)
..\AeroData\Cylinder.dat    FoilNm      -     Names of the airfoil files [NumFoil lines] (quoted strings)
..\AeroData\FFA-W3-600.dat
..\AeroData\FFA-W3-480.dat
..\AeroData\FFA-W3-360.dat
..\AeroData\FFA-W3-301.dat
..\AeroData\FFA-W3-241.dat
38          BldNodes    -     Number of blade nodes used for analysis (-)
RNodes      AeroTwst    DRNodes     Chord Nfoil PrnElm
```

```
3.76        14.5        3.22        4.573 1     NOPRINT
6.505       14.5        2.27        4.573 1     NOPRINT
9.25        14.436      3.22        4.632 1     NOPRINT
11.882      13.882      2.044       4.792 2     NOPRINT
14.401      12.536      2.994       4.988 2     NOPRINT
16.969      10.602      2.142       5.160 3     NOPRINT
19.586      8.886       3.092       5.257 3     NOPRINT
22.225      7.8         2.186       5.273 4     NOPRINT
24.884      7.023       3.132       5.222 4     NOPRINT
27.527      6.386       2.154       5.118 5     NOPRINT
30.153      5.787       3.098       4.974 5     NOPRINT
32.778      5.239       2.152       4.803 5     NOPRINT
35.404      4.681       3.1         4.611 5     NOPRINT
37.923      4.108       1.938       4.414 6     NOPRINT
40.336      3.532       2.888       4.217 6     NOPRINT
42.748      2.942       1.936       4.013 6     NOPRINT
45.161      2.348       2.89        3.805 6     NOPRINT
47.574      1.76        1.936       3.598 6     NOPRINT
49.781      1.235       2.478       3.409 6     NOPRINT
51.785      0.777       1.53        3.240 6     NOPRINT
53.788      0.339       2.476       3.074 6     NOPRINT
55.792      -0.077      1.532       2.910 6     NOPRINT
57.795      -0.47       2.474       2.750 6     NOPRINT
59.562      -0.798      1.06        2.612 6     NOPRINT
61.093      -1.068      2.002       2.496 6     NOPRINT
62.624      -1.331      1.06        2.383 6     NOPRINT
64.155      -1.588      2.002       2.271 6     NOPRINT
65.687      -1.843      1.062       2.163 6     NOPRINT
67.001      -2.061      1.566       2.073 6     NOPRINT
68.099      -2.243      0.63        1.997 6     NOPRINT
69.197      -2.426      1.566       1.917 6     NOPRINT
70.295      -2.609      0.63        1.828 6     NOPRINT
71.393      -2.787      1.566       1.726 6     NOPRINT
72.349      -2.937      0.346       1.624 6     NOPRINT
73.164      -3.059      1.284       1.520 6     NOPRINT
73.978      -3.172      0.344       1.389 6     NOPRINT
74.792      -3.278      1.284       1.212 6     NOPRINT
75.606      -3.384      0.344       0.939 6     NOPRINT
```

10MW AeroDyn file

Remark: Only input variables that change compared to the 7.5MW AeroDyn Input file are listed

```
DTU 10 MW offshore baseline aerodynamic input properties
119.0      HH          - Wind reference (hub) height [TowerHt+Twr2Shft+OverHang*SIN(ShftTilt)] (m)
1.225      AirDens     - Air density (kg/m^3)
  38       BldNodes    - Number of blade nodes used for analysis (-)
RNodes     AeroTwst   DRNodes    Chord Nfoil PrnElm
4.4100     14.500     3.2200     5.380 1     NOPRINT
7.6300     14.500     3.2200     5.380 1     NOPRINT
10.8500    14.436     3.2200     5.449 1     NOPRINT
13.9375    13.882     2.9550     5.638 2     NOPRINT
16.8925    12.536     2.9550     5.868 2     NOPRINT
19.9050    10.602     3.0700     6.071 3     NOPRINT
22.9750    8.886      3.0700     6.185 3     NOPRINT
26.0700    7.800      3.1200     6.203 4     NOPRINT
29.1900    7.023      3.1200     6.143 4     NOPRINT
32.2900    6.386      3.0800     6.021 5     NOPRINT
35.3700    5.787      3.0800     5.852 5     NOPRINT
38.4500    5.239      3.0800     5.650 5     NOPRINT
41.5300    4.681      3.0800     5.425 5     NOPRINT
44.4850    4.108      2.8300     5.193 6     NOPRINT
47.3150    3.532      2.8300     4.961 6     NOPRINT
50.1450    2.942      2.8300     4.721 6     NOPRINT
52.9750    2.348      2.8300     4.477 6     NOPRINT
55.8050    1.760      2.8300     4.233 6     NOPRINT
```

```
58.3950    1.235      2.3500     4.011 6    NOPRINT
60.7450    0.777      2.3500     3.812 6    NOPRINT
63.0950    0.339      2.3500     3.616 6    NOPRINT
65.4450    -0.077     2.3500     3.423 6    NOPRINT
67.7950    -0.470     2.3500     3.235 6    NOPRINT
69.8680    -0.798     1.7960     3.073 6    NOPRINT
71.6640    -1.068     1.7960     2.936 6    NOPRINT
73.4600    -1.331     1.7960     2.803 6    NOPRINT
75.2560    -1.588     1.7960     2.672 6    NOPRINT
77.0520    -1.843     1.7960     2.545 6    NOPRINT
78.5940    -2.061     1.2880     2.439 6    NOPRINT
79.8820    -2.243     1.2880     2.349 6    NOPRINT
81.1700    -2.426     1.2880     2.255 6    NOPRINT
82.4580    -2.609     1.2880     2.150 6    NOPRINT
83.7460    -2.787     1.2880     2.030 6    NOPRINT
84.8676    -2.937     0.9552     1.910 6    NOPRINT
85.8228    -3.059     0.9552     1.788 6    NOPRINT
86.7780    -3.172     0.9552     1.634 6    NOPRINT
87.7332    -3.278     0.9552     1.426 6    NOPRINT
88.6884    -3.384     0.9552     1.105 6    NOPRINT
```

HydroDyn

7.5MW HydroDyn file – Scaled

------- HydroDyn v2.00.* Input File ----------

NREL 5.0 MW offshore baseline floating platform HydroDyn input properties for the OC4 semisubmersible (platform approximated by a cylinder).

False	Echo	- Echo the input file data (flag)
---------- ENVIRONMENTAL CONDITIONS ----------		
1025.0	WtrDens	- Water density (kg/m^3)
200.0	WtrDpth	- Water depth (meters)
0.0	MSL2SWL	- Offset between still-water level and mean sea level (meters) [positive upward; must be zero if HasWAMIT=TRUE]
---------- WAVES ----------		
2	WaveMod	- Incident wave kinematics model {0: none=still water, 1: plane progressive (regular), 1P#: plane progressive with user-specified phase, 2: JONSWAP/Pierson-Moskowitz spectrum (irregular), 3: White noise spectrum, 4: user-defined spectrum from routine UserWaveSpctrm (irregular), 5: GH Bladed wave data [option 5 is invalid for HasWAMIT = TRUE]} (switch)
0	WaveStMod	- Model for stretching incident wave kinematics to instantaneous free surface {0: none=no stretching, 1: vertical stretching, 2: extrapolation stretching, 3: Wheeler stretching} (switch) [unused when WaveMod=0 or when HasWAMIT = TRUE]
3630.0	WaveTMax	- Analysis time for incident wave calculations (sec) [unused when WaveMod=0] [determines WaveDOmega=2Pi/WaveTMax in the IFFT]
0.25	WaveDT	- Time step for incident wave calculations (sec) [unused when WaveMod=0] [0.1<=WaveDT<=1.0 recommended] [determines WaveOmegaMax=Pi/WaveDT in the IFFT]
6.0	WaveHs	- Significant wave height of incident waves (meters) [used only when WaveMod=1, 2, or 3]
10.0	WaveTp	- Peak-spectral period of incident waves (sec) [used only when WaveMod=1 or 2]
DEFAULT	WavePkShp	- Peak-shape parameter of incident wave spectrum (-) or DEFAULT (unquoted string) [used only when WaveMod=2] [use 1.0 for Pierson-Moskowitz]
0.0	WvLowCOff	- Low cut-off frequency or lower frequency limit of the wave spectrum beyond which the wave spectrum is zeroed (rad/s) [used only when WaveMod=2, 4, or 5]
500.0	WvHiCOff	- High cut-off frequency or upper frequency limit of the wave spectrum beyond which the wave spectrum is zeroed (rad/s) [used only when WaveMod=2, 4, or 5]
0.0	WaveDir	- Incident wave propagation heading direction (degrees) [unused when WaveMod=0 or 5]

```
123456789       WaveSeed(1)    - First  random seed of incident waves [-2147483648 to 2147483647] (-) [unused when WaveMod=0 or 5]
1011121314    WaveSeed(2)    - Second random seed of incident waves [-2147483648 to 2147483647] (-) [unused when WaveMod=0 or 5]
FALSE           WaveNDAmp    - Flag for normally distributed amplitudes (flag)
""              GHWvFile       - Root name of GH Bladed files containing wave data (quoted string) [used only when WaveMod=5]
1               NWaveElev      - Number of points where the incident wave elevations can be computed (-) [maximum of 9 output locations]
0               WaveElevxi     - List of xi-coordinates for points where the incident wave elevations can be output (meters) [NWaveElev points, separated by
                                 commas or white space; ususued if NWaveElev = 0]
0               WaveElevyi     - List of yi-coordinates for points where the incident wave elevations can be output (meters) [NWaveElev points, separated by
                                 commas or white space; ususued if NWaveElev = 0]
---------------------- CURRENT ------------------------------------------------
0               CurrMod        - Current profile model {0: none=no current, 1: standard, 2: user-defined from routine UserCurrent} (switch)
0.0             CurrSSV0       - Sub-surface current velocity at still water level (m/s) [used only when CurrMod=1]
DEFAULT         CurrSSDir      - Sub-surface current heading direction (degrees) or DEFAULT (unquoted string) [used only when CurrMod=1]
20.0            CurrNSRef      - Near-surface current reference depth (meters) [used only when CurrMod=1]
0.0             CurrNSV0       - Near-surface current velocity at still water level (m/s) [used only when CurrMod=1]
0.0             CurrNSDir      - Near-surface current heading direction (degrees) [used only when CurrMod=1]
0.0             CurrDIV        - Depth-independent current velocity (m/s) [used only when CurrMod=1]
0.0             CurrDIDir      - Depth-independent current heading direction (degrees) [used only when CurrMod=1]
---------------------- FLOATING PLATFORM ---------------------------------------
TRUE            HasWAMIT       - Using WAMIT (flag)
"..\HydroData\marin_semi" WAMITFile    - Root name of WAMIT output files
1.13            WAMITULEN      - Characteristic body length scale used to redimensionalize WAMIT output (meters)
1.994E4         PtfmVol0       - Displaced volume of water when the platform is in its undisplaced position (m^3)
0.0             PtfmCOBxt      - The xt offset of the center of buoyancy (COB) from the platform reference point (meters)
0.0             PtfmCOByt      - The yt offset of the center of buoyancy (COB) from the platform reference point (meters)
1               RdtnMod        - Radiation memory-effect model {0: no memory-effect calculation, 1: convolution, 2: state-space} (switch)
60.0            RdtnTMax       - Analysis time for wave radiation kernel calculations (sec) [determines RdtnDOmega=Pi/RdtnTMax in the cosine transform]
0.0125          RdtnDT         - Time step for wave radiation kernel calculations (sec) [DT<=RdtnDT<=0.1 recommended]
---------------------- FLOATING PLATFORM FORCE FLAGS  -------------------------
```

```
True             PtfmSgF        - Platform horizontal surge translation force (flag) or DEFAULT
True             PtfmSwF        - Platform horizontal sway translation force (flag) or DEFAULT
True             PtfmHvF        - Platform vertical heave translation force (flag) or DEFAULT
True             PtfmRF         - Platform roll tilt rotation force (flag) or DEFAULT
True             PtfmPF         - Platform pitch tilt rotation force (flag) or DEFAULT
True             PtfmYF         - Platform yaw rotation force (flag) or DEFAULT
---------------------- FLOATING PLATFORM ADDITIONAL STIFFNESS AND DAMPING  -----
   0.0      0.0      0.0   0.0   0.0        0.0   AddF0    - Additional preload (N, N-m)
   0.0      0.0      0.0   0.0   0.0        0.0   AddCLin  - Additional linear stiffness (N/m, N/rad, N-m/m, N-m/rad)
   0.0      0.0      0.0   0.0   0.0        0.0
   0.0      0.0      0.0   0.0   0.0        0.0
   0.0      0.0      0.0   0.0   0.0        0.0
   0.0      0.0      0.0   0.0   0.0        0.0
   0.0      0.0      0.0   0.0   0.0        0.0
   0.0      0.0      0.0   0.0   0.0        0.0   AddBLin  - Additional linear damping(N/(m/s), N/(rad/s), N-m/(m/s), N-m/(rad/s))
   0.0      0.0      0.0   0.0   0.0        0.0
   0.0      0.0      0.0   0.0   0.0        0.0
   0.0      0.0      0.0   0.0   0.0        0.0
   0.0      0.0      0.0   0.0   0.0        0.0
   0.0      0.0      0.0   0.0   0.0        0.0
504375.5      0.0      0.0   0.0   0.0        0.0   AddBQuad - Additional quadratic drag(N/(m/s)^2, N/(rad/s)^2, N-m(m/s)^2, N-m/(rad/s)^2)
   0.0   504375.5      0.0   0.0   0.0        0.0
   0.0      0.0   4954372   0.0   0.0        0.0
   0.0      0.0      0.0 6.413E10 0.0        0.0
   0.0      0.0      0.0   0.0   6.413E10     0.0
   0.0      0.0      0.0   0.0   0.0        7.072E9
---------------------- HEAVE COEFFICIENTS -------------------------------------
1            NHvCoef       - Number of heave coefficients (-)
HvCoefID         HvCd    HvCa
```

(-) (-) (-)
1 0.0 0.0
---------- MEMBER JOINTS ----------
2 NJoints - Number of joints (-) [must be exactly 0 or at least 2]
JointID Jointx Jointy Jointz JointHvID JointOvrlp [JointOvrlp= 0: do nothing at joint, 1: eliminate overlaps by calculating super member]
(-) (m) (m) (m) (-) (switch)
1 0.0 0.0 -22.61 1 0 - Cylinder
2 0.0 0.0 11.30 1 0 - Cylinder
---------- MEMBER CROSS-SECTION PROPERTIES ----------
1 NPropSets - Number of member property sets (-)
PropSetID PropD PropThck
(-) (m) (m)
1 53.675 0.06 - Diameter and Thickness Cylinder
---------- SIMPLE HYDRODYNAMIC COEFFICIENTS (model 1) ----------
SimplCd SimplCdMG SimplCa SimplCaMG
(-) (-) (-) (-)
0.6 0.0 0.0 0.0
---------- DEPTH-BASED HYDRODYNAMIC COEFFICIENTS (model 2) ---------
0 NCoefDpth - Number of depth-dependent coefficients (-)
Dpth DpthCd DpthCdMG DpthCa DpthCaMG
(m) (-) (-) (-) (-)
---------- MEMBER-BASED HYDRODYNAMIC COEFFICIENTS (model 3) --------
0 NCoefMembers - Number of member-based coefficients (-)
MemberID MemberCd1 MemberCd2 MemberCdMG1 MemberCdMG2 MemberCa1 MemberCa2 MemberCaMG1 MemberCaMG2
(-) (-) (-) (-) (-) (-) (-) (-) (-)
---------- MEMBERS ----------
1 NMembers - Number of members (-)
MemberID MJointID1 MJointID2 MPropSetID1 MPropSetID2 MDivSize MCoefMod PropWAMIT [MCoefMod=1: use simple coeff table, 2: use depth-based coeff table, 3: use member-based coeff table] [PropWAMIT = TRUE if member is modeled in WAMIT]

```
(-)       (-)       (-)       (-)       (-)         (m)      (switch)   (flag)
 1         1         2         1         1          0.5       1         TRUE          - Cylinder
---------------------- FILLED MEMBERS ---------------------------------------------
0            NFillGroups     - Number of filled member groups (-) [If FillDens = DEFAULT, then FillDens = WtrDens; FillFSLoc is related to MSL2SWL]
FillNumM FillMList            FillFSLoc     FillDens
(-)      (-)                    (m)          (kg/m^3)
---------------------- MARINE GROWTH ----------------------------------------------
0            NMGDepths      - Number of marine-growth depths specified (-)
MGDpth     MGThck       MGDens
(m)        (m)          (kg/m^3)
---------------------- MEMBER OUTPUT LIST -----------------------------------------
  0          NMOutputs      - Number of member outputs (-) [must be < 10]
MemberID   NOutLoc    NodeLocs [NOutLoc < 10; node locations are normalized distance from the start of the member, and must be >=0 and <= 1] [unused if
NMOutputs=0]
 (-)       (-)       (-)
---------------------- JOINT OUTPUT LIST ------------------------------------------
  0         NJOutputs      - Number of joint outputs [Must be < 10 ]
---------------------- OUTPUT -----------------------------------------------------
False              HDSum          - Output a summary file [flag]
False              OutAll         - Output all user-specified member and joint loads (only at each member end, not interior locations) [flag]
2                  OutSwtch       - Output requested channels to: [1=Hydrodyn.out, 2=GlueCode.out,  3=both files]
"ES11.4e2"         OutFmt         - Output format for numerical results (quoted string) [not checked for validity!]
"A11"              OutSFmt        - Output format for header strings (quoted string) [not checked for validity!]
---------------------- FLOATING PLATFORM OUTPUTS ----------------------------------
"Wave1Elev"                       - Wave elevation at the platform reference point (0,  0)
END of Floating platform outputs
---------------------- MESH-BASED OUTPUTS -----------------------------------------
END of mesh-based outputs and HydroDyn input file (the word "END" must appear in the first 3 columns of this last line).
```

10MW HydroDyn file - Scaled

Remark: Only input variables that change compared to the 7.5MW HydroDyn Input file are listed

```
1.26              WAMITULEN    - Characteristic body length scale used to redimensionalize WAMIT output (meters)
2.729E4           PtfmVol0     - Displaced volume of water when the platform is in its undisplaced position (m^3)

627102.0      0.0       0.0   0.0   0.0        0.0   AddBQuad - Additional quadratic drag(N/(m/s)^2, N/(rad/s)^2, N-m(m/s)^2, N-m/(rad/s)^2)
    0.0   627102.0      0.0   0.0   0.0        0.0
    0.0       0.0   6159888   0.0   0.0        0.0
    0.0       0.0       0.0 1.0468E11 0.0        0.0
    0.0       0.0       0.0   0.0   1.0468E11    0.0
    0.0       0.0       0.0   0.0   0.0        1.154E10

---------------------- MEMBER JOINTS ----------------------------------------------
2             NJoints       - Number of joints (-)   [must be exactly 0 or at least 2]
JointID   Jointx     Jointy     Jointz     JointHvID  JointOvrlp   [JointOvrlp= 0: do nothing at joint, 1: eliminate overlaps by calculating super member]
(-)       (m)        (m)        (m)        (-)      (switch)
 1         0.0        0.0      -25.21       1        0              - Start location of Cylinder
 2         0.0        0.0       12.61       1        0              - End location of Cylinder
```

ElastoDyn

7.5MW ElastoDyn file - Scaled

```
------- ELASTODYN V1.01.* INPUT FILE -------------------------------------------
---------------------- SIMULATION CONTROL --------------------------------------
False           Echo        - Echo input data to "<RootName>.ech" (flag)
3               Method      - Integration method: {1: RK4, 2: AB4, or 3: ABM4} (-)
0.0125          DT          - Integration time step (s)
---------------------- ENVIRONMENTAL CONDITION ---------------------------------
9.80665         Gravity     - Gravitational acceleration (m/s^2)
---------------------- DEGREES OF FREEDOM --------------------------------------
False           FlapDOF1    - First flapwise blade mode DOF (flag)
False           FlapDOF2    - Second flapwise blade mode DOF (flag)
False           EdgeDOF     - First edgewise blade mode DOF (flag)
False           TeetDOF     - Rotor-teeter DOF (flag) [unused for 3 blades]
True            DrTrDOF     - Drivetrain rotational-flexibility DOF (flag)
True            GenDOF      - Generator DOF (flag)
True            YawDOF      - Yaw DOF (flag)
False           TwFADOF1    - First fore-aft tower bending-mode DOF (flag)
False           TwFADOF2    - Second fore-aft tower bending-mode DOF (flag)
False           TwSSDOF1    - First side-to-side tower bending-mode DOF (flag)
False           TwSSDOF2    - Second side-to-side tower bending-mode DOF (flag)
True            PtfmSgDOF   - Platform horizontal surge translation DOF (flag)
True            PtfmSwDOF   - Platform horizontal sway translation DOF (flag)
True            PtfmHvDOF   - Platform vertical heave translation DOF (flag)
True            PtfmRDOF    - Platform roll tilt rotation DOF (flag)
True            PtfmPDOF    - Platform pitch tilt rotation DOF (flag)
```

```
True            PtfmYDOF    - Platform yaw rotation DOF (flag)
---------------------- INITIAL CONDITIONS -------------------------------------
0               OoPDefl     - Initial out-of-plane blade-tip displacement (meters)
0               IPDefl      - Initial in-plane blade-tip deflection (meters)
0               BlPitch(1)  - Blade 1 initial pitch (degrees)
0               BlPitch(2)  - Blade 2 initial pitch (degrees)
0               BlPitch(3)  - Blade 3 initial pitch (degrees) [unused for 2 blades]
0               TeetDefl    - Initial or fixed teeter angle (degrees) [unused for 3 blades]
0               Azimuth     - Initial azimuth angle for blade 1 (degrees)
0               RotSpeed    - Initial or fixed rotor speed (rpm)
0               NacYaw      - Initial or fixed nacelle-yaw angle (degrees)
0               TTDspFA     - Initial fore-aft tower-top displacement (meters)
0               TTDspSS     - Initial side-to-side tower-top displacement (meters)
0               PtfmSurge   - Initial or fixed horizontal surge translational displacement of platform (meters)
0               PtfmSway    - Initial or fixed horizontal sway translational displacement of platform (meters)
0               PtfmHeave    - Initial or fixed vertical heave translational displacement of platform (meters)
0               PtfmRoll    - Initial or fixed roll tilt rotational displacement of platform (degrees)
0               PtfmPitch   - Initial or fixed pitch tilt rotational displacement of platform (degrees)
0               PtfmYaw     - Initial or fixed yaw rotational displacement of platform (degrees)
---------------------- TURBINE CONFIGURATION ----------------------------------
3               NumBl       - Number of blades (-)
75.778          TipRad      - The distance from the rotor apex to the blade tip (meters)
2.15            HubRad      - The distance from the rotor apex to the blade root (meters)
-2.5            PreCone(1)  - Blade 1 cone angle (degrees)
-2.5            PreCone(2)  - Blade 2 cone angle (degrees)
-2.5            PreCone(3)  - Blade 3 cone angle (degrees) [unused for 2 blades]
0               HubCM       - Distance from rotor apex to hub mass [positive downwind] (meters)
0               UndSling    - Undersling length [distance from teeter pin to the rotor apex] (meters) [unused for 3 blades]
0               Delta3      - Delta-3 angle for teetering rotors (degrees) [unused for 3 blades]
```

0	AzimB1Up	- Azimuth value to use for I/O when blade 1 points up (degrees)
-6.06	OverHang	- Distance from yaw axis to rotor apex [3 blades] or teeter pin [2 blades] (meters)
1.912	ShftGagL	- Distance from rotor apex [3 blades] or teeter pin [2 blades] to shaft strain gages [positive for upwind rotors] (meters)
-5	ShftTilt	- Rotor shaft tilt angle (degrees)
2.2935	NacCMxn	- Downwind distance from the tower-top to the nacelle CM (meters)
0	NacCMyn	- Lateral distance from the tower-top to the nacelle CM (meters)
2.075	NacCMzn	- Vertical distance from the tower-top to the nacelle CM (meters)
-3.09528	NcIMUxn	- Downwind distance from the tower-top to the nacelle IMU -3.09528 (meters)
0.0	NcIMUyn	- Lateral distance from the tower-top to the nacelle IMU (meters)
2.23336	NcIMUzn	- Vertical distance from the tower-top to the nacelle IMU 2.23336(meters)
2.35628	Twr2Shft	- Vertical distance from the tower-top to the rotor shaft (meters)
101.615	TowerHt	- Height of tower above ground level [onshore] or MSL [offshore] (meters)
11.3	TowerBsHt	- Height of tower base above ground level [onshore] or MSL [offshore] (meters)
0	PtfmCMxt	- Downwind distance from the ground level [onshore] or MSL [offshore] to the platform CM (meters)
0	PtfmCMyt	- Lateral distance from the ground level [onshore] or MSL [offshore] to the platform CM (meters)
-15.21	PtfmCMzt	- Vertical distance from the ground level [onshore] or MSL [offshore] to the platform CM (meters)
-0	PtfmRefzt	- Vertical distance from the ground level [onshore] or MSL [offshore] to the platform reference point (meters)
---------- MASS AND INERTIA ----------		
0	TipMass(1)	- Tip-brake mass, blade 1 (kg)
0	TipMass(2)	- Tip-brake mass, blade 2 (kg)
0	TipMass(3)	- Tip-brake mass, blade 3 (kg) [unused for 2 blades]
81150	HubMass	- Hub mass (kg)
220798.5	HubIner	- Hub inertia about rotor axis [3 blades] or teeter axis [2 blades] (kg m^2)
1017.3	GenIner	- Generator inertia about HSS (kg m^2)
343018	NacMass	- Nacelle mass (kg)
4.96E+06	NacYIner	- Nacelle inertia about yaw axis (kg m^2)
0	YawBrMass	- Yaw bearing mass (kg)
19403070	PtfmMass	- Platform mass (kg)
1.204954E+10	PtfmRIner	- Platform inertia for roll tilt rotation about the platform CM (kg m^2)

```
1.204954E+10   PtfmPIner        - Platform inertia for pitch tilt rotation about the platform CM (kg m^2)
2.166154E+10   PtfmYIner        - Platfrom inertia for yaw rotation about the platform CM (kg m^2)
---------------------- BLADE -----------------------------------------------------
"..\7.5MW_Blade.dat"    BldFile(1)  - Name of file containing properties for blade 1 (quoted string)
"..\7.5MW_Blade.dat"    BldFile(2)  - Name of file containing properties for blade 2 (quoted string)
"..\7.5MW_Blade.dat"    BldFile(3)  - Name of file containing properties for blade 3 (quoted string) [unused for 2 blades]
---------------------- ROTOR-TEETER ----------------------------------------------
        0   TeetMod     - Rotor-teeter spring/damper model {0: none, 1: standard, 2: user-defined from routine UserTeet} (switch) [unused for 3 blades]
        0   TeetDmpP    - Rotor-teeter damper position (degrees) [used only for 2 blades and when TeetMod=1]
        0   TeetDmp     - Rotor-teeter damping constant (N-m/(rad/s)) [used only for 2 blades and when TeetMod=1]
        0   TeetCDmp    - Rotor-teeter rate-independent Coulomb-damping moment (N-m) [used only for 2 blades and when TeetMod=1]
        0   TeetSStP    - Rotor-teeter soft-stop position (degrees) [used only for 2 blades and when TeetMod=1]
        0   TeetHStP    - Rotor-teeter hard-stop position (degrees) [used only for 2 blades and when TeetMod=1]
        0   TeetSSSp    - Rotor-teeter soft-stop linear-spring constant (N-m/rad) [used only for 2 blades and when TeetMod=1]
        0   TeetHSSp    - Rotor-teeter hard-stop linear-spring constant (N-m/rad) [used only for 2 blades and when TeetMod=1]
---------------------- DRIVETRAIN ------------------------------------------------
      100   GBoxEff     - Gearbox efficiency (%)
       50   GBRatio     - Gearbox ratio (-)
2.452936425E+09   DTTorSpr    - Drivetrain torsional spring (N-m/rad)
 9.24056E+06   DTTorDmp    - Drivetrain torsional damper (N-m/(rad/s))
---------------------- FURLING ---------------------------------------------------
False         Furling     - Read in additional model properties for furling turbine (flag) [must currently be FALSE)
"Dummy"       FurlFile    - Name of file containing furling properties (quoted string) [unused when Furling=False]
---------------------- TOWER -----------------------------------------------------
       20   TwrNodes    - Number of tower nodes used for analysis (-)
"..\7.5MW_Tower.dat"    TwrFile     - Name of file containing tower properties (quoted string)
---------------------- OUTPUT ----------------------------------------------------
False          SumPrint    - Print summary data to "<RootName>.sum" (flag)
        1   OutFile     - Switch to determine where output will be placed: {1: in module output file only; 2: in glue code output file only; 3: both} (currently unused)
```

True TabDelim - Use tab delimiters in text tabular output file? (flag) (currently unused)

"ES10.3E2" OutFmt - Format used for text tabular output (except time). Resulting field should be 10 characters. (quoted string) [not checked for validity!] (currently unused)

0 TStart - Time to begin tabular output (s) (currently unused)

1 DecFact - Decimation factor for tabular output {1: output every time step} (-) (currently unused)

0 NTwGages - Number of tower nodes that have strain gages for output [0 to 9] (-)

1,2 TwrGagNd - List of tower nodes that have strain gages [1 to TwrNodes] (-) [unused if NTwGages=0]

3 NBlGages - Number of blade nodes that have strain gages for output [0 to 9] (-)

5, 9, 13 BldGagNd - List of blade nodes that have strain gages [1 to BldNodes] (-) [unused if NBlGages=0]

OutList - The next line(s) contains a list of output parameters. See OutListParameters.xlsx for a listing of available output channels, (-)

END of input file (the word "END" must appear in the first 3 columns of this last OutList line)

7.5MW ElastoDyn file – Reduced Draft

Remark: Only input variables that change compared to the 7.5MW ElastoDyn Input file are listed

10.00 TowerBsHt - Height of tower base above ground level [onshore] or MSL [offshore] (meters)

0 PtfmCMxt - Downwind distance from the ground level [onshore] or MSL [offshore] to the platform CM (meters)

0 PtfmCMyt - Lateral distance from the ground level [onshore] or MSL [offshore] to the platform CM (meters)

-13.64 PtfmCMzt - Vertical distance from the ground level [onshore] or MSL [offshore] to the platform CM (meters)

-0 PtfmRefzt - Vertical distance from the ground level [onshore] or MSL [offshore] to the platform reference point (meters)

1.253E+10 PtfmRIner - Platform inertia for roll tilt rotation about the platform CM (kg m^2)

1.253E+10 PtfmPIner - Platform inertia for pitch tilt rotation about the platform CM (kg m^2)

2.235E+10 PtfmYIner - Platfrom inertia for yaw rotation about the platform CM (kg m^2)

10MW ElastoDyn file – Scaled

Remark: Only input variables that change compared to the 7.5MW ElastoDyn Input file are listed

---------- TURBINE CONFIGURATION ----------

3	NumBl	- Number of blades (-)
89.166	TipRad	- The distance from the rotor apex to the blade tip (meters)
2.8	HubRad	- The distance from the rotor apex to the blade root (meters)
-7.1	OverHang	- Distance from yaw axis to rotor apex [3 blades] or teeter pin [2 blades] (meters)
1.912	ShftGagL	- Distance from rotor apex [3 blades] or teeter pin [2 blades] to shaft strain gages [positive for upwind rotors] (meters)
-5	ShftTilt	- Rotor shaft tilt angle (degrees)
2.687	NacCMxn	- Downwind distance from the tower-top to the nacelle CM (meters)
0	NacCMyn	- Lateral distance from the tower-top to the nacelle CM (meters)
2.45	NacCMzn	- Vertical distance from the tower-top to the nacelle CM (meters)
-3.09528	NcIMUxn	- Downwind distance from the tower-top to the nacelle IMU -3.09528 (meters)
2.23336	NcIMUzn	- Vertical distance from the tower-top to the nacelle IMU 2.23336(meters)
2.75	Twr2Shft	- Vertical distance from the tower-top to the rotor shaft (meters)
115.63	TowerHt	- Height of tower above ground level [onshore] or MSL [offshore] (meters)
12.61	TowerBsHt	- Height of tower base above ground level [onshore] or MSL [offshore] (meters)
-16.97	PtfmCMzt	- Vertical distance from the ground level [onshore] or MSL [offshore] to the platform CM (meters)

---------- MASS AND INERTIA ----------

105520	HubMass	- Hub mass (kg)
325671	HubIner	- Hub inertia about rotor axis [3 blades] or teeter axis [2 blades] (kg m^2)
1500.5	GenIner	- Generator inertia about HSS (kg m^2)
446036	NacMass	- Nacelle mass (kg)
7.326346E+06	NacYIner	- Nacelle inertia about yaw axis (kg m^2)
26598228	PtfmMass	- Platform mass (kg)
2.023776E+010	PtfmRIner	- Platform inertia for roll tilt rotation about the platform CM (kg m^2)
2.023776E+010	PtfmPIner	- Platform inertia for pitch tilt rotation about the platform CM (kg m^2)
3.647042E+010	PtfmYIner	- Platfrom inertia for yaw rotation about the platform CM (kg m^2)

10MW ElastoDyn file – Reduced Draft

Remark: Only input variables that change compared to the 7.5MW ElastoDyn Input file are listed

-13.46 PtfmCMzt - Vertical distance from the ground level [onshore] or MSL [offshore] to the platform CM (meters)

26598228 PtfmMass - Platform mass (kg)
2.023776E+010 PtfmRIner - Platform inertia for roll tilt rotation about the platform CM (kg m^2)
2.023776E+010 PtfmPIner - Platform inertia for pitch tilt rotation about the platform CM (kg m^2)
3.813084E+010 PtfmYIner - Platfrom inertia for yaw rotation about the platform CM (kg m^2)

ServoDyn

Remark: The ServoDyn input differs mainly in the turbine-related control strategy, which has been modified based on the NREL 5MW OWT design by Cyril Godreau

------- SERVODYN V1.01.* INPUT FILE --
---------------------- SIMULATION CONTROL --------------------------------------
False Echo - Echo input data to <RootName>.ech (flag)
0.0125 DT - Communication interval for controllers (s)
---------------------- PITCH CONTROL ---
5 PCMode - Pitch control mode {0: none, 1: user-defined from routine PitchCntrl, 2: user-defined from Simulink, 5: user-defined from Bladed-style DLL}
0 TPCOn - Time to enable active pitch control (s) [unused when PCMode=0]
9999.9 TPitManS(1) - Time to start override pitch maneuver for blade 1 and end standard pitch control (s)
9999.9 TPitManS(2) - Time to start override pitch maneuver for blade 2 and end standard pitch control (s)
9999.9 TPitManS(3) - Time to start override pitch maneuver for blade 3 and end standard pitch control (s) [unused for 2 blades]
2 PitManRat(1) - Pitch rate at which override pitch maneuver heads toward final pitch angle for blade 1 (deg/s)
2 PitManRat(2) - Pitch rate at which override pitch maneuver heads toward final pitch angle for blade 2 (deg/s)

2 PitManRat(3) - Pitch rate at which override pitch maneuver heads toward final pitch angle for blade 3 (deg/s) [unused for 2 blades]

0 BlPitchF(1) - Blade 1 final pitch for pitch maneuvers (degrees)

0 BlPitchF(2) - Blade 2 final pitch for pitch maneuvers (degrees)

0 BlPitchF(3) - Blade 3 final pitch for pitch maneuvers (degrees) [unused for 2 blades]

---------- GENERATOR AND TORQUE CONTROL ----------

5 VSContrl - Variable-speed control mode {0: none, 1: simple VS, 2: user-defined from routine UserVSCont, 3: user-defined from Simulink 5: user-defined from Bladed-style DLL} (switch)

2 GenModel - Generator model {1: simple, 2: Thevenin, 3: user-defined from routine UserGen} (switch) [used only when VSContrl=0]

94.4 GenEff - Generator efficiency [ignored by the Thevenin and user-defined generator models] (%)

True GenTiStr - Method to start the generator {T: timed using TimGenOn, F: generator speed using SpdGenOn} (flag)

True GenTiStp - Method to stop the generator {T: timed using TimGenOf, F: when generator power = 0} (flag)

9999.9 SpdGenOn - Generator speed to turn on the generator for a startup (HSS speed) (rpm) [used only when GenTiStr=False]

0 TimGenOn - Time to turn on the generator for a startup (s) [used only when GenTiStr=True]

9999.9 TimGenOf - Time to turn off the generator (s) [used only when GenTiStp=True]

---------- SIMPLE VARIABLE-SPEED TORQUE CONTROL ----------

9999.9 VS_RtGnSp - Rated generator speed for simple variable-speed generator control (HSS side) (rpm) [used only when VSContrl=1]

9999.9 VS_RtTq - Rated generator torque/constant generator torque in Region 3 for simple variable-speed generator control (HSS side) (N-m) [used only when VSContrl=1]

9999.9 VS_Rgn2K - Generator torque constant in Region 2 for simple variable-speed generator control (HSS side) (N-m/rpm^2) [used only when VSContrl=1]

9999.9 VS_SlPc - Rated generator slip percentage in Region 2 1/2 for simple variable-speed generator control (%) [used only when VSContrl=1]

---------- SIMPLE INDUCTION GENERATOR ----------

9999.9 SIG_SlPc - Rated generator slip percentage (%) [used only when VSContrl=0 and GenModel=1]

9999.9 SIG_SySp - Synchronous (zero-torque) generator speed (rpm) [used only when VSContrl=0 and GenModel=1]

9999.9 SIG_RtTq - Rated torque (N-m) [used only when VSContrl=0 and GenModel=1]

9999.9 SIG_PORt - Pull-out ratio (Tpullout/Trated) (-) [used only when VSContrl=0 and GenModel=1]

---------- THEVENIN-EQUIVALENT INDUCTION GENERATOR ----------

9999.9 TEC_Freq - Line frequency [50 or 60] (Hz) [used only when VSContrl=0 and GenModel=2]

9998 TEC_NPol - Number of poles [even integer > 0] (-) [used only when VSContrl=0 and GenModel=2]

9999.9 TEC_SRes - Stator resistance (ohms) [used only when VSContrl=0 and GenModel=2]

9999.9 TEC_RRes - Rotor resistance (ohms) [used only when VSContrl=0 and GenModel=2]
9999.9 TEC_VLL - Line-to-line RMS voltage (volts) [used only when VSContrl=0 and GenModel=2]
9999.9 TEC_SLR - Stator leakage reactance (ohms) [used only when VSContrl=0 and GenModel=2]
9999.9 TEC_RLR - Rotor leakage reactance (ohms) [used only when VSContrl=0 and GenModel=2]
9999.9 TEC_MR - Magnetizing reactance (ohms) [used only when VSContrl=0 and GenModel=2]
---------- HIGH-SPEED SHAFT BRAKE ----------
1 HSSBrMode - HSS brake model {1: simple, 2: user-defined from routine UserHSSBr, 3: user-defined from Labview, 5: user-defined from Bladed-style DLL} (switch)
9999.9 THSSBrDp - Time to initiate deployment of the HSS brake (s)
0.6 HSSBrDT - Time for HSS-brake to reach full deployment once initiated (sec) [used only when HSSBrMode=1]
28116.2 HSSBrTqF - Fully deployed HSS-brake torque (N-m)
---------- NACELLE-YAW CONTROL ----------
5 YCMode - Yaw control mode {0: none, 1: simple, 2: user-defined from routine UserYawCont, 3: user-defined from Simulink/Labview, 5: user-defined from Bladed-style DLL} (switch)
9999.9 TYCOn - Time to enable active yaw control (s) [unused when YCMode=0]
0 YawNeut - Neutral yaw position--yaw spring force is zero at this yaw (degrees)
9.02832E+09 YawSpr - Nacelle-yaw spring constant (N-m/rad)
1.916E+07 YawDamp - Nacelle-yaw damping constant (N-m/(rad/s))
9999.9 TYawManS - Time to start override yaw maneuver and end standard yaw control (s)
2 YawManRat - Yaw maneuver rate (in absolute value) (deg/s)
0 NacYawF - Final yaw angle for override yaw maneuvers (degrees)
---------- BLADED INTERFACE ----------
"..\DISCON_7_5MWDTU_win32.dll" DLL_FileName - Name/location of the dynamic library {.dll [Windows] or .so [Linux]} in the Bladed-DLL format (-) [used only with Bladed Interface]
0 NacYaw_North - Reference yaw angle of the nacelle when the upwind end points due North (deg) [used only with Bladed Interface]
0 Ptch_Cntrl - Record 28: Use individual pitch control {0: collective pitch; 1: individual pitch control} (switch) [used only with Bladed Interface]
0 Ptch_SetPnt - Record 5: Below-rated pitch angle set-point (deg) [used only with Bladed Interface]
0 Ptch_Min - Record 6: Minimum pitch angle (deg) [used only with Bladed Interface]
0 Ptch_Max - Record 7: Maximum pitch angle (deg) [used only with Bladed Interface]
0 PtchRate_Min - Record 8: Minimum pitch rate (most negative value allowed) (deg/s) [used only with Bladed Interface]

```
        0   PtchRate_Max - Record  9: Maximum pitch rate  (deg/s) [used only with Bladed Interface]
        0   Gain_OM      - Record 16: Optimal mode gain (Nm/(rad/s)^2) [used only with Bladed Interface]
        0   GenSpd_MinOM - Record 17: Minimum generator speed (rpm) [used only with Bladed Interface]
        0   GenSpd_MaxOM - Record 18: Optimal mode maximum speed (rpm) [used only with Bladed Interface]
        0   GenSpd_Dem   - Record 19: Demanded generator speed above rated (rpm) [used only with Bladed Interface]
        0   GenTrq_Dem   - Record 22: Demanded generator torque above rated (Nm) [used only with Bladed Interface]
        0   GenPwr_Dem   - Record 13: Demanded power (W) [used only with Bladed Interface]
---------------------- BLADED INTERFACE TORQUE-SPEED LOOK-UP TABLE ----------
        0   DLL_NumTrq   - Record 26: No. of points in torque-speed look-up table {0 = none and use the optimal mode parameters; nonzero = ignore the optimal mode PARAMETERs by setting Record 16 to 0.0} (-) [used only with Bladed Interface]
 GenSpd_TLU   GenTrq_TLU
 (rpm)          (Nm)
---------------------- OUTPUT ----------------------------------------------------
False          SumPrint     - Print summary data to <RootName>.sum (flag) (currently unused)
        1   OutFile      - Switch to determine where output will be placed: {1: in module output file only; 2: in glue code output file only; 3: both} (currently unused)
True           TabDelim     - Use tab delimiters in text tabular output file? (flag) (currently unused)
"ES10.3E2"    OutFmt       - Format used for text tabular output (except time).  Resulting field should be 10 characters. (quoted string) (currently unused)
        0   TStart       - Time to begin tabular output (s) (currently unused)
           OutList      - The next line(s) contains a list of output parameters.  See OutListParameters.xlsx for a listing of available output channels, (-)
GenPwr                   - Electrical generator power and torque
GenTq                    - Electrical generator power and torque
END of input file (the word "END" must appear in the first 3 columns of this last OutList line)
---------------------------------------------------------------------------------------
```

C Technical Drawings Platforms

REVISION HISTORY			
REV	DESCRIPTION	DATE	APPROVED

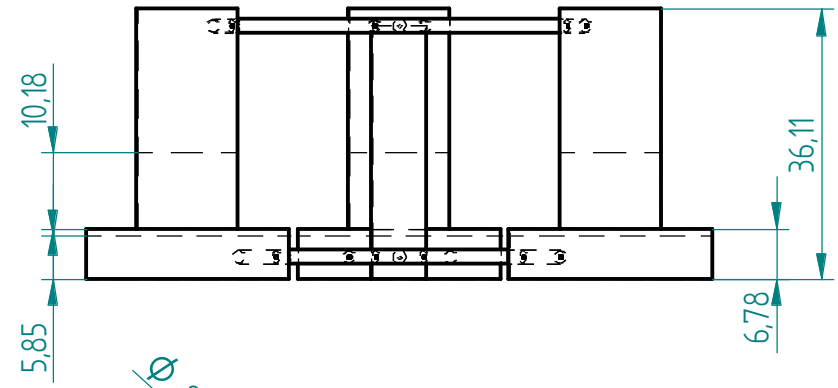

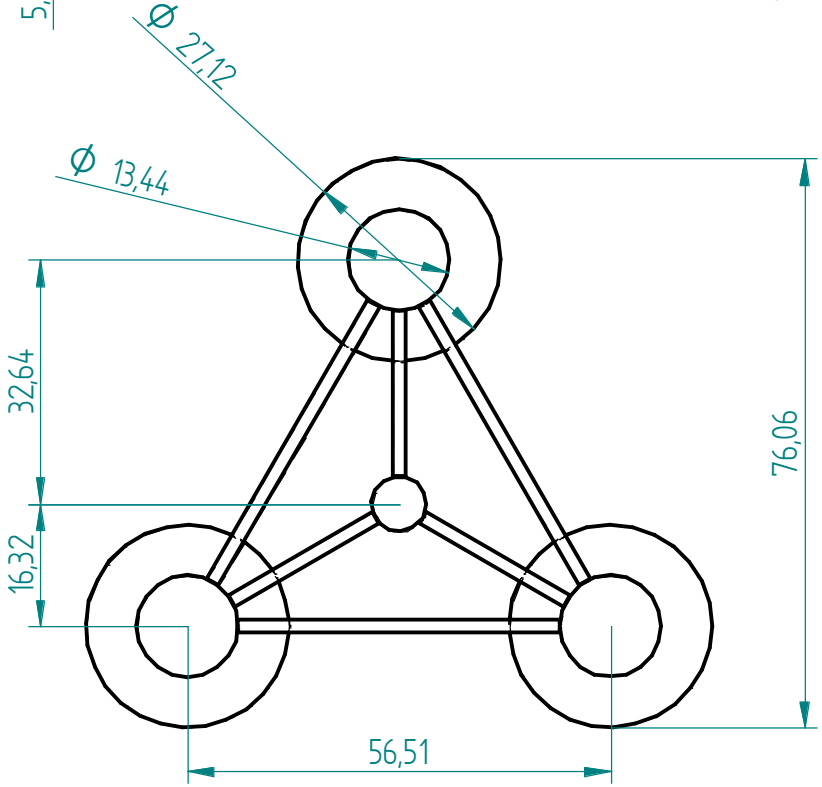

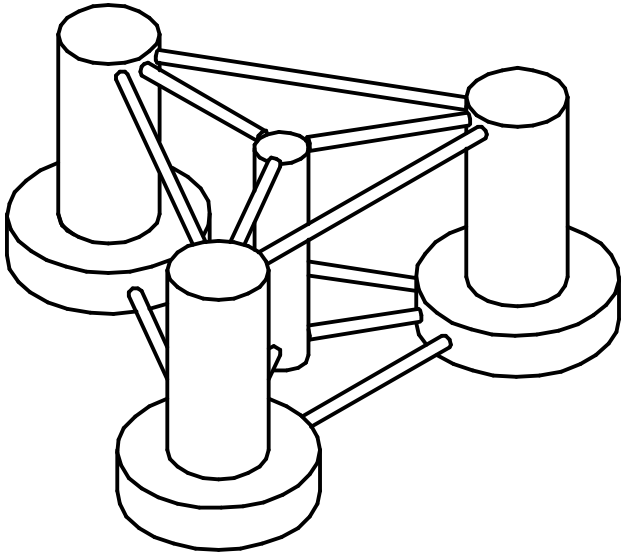

	NAME	DATE
DRAWN	Johannes	10.07.2014
CHECKED	George	
ENG APPR		
MGR APPR		

UNLESS OTHERWISE SPECIFIED
DIMENSIONS ARE IN METERS

Solid Edge

TITLE
7.5MW SCALED

SIZE	DWG NO	REV
A4		

FILE NAME: _1466513028

SCALE: 1:1000	WEIGHT:	SHEET 1 OF 1

REVISION HISTORY			
REV	DESCRIPTION	DATE	APPROVED

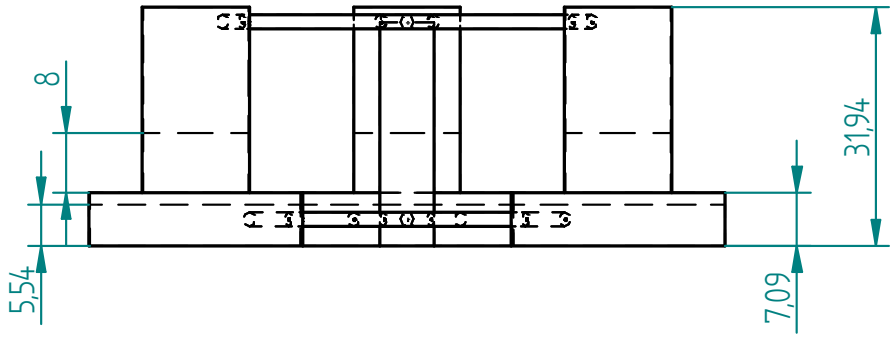

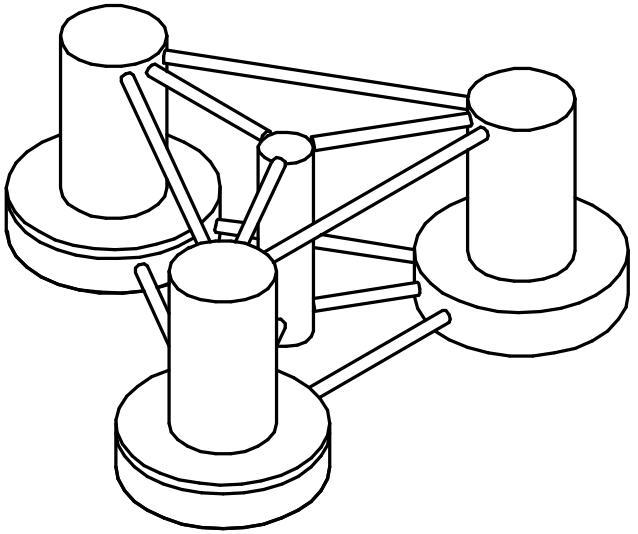

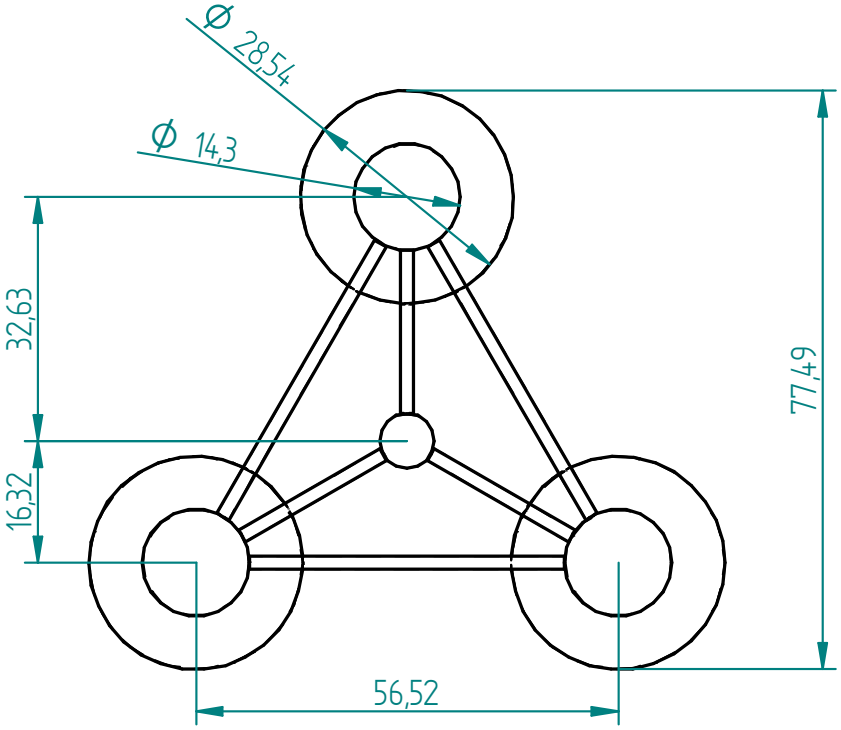

	NAME	DATE
DRAWN	Johannes	
CHECKED	George	
ENG APPR		
MGR APPR		

UNLESS OTHERWISE SPECIFIED
DIMENSIONS ARE IN METERS

Solid Edge

TITLE
7.5MW REDUCED DRAFT

SIZE	DWG NO	REV
A4		

FILE NAME: _1466517802

SCALE: 1:1000	WEIGHT:	SHEET 1 OF 1

REVISION HISTORY			
REV	DESCRIPTION	DATE	APPROVED

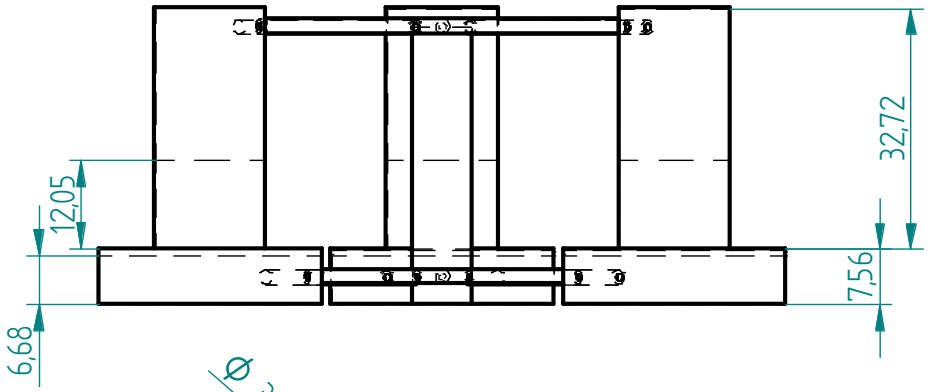

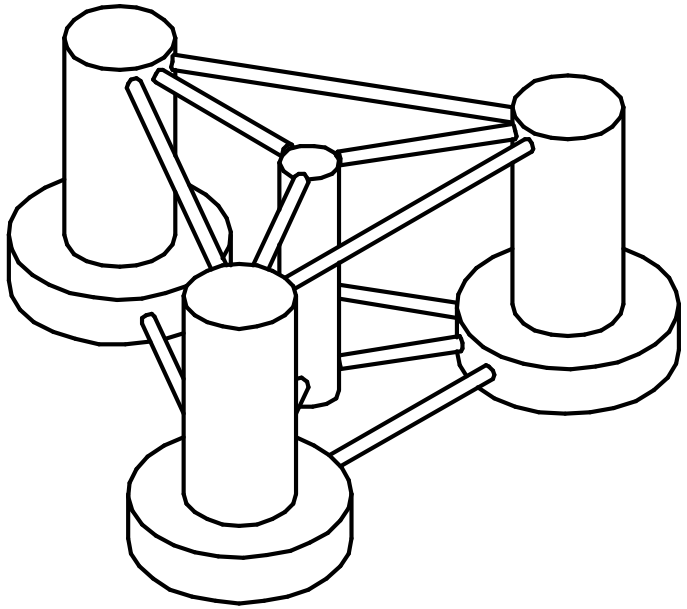

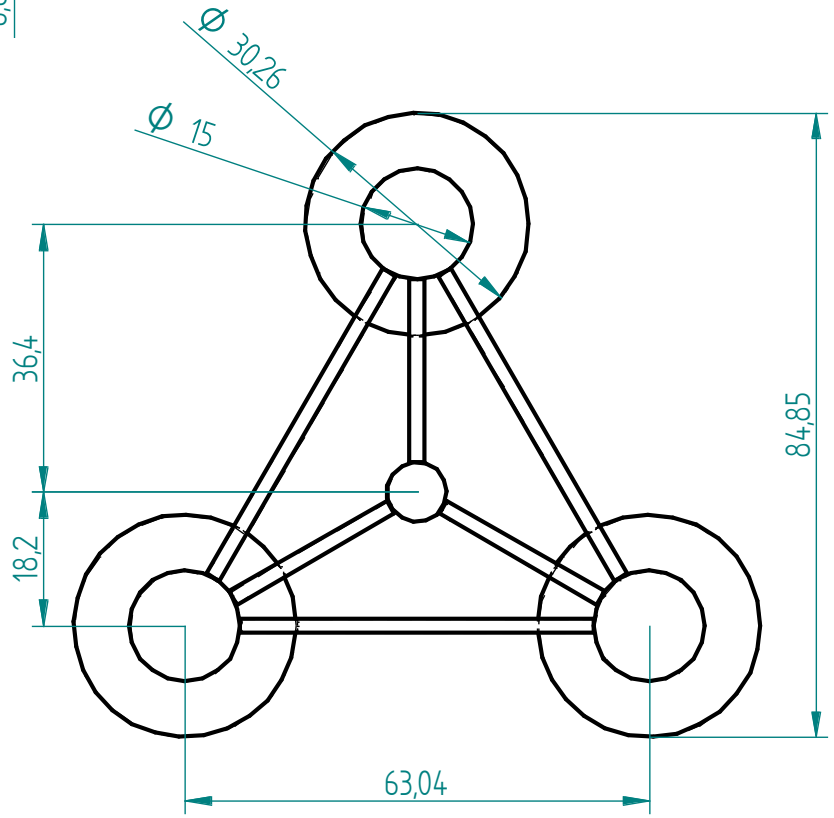

	NAME	DATE
DRAWN	Johannes	
CHECKED	George	
ENG APPR		
MGR APPR		

UNLESS OTHERWISE SPECIFIED
DIMENSIONS ARE IN METERS

Solid Edge

TITLE
10MW SCALED

SIZE	DWG NO	REV
A4		

FILE NAME: _1466518532

SCALE:	WEIGHT:	SHEET 1 OF 1

REVISION HISTORY			
REV	DESCRIPTION	DATE	APPROVED

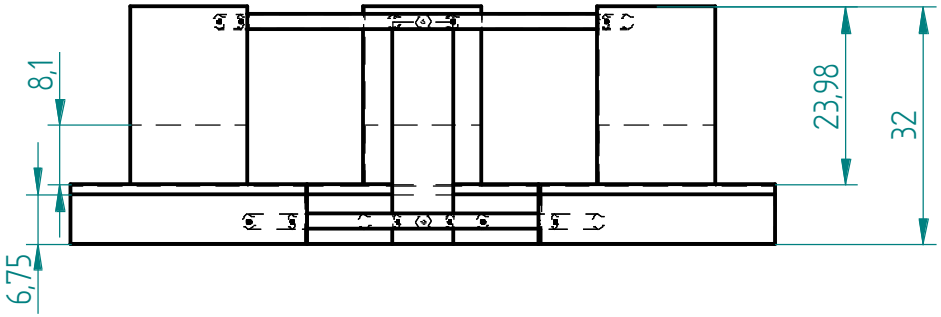

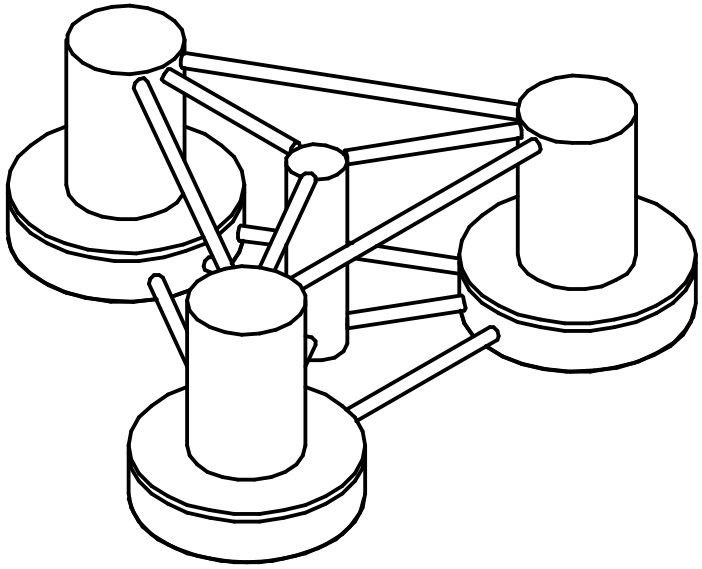

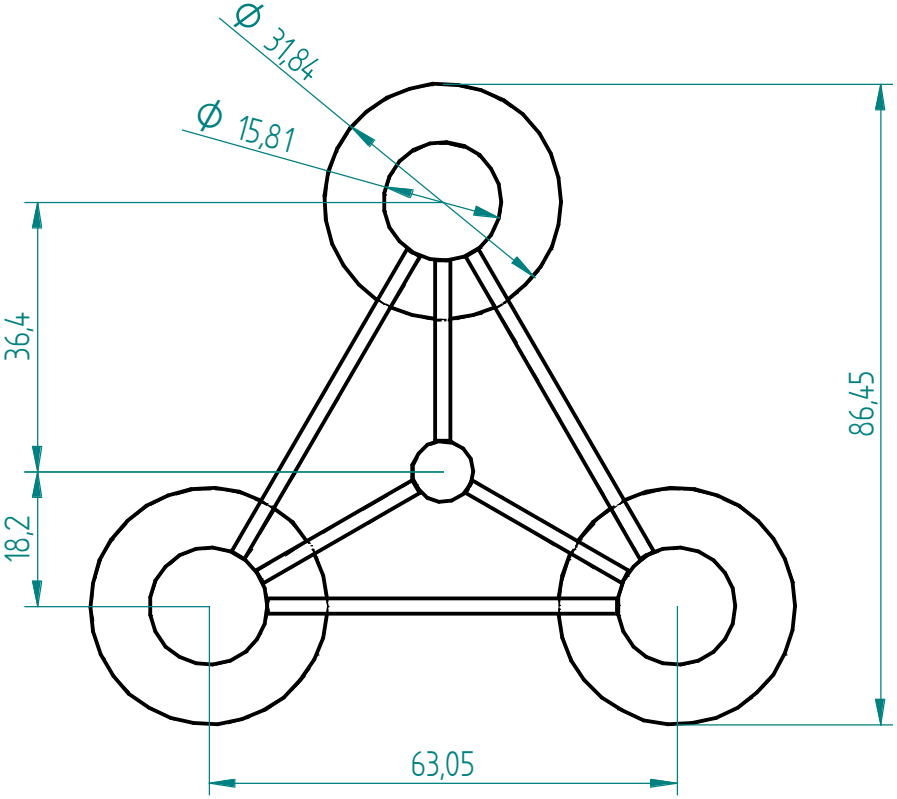

	NAME	DATE
DRAWN	Johannes	
CHECKED	George	
ENG APPR		
MGR APPR		

UNLESS OTHERWISE SPECIFIED
DIMENSIONS ARE IN METERS

Solid Edge

TITLE
10MW REDUCED DRAFT

SIZE	DWG NO	REV
A4		

FILE NAME: _1466519169

SCALE:	WEIGHT:	SHEET 1 OF 1